IDENTIFICATION OF NOVEL ESTROGEN RECEPTOR INHIBITORS FOR THE TREATMENT OF HORMONE RESISTANT BREAST CANCER

by

Kriti Singh

MSc., Assam Agricultural University, India, 2007

A THESIS SUBMITTED IN PARTIAL FULFILLMENT OF

THE REQUIREMENTS FOR THE DEGREE OF

DOCTOR OF PHILOSOPHY

in

THE FACULTY OF GRADUATE AND POSTDOCTORAL STUDIES

(Experimental Medicine)

THE UNIVERSITY OF BRITISH COLUMBIA

(Vancouver)

May 2017

Abstract

Estrogen receptor alpha positive (ERα+) disease constitutes approximately 75% of all breast cancer (BCa) cases. However resistance to hormone therapy is observed in early-stage as well as in metastatic disease. Importantly, 70% of ERα+ primary tumors retain active ERα when they metastasize and, therefore, ERα continues to play a role in the resistant form of the disease. Moreover, the effectiveness of conventional hormone therapies is hampered due to gain-of-function mutations that may render the receptor constitutively active. Thus drugs that target the ERα estrogen binding site can become ineffective with time. Moreover, cross-talk between ERα and activated growth factor receptors, or their downstream kinases have shown to play a major role in activating ERα even in the absence of estradiol. Taken together, these observations highlight the importance of developing therapeutics that target alternative sites on the receptor, for instance, those that directly act on the co-activator binding pocket called activation function-2 (AF2) site.

Using methods of *in-silico* screening followed by a systematic computer-guided lead optimization process, we were able to develop several promising small-molecule inhibitors that target the AF2 functional site of ERs. This thesis describes the establishment of an experimental pipeline and development of such inhibitors. The identified lead compound VPC-16606 effectively blocked ERα-co-activator interactions, demonstrated a strong anti-proliferative effect against a panel of ERα+ cells including Tamoxifen-resistant cells and down-regulated ERα-dependent genes. Most importantly, VPC-16606 successfully inhibited known constitutively active mutant forms of ERα observed in clinical settings where BCa patients have relapsed on aromatase inhibitors. Furthermore, the compound also reduced tumor burden *in vivo*.

Overall, these studies helped to identify a novel class of ERα AF2 inhibitors which have the potential to effectively inhibit ERα activity by a unique mechanism and to circumvent the issue of hormone resistance in BCa patients.

Preface

1. Work described in Chapter 3 has been published [**Singh K**, Munuganti RS, Leblanc E, Lin YL, Leung E, Lallous N, Butler M, Cherkasov A, Rennie PS. *In silico* discovery and validation of potent small-molecule inhibitors targeting the activation function 2 site of human oestrogen receptor α. *Breast Cancer Res*. (**2015**) 25;17,27]. Drs. Rennie and Cherkasov are senior authors, and they supervised this project throughout the concept formation to manuscript revision. I performed all the wet-lab experiments, as well as drafted and revised the manuscript. Dr. Munuganti performed all the computational experiments. Drs. Leblanc E, Lallous N and Butler helped in the biological evaluation of the inhibitors. Dr. Leung E provided Tamoxifen-resistant breast cancer cell lines. Lin YL performed compound screening.

2. Work described in Chapter 4 will be submitted for publication [**Singh K,** Munuganti RS, Lallous N, Zhang K, Dalal K, Yoon S, Sharma A, Yamazaki T, Santos ND, Bally M, Cherkasov A, Rennie PS. Benzothiophenone Derivatives Targeting Mutant Forms of Estrogen Receptor- α in Hormone Resistant Breast Cancers. (**2017**), manuscript submitted. Drs. Rennie and Cherkasov are senior authors, and they supervised this project throughout the concept formation to manuscript revision. I performed all the wet-lab experiments, as well as drafted and revised the manuscript. Dr. Munuganti and Yamazaki performed all the computational experiments. Drs. Lallous, Leblanc and Dalal and Sharma A helped in the biological evaluation of the inhibitors. Dr. Santos performed *in vivo* experiment whereas Dr. Bally M supervised *in vivo* study. Zhang K prepared MCF7LUC cells. Yoon S performed drug screening.

Materials and methods described in Chapter 2 have been described in above mentioned research papers.

Table of Contents

List of Tables

List of Figures

List of Abbreviations

AF1: Activation function 1

AF2: Activation function 2

AR: Androgen receptor

AI: Aromatase inhibitors

BCa: Breast cancer

BLI: BioLayer Interferometry

DBD: DNA-binding domains

E2: Estradiol

EBS: E2-binding site

ER: Estrogen receptor

ERE: Estrogen response elements

FSH: Follicle-stimulating hormone

GR: Glucocorticoid receptor

GnRH: Gonadotropin-releasing hormone

LBD: Ligand-binding domains

LH: Luteinizing hormone

MARCoNI: Microarray assay for real time co-regulator nuclear receptor interaction

MD: Molecular dynamics

NTD: N-terminal domains

OHT: 4-HydroxyTamoxifen

PR: Progesterone receptor

TamR: Tamoxifen-resistant cells

TR-FRET: Time-resolved fluorescence resonance energy transfer

WT: Wild type

Acknowledgements

Chapter 1: Introduction

1.1   Breast cancer

Breast cancer (BCa) is one of the most challenging oncologic problems and the second leading cause of cancer-related death in women worldwide. In 2016, BCa continues to be the most common (up to 25%) cancers in Canadian women. It has been estimated that on an average 5,000 Canadians (14% of all cancer related death cases) will die from it every year.[1]

BCa originates from the epithelial cells of the mammary gland. The ducts are lined with luminal epithelial cells , which give rise to the majority of BCa cases.[2] It is a complex disease with various risk factors associated to age, race, lifestyle patterns, genetic and nutritional factors.[3]

The steroid hormone, Estradiol (E2), plays an important role in the progression of BCa, and a majority of the human breast cancers start out as estrogen-dependent and express the estrogen receptor (ER). The biological effects of estrogen are mediated by its binding to one of the structurally and functionally distinct forms of ER, α and β.[4] ERα is the major ER subtype present in the mammary epithelium and plays a critical role in mammary gland biology as well as in BCa progression.[5] It has been reported that ERα+ disease constitutes approximately 75% of all BCa cases[6] and its treatment with anti-estrogens such as Tamoxifen has been the main therapeutic avenue for more than 30 years. This approach targets hormone-dependent BCa with an aim to block binding of E2 to the ERα. While treatment with Tamoxifen can initially suppress BCa growth, it becomes ineffective upon long term therapy.[7] One third of women treated with Tamoxifen for 5 years develop recurrent disease within 15 years.[8] It has been shown that the growth of Tamoxifen-resistant cells (TamR) is highly dependent on ERα. In addition, biopsies

from BCa patients who relapsed on Tamoxifen indicated that the ERα expression was still retained in more than 50% of cases.[9] Importantly, 70% of ERα+ primary tumors also retain the ERα when they metastasize.[10] These findings confirm the ERα as the major validated target in ERα-positive Tamoxifen resistant and metastatic BCa.

1.2 Subtypes of breast cancer

Table 1.1. Molecular subtype signatures of BCa.

Category	Signature genes	Signaling Pathways	Clinical grade	Therapeutic options	5-year survival (%)
Luminal A	ER+ and/or PR+, HER2-,CK8/18+; GATA 3, XBP 1, FOXA1 and ADH1B gene overexpression	Estradiol response	I	Tamoxifen and Arimidex	95
Luminal B	ER+ and/or PR+,HER2+, CK8/18+, FGFR1, HER1,Ki-67 and/or cyclin E1, CCNB1 and MYBL2 overexpression	IGF-1,FGF, PI3K	II (III also observed)	Bevacizumab combined with Paclitaxel, Tamoxifen combined with agents against IGF‑1R, FGFR, PI3K and EGFR/HER2	50
ErbB2/HER2+	ER‑ and/or PR‑,HER2+ and GRB7 overexpression	IGF-1, HER2	More likely III	Herceptin, Lapatinib. For patients with resistance to Herceptin, combined with a PI3K/mTOR inhibitor	30

Category	Signature genes	Signaling Pathways	Clinical grade	Therapeutic options	5-year survival (%)
Basal-like	Marker genes: ER‑ and/or PR‑, HER2‑ ,CK5/6+, CK14+, CK17+, EGFR+, HER1 and/or c‑Kit, FOXC1, p63,P‑cadherin, vimentin and laminin overexpression	IGF-1, Wntβ-catenin	More likely III	Chemotherapy; anti-angiogenic agents, platinum salts and PARP inhibitors	30

ER, estrogen receptor; PR, progesterone receptor; HER2, human epidermal growth factor receptor 2; GATA‑3, GATA binding protein 3; XBP‑1, X‑box binding protein 1; FOXA1, fork head box A1; FGFR1, fibroblast growth factor receptor 1; MYBL2, myeloblastosis oncogene-like 2; CK, cytokeratin; ADH, alcohol dehydrogenase; GRB, growth factor receptor-bound protein; IGF, insulin-like growth factor; PI3K, phosphatidylinositol-3-kinase; mTOR, mammalian target of rapamycin; PARP, poly ADP ribose polymerase.

1.3 Estrogens

Estrogens are a group of steroid compounds which function as the primary female sex hormones. Estrogens are mainly produced by the ovaries and adrenal cortex and display a wide range of physiological functions ranging from regulation of the menstrual cycle to modulating brain function and bone density.[11, 12] Although, the predominant form of estrogen is E2, lower levels of E2 metabolites, Estrone and Estriol are also present in humans (Figure 1.1). It has been reported that E2 controls many aspects of human physiology, including development,

reproduction and homeostasis, through regulation of the transcriptional activity of its cognate receptors.[13]

Synthesis of estrogen is regulated by the hypothalamic-pituitary-ovarian axis and begins by anterior pituitary release of luteinizing hormone (LH) and follicle-stimulating hormone (FSH) in response to the hypothalamic peptide gonadotropin-releasing hormone (GnRH). Further, LH stimulates androgen (male sex hormones: androstenedione and testosterone) production, whereas FSH upregulates aromatase, which catalyzes the rate-limiting and final step of estrogen biosynthesis *i.e.* the aromatization of androgen to estrogen (Figure 1.1). During ovulation, E2 production increases up to ten fold. Higher levels of estrogen in turn act via negative feedback to regulate estrogen production to inhibit the release of GnRH, LH, and FSH.[14]

In premenopausal women, the hypothalamic-pituitary-ovarian axis is functional, with estrogen levels changing dramatically throughout the menstrual cycle. However, ovarian estrogen biosynthesis is minimal in postmenopausal women and circulating estrogen is derived mainly from aromatization of adrenal androgen. Hence, adipose tissue becomes the main source of estrogen production in obese postmenopausal women.[15] As a result, pre- and post-menopausal groups respond differently to aromatase inhibitors (AIs), a category of anti-estrogen therapy used to treat BCa. AIs are much more efficacious in post-menopausal women, whose hypothalamic-pituitary-ovarian axis is no longer active.
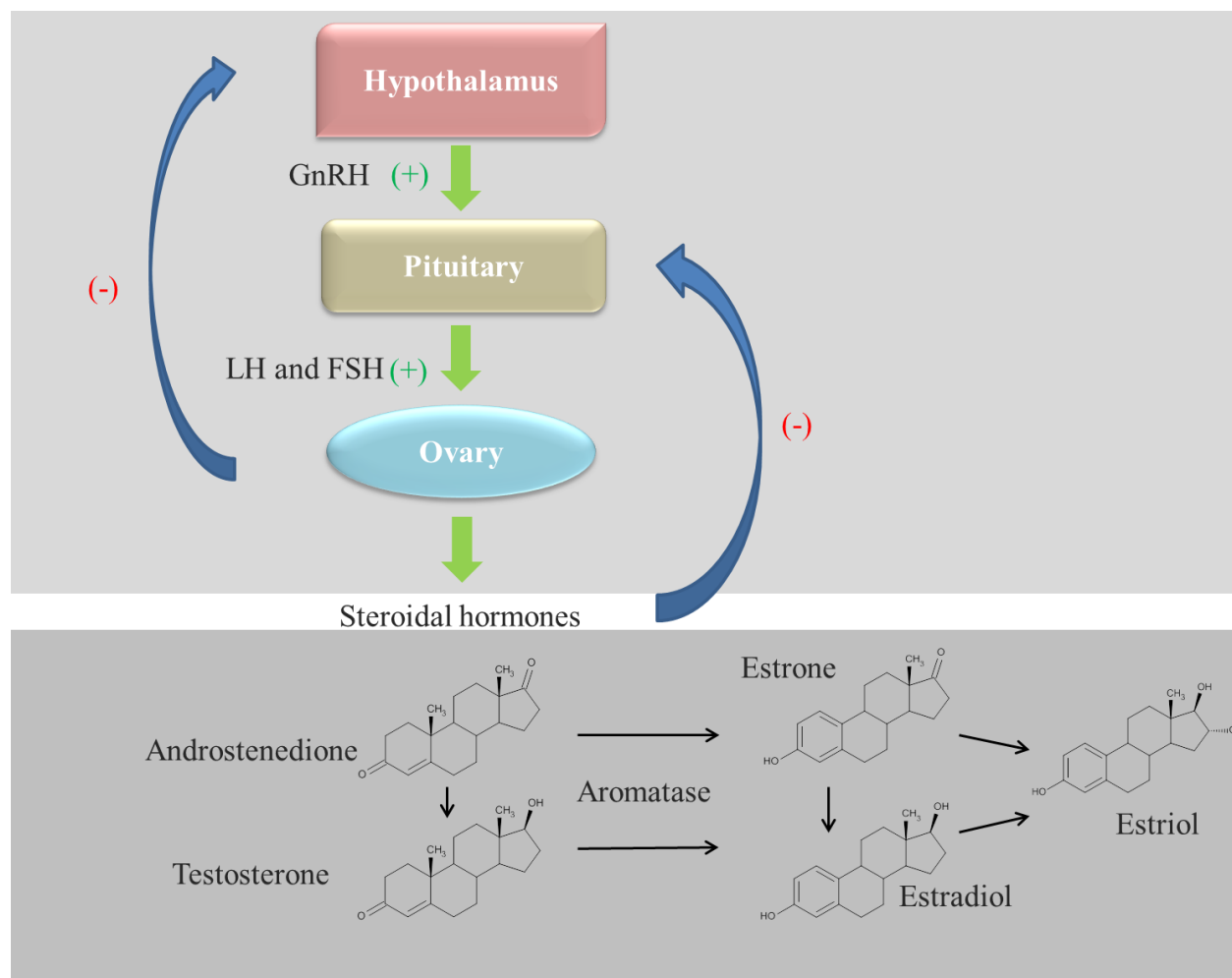
Figure 1.1. Hypothalamic-pituitary-ovarian axis and chemical synthesis of estrogens.

1.4 Estrogen receptor

Estrogen mediates its biological effects in target tissues primarily by binding to specific intracellular receptors, ERα and ERβ (NR3A1 and NR3A2, respectively). They are the products of separate genes, *ESR1* and *ESR2* present on chromosomes 6 and 14 respectively. ERα and ERβ are widely expressed in many tissues, such as the uterus, ovary, mammary gland, prostate, lung, and brain. The expression levels and subtypes of ER are primary factors that determine tissue-specific estrogen responsiveness.[4, 16] Both ERα and ERβ are members of the nuclear hormone

receptor superfamily that contain modular structures and discrete functional domains. ERα and ERβ are highly homologous (~96%) in their DNA-binding domains (DBDs) and possess moderate (53%) sequence identity in their ligand-binding domains (LBDs). The major functional difference between ERα and ERβ appears to be determined by the hormone-independent transcriptional activation function (AF1) domains in their respective N-terminal region.[17] The pro-oncogenic effect of estrogen is mediated primarily by ERα activation of target genes that promote cell proliferation or decrease apoptosis. Genetic and pharmacological lesions directed against either ERα or ERβ show that these two receptors exert opposing effects on cell proliferation and apoptosis.[18, 19]

ER functions as a ligand activated transcription factor to regulate the expression of multiple target genes (Figure 1.2). Prior to estrogen binding, ERs are complexed with heat-shock Hsp90 and Hsp70 by multi-protein chaperone machinery formed specifically with the ligand binding domain.[20-22] The Hsp90/70-based chaperone machinery interacts with the unliganded ER to open the steroid-binding cleft to be accessed by a steroid. Moreover, this protein complex interacts in a dynamic fashion with a liganded, transformed receptor to facilitate its translocation along microtubular highways to the nucleus.[23] The binding of E2 to ER induces conformational changes in the protein that allow consequent dimerization of ER and facilitates its interaction with several co-activators. The ligand-bound ER dimers bind to specific DNA sequences termed estrogen response elements (EREs) and regulate transcription through interaction with transcription modulators and recruitment of the general transcription machinery (Figure 1.2).[24] The assembly and disassembly of the ER complex are extremely dynamic, and variation in gene expression among tissues under different conditions can greatly affect the final composition of the ER complex. ERs are subjected to a variety of post-translational modifications, which further

influence the stability, subcellular localization, transcriptional activity, and hormone sensitivity of the ER-nucleated transcriptional apparatus. Approximately 22 sites throughout ERα are subjected to various post-translational modifications[25] including phosphorylation, methylation, acetylation, SUMOylation, and ubiquitination.
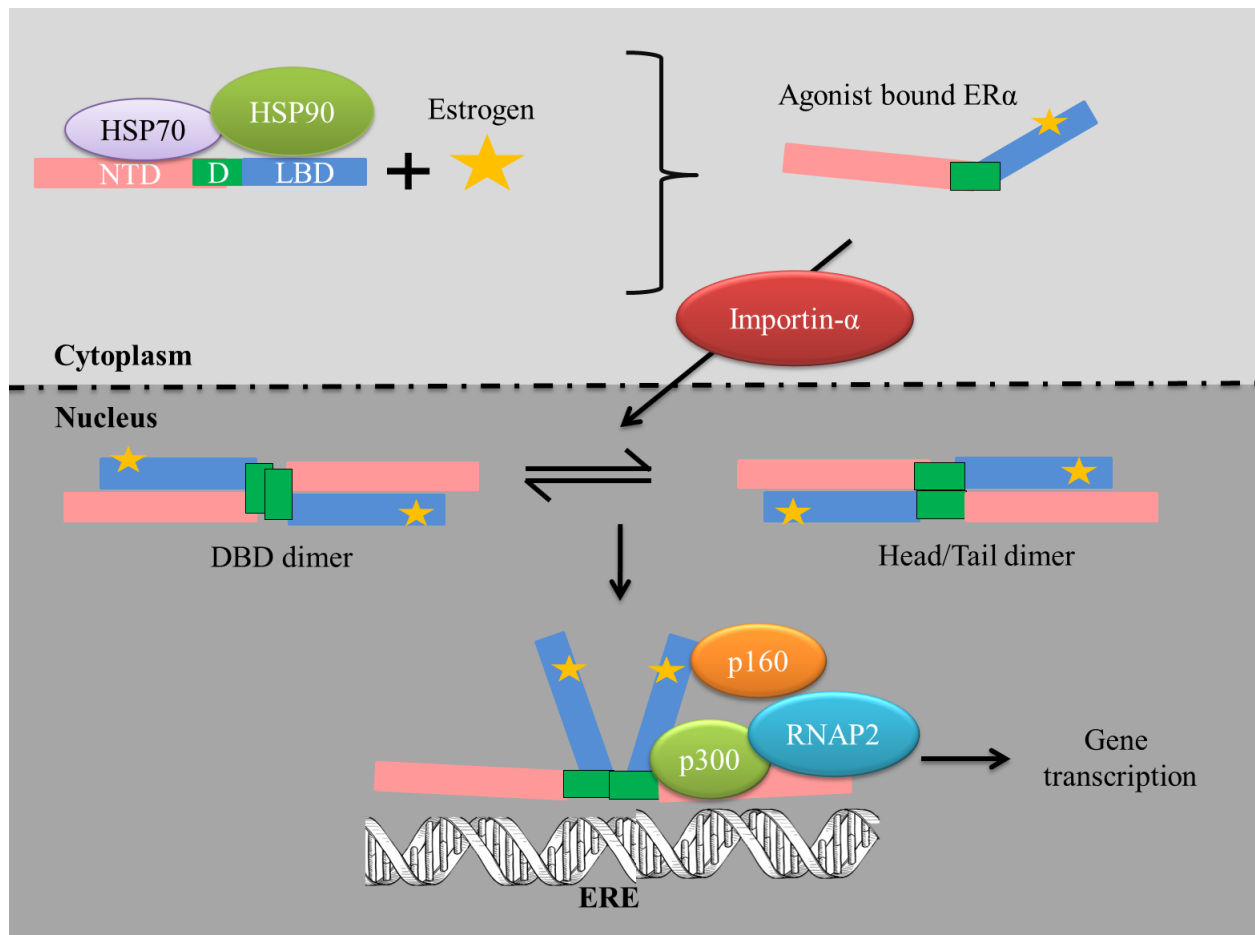
Figure 1.2. The signaling pathway of estrogen receptor. The ER domains are labeled as NTD - N-terminal domain, D - DNA binding domain, LBD - ligand binding domain.

1.5   Structural and functional aspects of ERα

ERα is a 66 KDa protein containing 595 amino acids. Even though steroidal nuclear receptors are implicated in different physiological processes, they all share the same modular structure and domain organization.[26] These regions participate in the formation of independent but interacting functional domains. The N-terminal domain (NTD or A/B region; encoded by exon 1) is involved in both inter-molecular and intra-molecular interactions as well as in the activation of gene transcription. The DNA binding domain (DBD or C region, encoded by exons 2, 3 and 4) allows ERα to dimerize and to bind to the specific ERE sequence on DNA through its two "zinc finger" structures. The hinge domain (D region, encoded by exon 4) has a role in receptor dimerization and in binding to chaperone heat-shock proteins. The ligand binding domain (LBD or E/F region, encoded by exon 5 to 8) comprises the estrogen binding site (EBS) and works, synergistically with the NTD in the regulation of gene transcription. Two activation function domains, AF1 and AF2, located within the NTD and LBD, respectively, are responsible for regulating the transcriptional activity of ERα (Figure 1.3A). To date, three-dimensional structure for the NTD is unavailable not only for the ERα but for the entire nuclear hormone receptor superfamily.

1.5.1   The N-terminal domain

Like other nuclear hormone receptors, the NTD of ERα possesses an intrinsically disordered conformation.[27-29] However, it has been reported that the disordered behavior of the ERα NTD plays a pivotal role in promoting molecular recognition by providing surfaces to be able to recruit specific binding partners.[30, 31] In 2001, Warnmark *et al* confirmed the flexible nature of the ERα NTD by circular dichroism method.[27] A secondary structural analysis of ERα

8

conducted by Combet *et al* using network protein sequence analysis revealed that ~67% of ERα NTD contains random coil conformation.[32] They hypothesized that the intrinsically disordered nature of NTD allows it to rapidly sample its environment until appropriate concentration and affinity of the binding partners are found, meaning that they may not be structured until they have recruited and bound their proper interaction partners. Therefore, NTD is a unique functional domain involved in protein–protein interactions[33-35] and in transcriptional activation of ERα specific target-gene expression.[33, 36, 37] The NTD of ER is solvent-exposed and contains the AF1 region and several phosphorylation and SUMOylation sites.[28, 38]

Several coregulatory proteins participate in ER target gene transcription. For example, Warnmark *et al* studied the role of TATA box-binding protein and reported that it has a central role in the basal transcription machinery of ERα. Surprisingly, TATA box-binding protein directly binds to the NTD of the ERα but fails to bind to ERβ NTD to potentiate ER-activated transcription. [27] This could be pertaining to the difference in both length and amino acid identity of ER isoforms.

Several research groups also studied the E2-independent transactivation mechanism of ERα NTD. It has been shown that when the AF1 domain is combined with the DBD, it can constitutively activate transcription of ERα.[28, 36, 38] However, it must be emphasized that full transcriptional activation by ERα requires functional synergy between AF1 domain and AF2 region, a co-activator recruitment site located on ERα LBD. Several lines of evidence suggested that AF1 shares features with the AF2 co-activator complex. To begin with, AF1 can mask weak mutations in AF2, suggesting that AF1 can compensate for reduced co-activator recruitment.[39] Further, AF1 and AF2 squelch each other's activity, suggesting that they compete for common limiting target molecules.[40] Finally, it has been demonstrated that the transcriptional activity of

isolated AF1 can be enhanced by introducing the free ER-LBD into the same cells.[41] Despite all this evidence, the reasons why AF1 synergizes with AF2 in some contexts, yet works independently in others, are unknown and yet to be explored.

1.5.2   The DNA-binding domain

The DBD plays a pivotal role in receptor dimerization and the binding of ERα to its ERE composed of a palindromic hexanucleotide ^{5}AGGTCAnnnTGACCT^3.[42, 43] The ERE sequences not only dictate the binding affinity of the ERα, but have also been shown to modulate the recruitment of co-activators.[44, 45]   Three-dimensional structure of the ERα has been solved using nuclear magnetic resonance as well as X-ray crystallographic techniques both alone and in complex with DNA.[46-48] The DBD-ERE interactions and ERE-facilitated dimerization are in part mediated through the P box and D box sequences in the Zinc finger domains (Figure 1.3B).

The DBD is folded into a globular shape, containing two α-helices perpendicular to one another, forming the base of the hydrophobic core. The ERα contains eight conserved Cys residues found in two groups of four. Each group is involved in the tetrahedral co-ordination of a single zinc atom. While P box actively interacts with the ERE nucleotides, the D box is present at the dimerization interface.[49, 50] Transcriptional regulation at the ERE can be mediated via two separate mechanisms of ER action: 1. Ligand bound ER can directly associate with specific response element sequences 2. ER may participate in a multiprotein, preinitiation complex and regulate gene transcription without a direct interaction with any DNA sequence.[51, 52] Together, these mechanisms highlight the complex role of co-activators and response elements in eliciting specificity in transcriptional output.

A)

B)
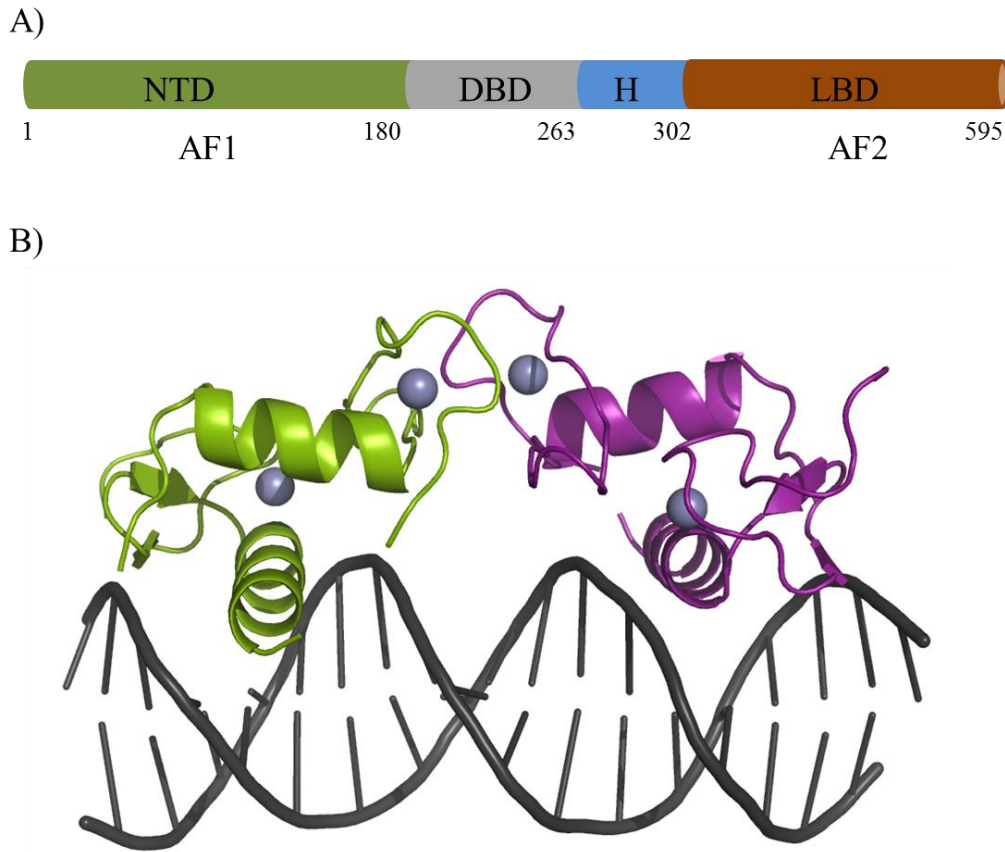
Figure 1.3. Structural details of ER*α* (A) Domain organization of the ER*α*. (B) Cartoon representations of the rat ER*α* monomer-DBD structure. Zinc ions are presented as spheres and the D-box is highlighted in green. The P-box is shown in purple color.

1.5.3   The hinge region

The D domain which follows DBD is known as a hinge region. Hinge region contains several sites for post-translational modifications and nuclear localization signal which gets unmasked upon ligand binding and serves as a flexible region connecting DBD and LBD.[53, 54] The hinge domain has a role in receptor dimerization and in binding to chaperone heat-shock proteins.[55]

1.5.4   The ligand-binding domain

Like other nuclear receptors, LBD (or E/F regions) consists of 12 helices. LBD recruits estrogens, preferably E2, which mediates further events including co-activator binding to AF2 receptor dimerization, nuclear translocation, and transactivation of target gene expression.[56] In an agonist bound form, ERα is spatially organized in a three-layered structure with helices 4, 5, 6, 8, and 9 lining up on one side by H1 and H3, and on the other side are helices 7, 10,and 11.[57] The first crystal structure of ERα LBD bound to its natural ligand E2 showed that E2 is buried in a highly hydrophobic environment.[57]

It has been observed that when LBD is complexed with the agonists such as E2 or diethylstilbestrol at EBS, H12 adopts a conformation in which it forms one side of a charge clamp that grips the ends of a short helix of signature motif (LxxLL/FxxLF) termed the NR box present in co-activator proteins that interact directly with the LBD (Figure 1.4A).[58-60] This surface exposed site is termed AF2 (shown in cyan color in figure 1.4A). Crystallographic information on ERα LBDs revealed that the AF2 surface consists of a cluster of residues from helices 3, 5, and 12 that form a hydrophobic patch on the surface of the E2 bound LBD. This hydrophobic patch recruits a panel of proteins called the p160s, which include GRIP1/TIF2,[61] SRC-1,[62] and RAC3/p/CIP/ACTR/AIB1.[63]

Elucidation of the three dimensional structure of LBD in complex with Raloxifene [57, 64]and 4-OH-Tamoxifen complex[59] has revealed that selective modulation of ER transcriptional activity can be achieved by altering the conformation of H12 *i.e.* formation of the AF2 site (Figure 1.4B). A well-known example is Tamoxifen preventing AF2 from adopting a charge-clamp conformation, thereby blocking AF2-dependent transcriptional activity (Figure 1.4B). It is evident that different ligands can induce different receptor conformations[65, 66] and that the

12

positioning of H12 is a key event that permits discrimination between estrogen agonists and antagonists.
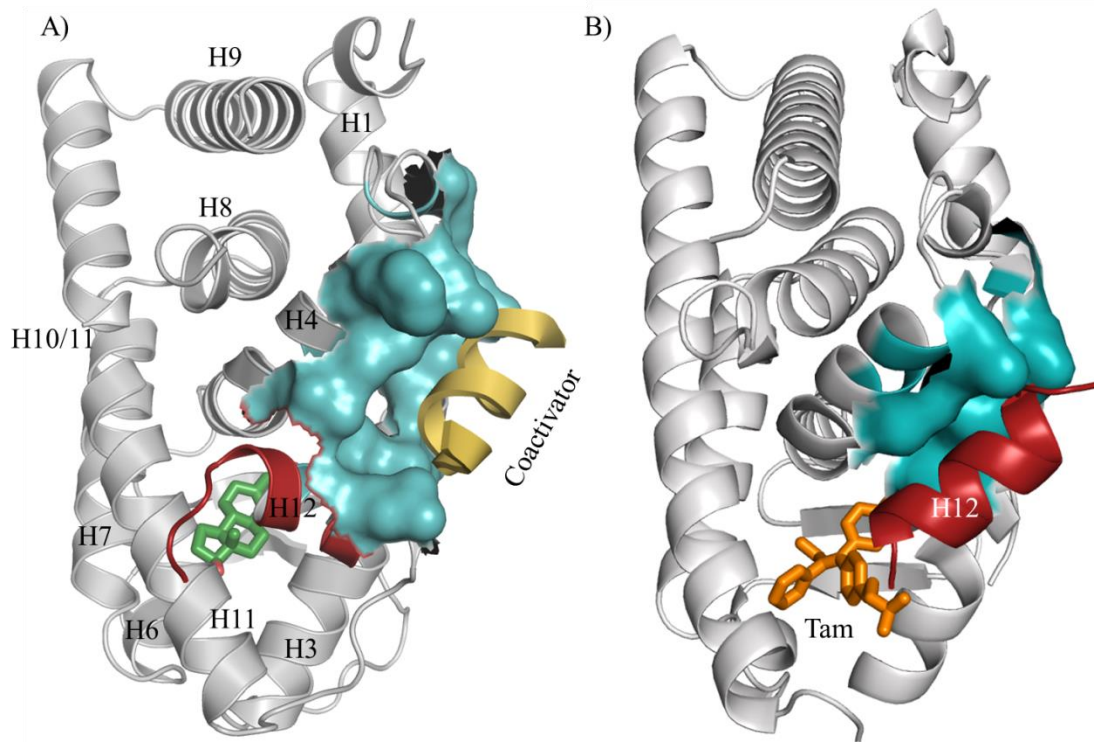
Figure 1.4. Agonist and antagonist models of ERα. (A) Binding of E2 (shown in green color) causes the movement of alpha helix-12 (shown in red color) such that it opens up the AF2 pocket (shown in cyan color). In this scenario, AF2 inhibitor directly prevents interaction between co-activators (shown in yellow color) and the receptor. (B) Binding of Tamoxifen (shown in orange color) to ERα leads to an antagonist conformation causing repositioning of alpha helix-12 (show in red color) such that it prevents AF2 formation and co-activator recruitment.

The AF2 pocket is a surface exposed hydrophobic groove that plays an important role in activation and functioning of the ERα. As shown in figure 1.5 it is flanked with regions of

positive and negative charges, "charge clamps", that are essential for binding ERα activation factors. AF2 is a highly conserved protein-protein interaction site and has also been extensively analyzed throughout this nuclear receptor family. It recruits a variety of co-activators and mediates diverse functions of the ERα. Recent findings suggest that ERα co-activators are differentially expressed in malignant tumors and their functions may be altered, leading to tumor progression. For example, co-activators such as SRC-3 have been shown to be amplified in breast cancer.[67] Hao *et al* suggested that AF2 can also directly recruit p300 co-activator, independently from E2 via Notch-1 signaling pathway which activates the ERα in BCa.[68] In addition, PELP1 factor that binds to AF2 site plays a pivotal role in ERα+ metastasis.[69] Collectively, these emerging findings implicate the role of AF2 mediated functions in BCa. **Hence, targeting AF2 site offers an alternative strategy to create new therapeutics for ERα in breast cancers.**
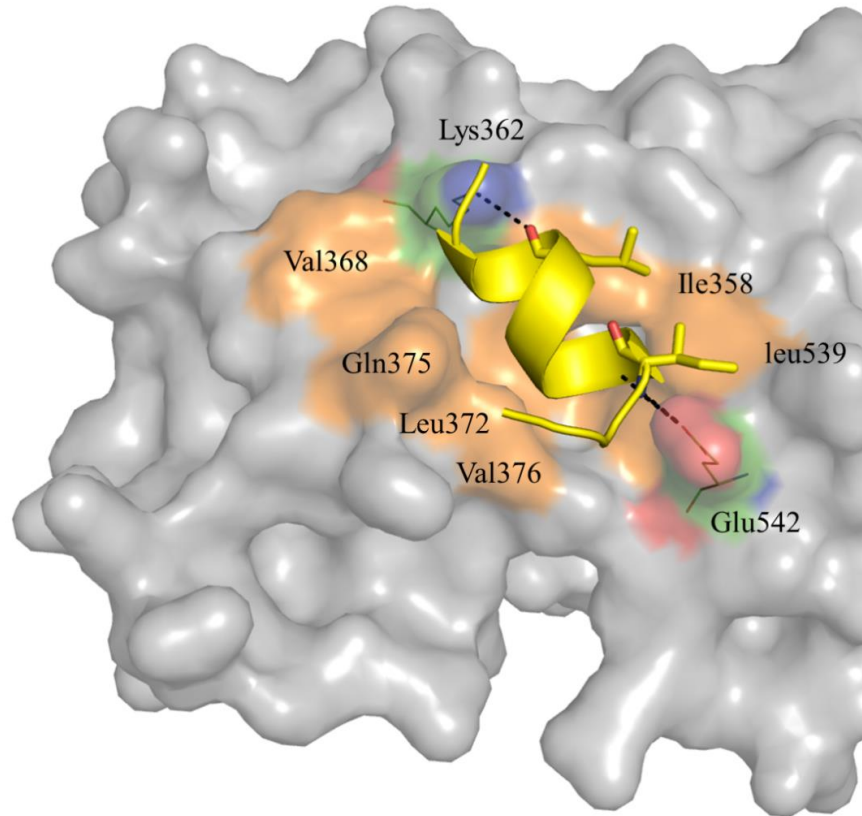
Figure 1.5. Graphical representation of the AF2 site. Charge clamp residues, Lys362 and Glu542, which stabilize the interaction with LxxLL motif, are highlighted in atomic color. SRC peptide is shown in yellow color. Hydrogen bonds formed between co-activator and charged residues are shown as black dotted lines. Hydrophobic residues are in brown.

1.6   ERα splice variants

Rapid progress in recent studies on genomic and cDNA sequences has accelerated the identification of ERα alternative splice variants in BCa[70, 71] and other tumors.[72-74] The ERα mRNA undergoes alternate splicing, generating transcripts containing single, double or multiple exon deletions resulting in 20 splice variants.[75] Out of them, ERα46, ERα36 and ERα80 variants

are explored in terms of their function and physiological significance and other forms are yet to be explored.

Splice variants ERα46 and ERα36 are most discussed as they are reported to oppose genomic actions of full length ERα66. In 2005, Penot *et al* identified the ERα46 isoform in the MCF7 breast cancer cell line.[76] This isoform is formed by skipping exon 1 encoding the NTD; hence, ERα46 is devoid of AF1 mediated activity. Unlike full length receptor, this truncated isoform does not mediate E2 dependent cell proliferation and high levels of this isoform have been shown to be associated with cell cycle arrest in the G0/G1 phase and a state of refraction to E2 stimulated growth, which is normally reached at hyper confluency of the cells.[76] The presence of ERα46 has also been confirmed in osteoblasts[77] and endothelial cells.[74]

The second truncated ERα isoform ERα36 was first described by Wang et al in 2005.[73] Unlike ERα46, ERα36 lacks both the AF1 and AF2 domains. However it has functional DBD, partial dimerization and LBD domains. With no functional activation domains ERα36does not have any direct transcriptional activity. ZhaoYi Wang and co-workers reported that ERα36 acts as a robust inhibitor of full length ERα dependent transactivation and it is mainly localized in the plasma membrane and works in a different way to full length protein.[78] Furthermore, ERα36 can activate non genomic ER pathways such as MAPK/ERK signaling in response to E2 which is of particular significance in response to anti-estrogens such as Tamoxifen.[78]

The ERα80 isoform was detected in the MCF7:2A cell line, which is a subclone of the MCF7 cell line derived from long term growth in the absence of E2. This ERα80 isoform was produced by duplication of exons 6 and 7.[79] No evident function has been described so far.

Apart from the above discussed isoforms, several other variants (ERαΔE2, ERαΔE3, ERαΔE4, ERαΔE5, ERαΔE6, ERαEΔ5,7, ERαEΔ7…) as a result of exon splicing deletions have been confirmed in human[75, 80] showing a dominant inhibitory effect in normal ER function.

1.7   Current advances in the development of ER inhibitors

1.7.1   Selective estrogen receptor modulators (SERMs)

SERMs are a category of therapeutic agents used for the prevention and treatment of diseases such as osteoporosis and BCa. Unlike pure agonists and antagonists, SERMs display a unique tissue-selective pharmacology *i.e.* they are agonists in some tissues (bone, liver, and the cardiovascular system), antagonists in other tissues (brain and breast), and mixed agonists/antagonists in the uterus. Among several SERMs that are currently being clinically used and newly developed, Tamoxifen (Nolvadex), Raloxifene (Evista) and Toremifene (Fareston) are well-known for their therapeutic advantages (Figure 1.6).

Tamoxifen is the first clinically relevant and the most widely used SERM.[81] It acts as an antagonist in the breast, therefore, it is often used as endocrine therapy for post-menopausal women with early-stage ER+ BCa. There is also evidence that Tamoxifen preserves bone density in postmenopausal patients.[82] However, it has been reported that prolonged treatment increases the risk for endometrial cancer.[83, 84] Thus, Tamoxifen behaves as an ER antagonist in the mammary gland and as an agonist in the uterus and bone.

Raloxifene is a benzothiophene SERM that acts as ER antagonist in breast and an agonist in bone. However, unlike Tamoxifen, it does not exert ER agonist properties in the uterus.[83, 84]Toremifene, a triphenylethylene derivative, is a relatively new anti-estrogen SERM with properties and side effects similar to Tamoxifen's.[85] Unlike Tamoxifen, it does not increase the

risk of endometrial cancer and the 4-hydroxy, N-desmethyl metabolite of this drug has not been shown to form detectable DNA adducts *in vitro*. However, the use of Toremifene in post-menopausal women with metastatic BCa has been restricted by the FDA.

1.7.2   Selective ER down-regulators (SERDs)

SERDs are a class of chemicals that induce a conformational shift of the receptor, resulting in ubiquitination and subsequent degradation of ERα, via the ubiquitin-proteasome system.[86, 87]Due to the unique and dual-function of SERDs *i.e.* ER antagonism and depletion, these compounds are used as endocrine agents upon failure of Tamoxifen or aromatase inhibitors in BCa patients. Fulvestrant is considered to be a first-in-class SERD (Figure 1.6).[88] Unfortunately, Fulvestrant has significant pharmaceutical liabilities (requiring intramuscular injection) that have negatively impacted its application.[89]GDC-0810[90] and AZD9694 are the second generation of degraders (Figure 1.6) developed having advantages associated with the SERD approach, while overcoming the limitations associated with Fulvestrant. These are non-steroidal, orally bioavailable dual function ER antagonists and down-regulators that induce potent, rapid proteasome-mediated ERα degradation in breast cancer cells. Currently they are in clinical trials.
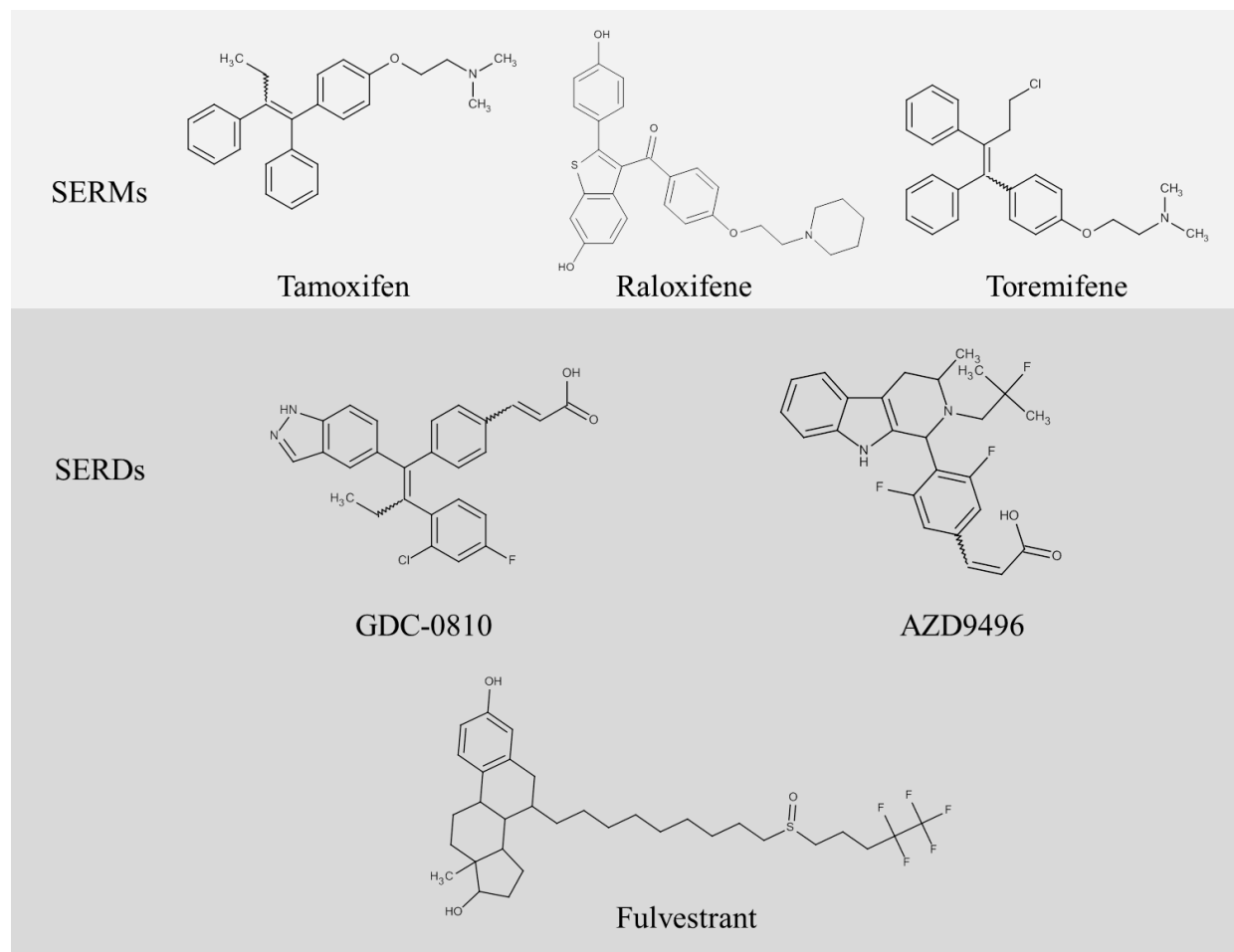
Figure 1.6. Chemical structures of clinically used and experimental selective ER modulators and down-regulators.

1.7.3 DNA-binding domain inhibitors

The DBD represents an alternative promising target to develop ER inhibitors. However, drug discovery at the DBD is very challenging since it is the most highly conserved domain in nuclear receptor family. Despite this several attempts have been made to develop inhibitors targeting ER DBD. XR5944, a topoisomerase inhibitor, was shown to inhibit ER binding to DNA. Punchihewa *et al* demonstrated that XR5944 inhibited ER transcriptional activity by binding to the DNA major groove and disrupting ER-ERE interactions.[91]

19

Electrophilic compounds such as disulfide benzamide (DIBA; Figure 1.7), and benzisothiazolone derivatives (BITA) were shown to inhibit proliferation of ER+ BCa cell lines with IC_{50} values around 25 μm. These compounds decreased binding of purified ERα to an ERE.[92, 93] A high-throughput screen using fluorescence anisotropy microplates identified theophylline, 8-[(benzylthio) methyl]-(7Cl, 8Cl) (TPBM).[94] Although TPBM disrupts estradiol-ERα complex binding to ERE, the actual binding site of TPBM on ER remains to be clarified.

1.7.4   Co-activator binding inhibitors

In 2004, Rodriguez and co-workers proposed an alternative strategy to target ERα using small-molecules.[95] They demonstrated that chemicals bearing pyrimidine moieties block the interaction of purified E2-activated ERα with a labeled SRC1 Box II peptide in a fluorescence polarization assay. In order to improve potency, Parent *et al* conducted structure-activity relationship studies around the pyrimidine core.[96] They reported molecules with the best exhibiting K_i values of 2–3 μM in a time-resolved fluorescence resonance energy transfer (TR-FRET) assay. Moreover, these values correlated with IC_{50} values measured against ERα-mediated transcription in HEC-1 cells co-transfected with an ERα plasmid and a luciferase reporter gene. Based on the pyrimidine de novo design, amphipathic benzenes were developed and these molecules show better solubility compared to pyrimidines due to their amphipathic nature.[97]

Researchers from Wyeth Pharmaceuticals performed a study that combined high-throughput mammalian two hybrid assays with virtual screening to identify novel co-activator binding inhibitors.[98] They reported guanylhydrazone compound ERI-05 (IC_{50} = 5.5 μM) that blocks the interactions of Gal4 DBD/hERα LBD fusion and SRC-1, SRC-3 or SRC-3/VP16

fusion in a mammalian two-hybrid assay performed in COS7 cells. Although ERI-05 reduced the expression of the ERα-regulated gene pS2 in MCF-7 cell line at 20 μM, it turned out to be toxic at higher concentrations. Subsequently, LaFrate *et al* made a library of these compounds, with some showing improved potency over ERI-05.[99] Since these compounds react covalently with nucleophilic residues in ERα, they could not be explored further. Additionally, peptide inhibitors (designed based on LxxLL motif) were reported to inhibit the interaction of ER with co-activators.[100-103] However, their application is limited by poor permeability and lack of specificity.
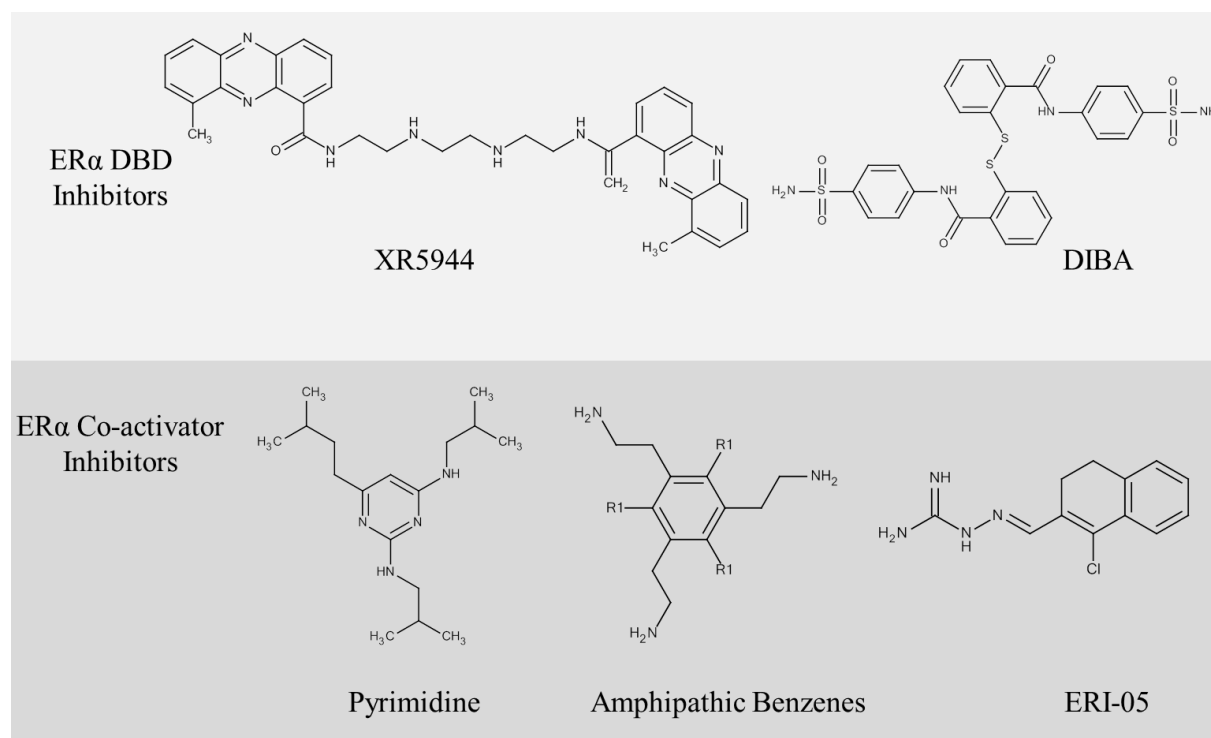
Figure 1.7. Chemical structures of compounds reported as ER DBD inhibitors and co-activator inhibitors in the literature.

1.8 Limitations of commercial anti-estrogens

It is a well-known fact that patients with ER+ BCa initially respond to therapeutic agents such as Tamoxifen or fulvestrant, but remissions are often followed by the acquisition of resistance and, ultimately, disease relapse. Several mechanisms of resistance to these anti-ER drugs have been studied and include the following: pharmacologic mechanisms, loss or modification in estrogen receptor expression, alterations in co-regulatory proteins and the regulation of the different signaling pathways that participate in different cellular processes such as survival, proliferation, stress, cell cycle, inhibition of apoptosis regulated by the Bcl-2 family, autophagy, altered expression of microRNA, and signaling pathways that regulate the epithelial-mesenchymal transition in the tumor microenvironment. Some proposed mechanisms are discussed below.

1.8.1 Loss or modification in ER expression

Since therapeutic effects of Tamoxifen are derived from its ability to mediate ER signaling as an ER antagonist, loss of its target, ER is attributed to resistance to therapy. It has been reported that 17–28% of patients with acquired resistance to Tamoxifen lose the expression of ERα.[104] Using T47D or ZR-75-1 cell lines Van den Berg et al[105] and Graham et al[106] demonstrated that loss of ER expression can occur due to transcriptional repression of the ER gene and population remodeling leading to overpopulation of ER-negative cells from seemingly heterogeneous ER-positive tumors. Further studies investigated epigenetic changes such as aberrant CpG island methylation of the ER promoter and histone deacetylation, resulting in a compact nucleosome structure that limits transcription.[107-109]

1.8.2   Alterations in co-regulatory proteins

The transcriptional regulatory activity of ER is mainly mediated by the formation of complexes with co-activator or co-repressor proteins. In general, co-activators bind to ER upon agonist binding, enhancing transcriptional activity. Conversely, recruitment of antagonists results in association of ER-corepressors complex. It has been demonstrated *in vitro* that co-activator proteins AIB1, PGC-1β and SRC1 enhance the agonistic activity of Tamoxifen.[35, 110] In patients receiving adjuvant Tamoxifen therapy, high levels of AIB1 alone or in combination with high levels of ERBB2/HER2 are associated with shorter disease-free survival in patients.[111] Further, Hao *et al* developed a model in which Notch-1 can activate the transcription of ERα-target genes via IKKα-dependent cooperative chromatin recruitment of Notch–CSL–MAML1 transcriptional complexes and ERα, which promotes the recruitment of p300. The authors suggested that Notch-1/ERα chromatin crosstalk mediates Notch signaling effects in ERα+ BCa cells and contributes to regulate the transcriptional functions of ERα itself.[68] A study using tissue microarrays and immunohistochemistry on a population of 1,162 BCa patients confirmed that increased PELP1 expression is associated with tumours of larger size and higher histological grade. It was confirmed that PELP1, a co-activator protein that binds to AF2 site, plays a pivotal role in ERα+ metastasis.[69]

1.8.3   Growth factor receptor signaling pathways

ER may initiate rapid cellular signaling via direct interaction with components of growth factor signaling pathways. Several studies have reported that overexpression of EGFR or erbB-2/HER2 in ER-positive, anti-estrogen-sensitive breast cancer confers resistance to Tamoxifen.[112, 113] It has been found that EGFR and HER2 not only reduce response to Tamoxifen but also

stimulate the growth of tumors.[114, 115] Shou *et al* demonstrated that Gefitinib (an inhibitor of erb-2/HER2) improved the antitumor effect of Tamoxifen and delayed the acquisition of resistance, Moreover, increased levels of phosphorylated p42/44 and p38 MAPK (both downstream of EGFR/HER2) were observed upon treatment with Gefitinib.[114]

Studies have found that overexpression of FGF-1R, or loss of the inositol polyphosphate phosphatase 4B (INPP4B), activate the PI3K pathway and also confer anti-estrogen resistance in patients with ERα+ BCa.[116, 117] PI3K is commonly activated in BCa cells by growth factor receptor tyrosine kinases or G-protein-coupled receptors. The signaling cascades triggered by PI3K, including PDK1, AKT and SGK among others, promote cell growth and survival.[117] Cyclin D1 is known to interact with ERα and can potentiate its transcriptional activity independently of estrogen and may not be inhibited by Tamoxifen.[118] Overexpression of cyclin D1 has been reported to result in a conformational change in ERα that induces receptor activation in the presence of Tamoxifen, which in turn promotes growth of MCF7 cells-indicating a change from antagonist to agonist.[119] Patients with cyclin D1 negative tumors show better relapse-free survival when they are treated with Tamoxifen,[120] whereas multiple clinical studies have demonstrated that overexpression of cyclin D1 is correlated with poor outcome on Tamoxifen treatment.[120, 121]

1.8.4   Pharmacological and metabolic aspects of anti-estrogen resistance

Decrease in intracellular concentrations of a certain drug is a general mechanism of drug resistance as a result of increased efflux or decreased influx.[122] Indeed, significantly lower intra-tumoral Tamoxifen concentrations were found in breast tumor samples that had been known to develop acquired resistance to Tamoxifen compared to those with de novo resistance.[123] It is

likely that reduced uptake of Tamoxifen from extracellular sources and lower availability of intracellular Tamoxifen could confer resistance, resulting in a lack of the intracellular Tamoxifen to effectively compete with E2 for binding to ER. Although the precise mechanisms for lower intracellular Tamoxifen levels remain unclear, potential mechanisms include the presence of microsomal anti-estrogen binding site proteins[124] or increased Tamoxifen efflux via multi-drug resistance P-glycoprotein drug pump. It has also been reported that the affinity of Tamoxifen for AEBS is particularly high at the 1 nM level, which is significantly greater than its affinity for the ER.[125]

1.8.5   ER mutations

Although diverse mechanisms of resistance to endocrine therapy have been described, recent evidence has identified acquired mutations in *ESR1* gene, which confer ligand independent- and constitutive receptor activation as a potential mechanism of resistance to the existing ERα inhibitors. [126-128] These gene mutations were originally reported in a small cohort of metastatic BCa cases in 1997.[129] In recent years, several independent groups performed studies utilizing next-generation sequencing approach and reported that such mutations are present in ~20% of advanced, metastatic tumor samples previously treated with aromatase inhibitors.[126-128] Interestingly, these mutations occur rarely in primary BCa samples. The most frequently occurring *ESR1* mutations are in LBD of ERα, generally clustering between amino acids 534–538 (part of Helix 12, located adjacent to the AF2 site), though mutations at other positions including S463 and L380 have also been described. Biochemical studies demonstrated that the Y537S mutation is constitutively active and results in increased interactions with co-activators at AF2 site in E2-independent fashion.[130] Consistent with this observation, ERα-

Y537S promotes hormone-independent transcription and proliferation of tumor cell growth and reduces the efficacy of conventional anti-ERα drugs that target EBS. Subsequent reports demonstrated that other ERα LBD mutations similarly confer constitutive, ligand-independent activation.[127, 128, 131] Overall, this finding suggests that certain mutant ERα proteins offer significant growth advantage to the BCa cells. Currently prospective clinical trials are evaluating the effect of using higher-doses of SERMs in *ESR1* mutant BCa cases. But due to dual agonist/antagonist activity of SERMs, such an approach increases the risk of a second type of cancers such as endometrial cancer.

Since AF2 inhibitors reported in this study block co-activator recruitment directly at the AF2 pocket, it can be anticipated that they would be effective against mutant forms of ERα. One of the AF2 inhibitors described in this research has been evaluated against all mutant forms (discussed in detail in Chapter 4). We believe that such drug proto-types offer substantial therapeutic benefit even for patients expressing mutated forms of the receptor.

1.9   Objective and rationale of the study

Tamoxifen, an ERα EBS binder, is frequently used to prevent recurrence as well as a treatment for advanced, recurrent or metastatic forms of BCa. While treatment with Tamoxifen is usually very effective initially in controlling disease, its effectiveness is often temporary due to progression of tumour cells to a hormone-resistant state. In most cases of BCa, ERα expression persists and still directs hormonal signaling and growth, but the tumours no longer respond to conventional therapies. Hence, there is an urgent need to develop new types of therapeutics that exhibit entirely novel mode of ERα inhibition. For instance, rather than blocking E2 binding to

the ERα, such new drugs could target co-activator recruitment sites and block further protein-protein interactions.

A novel strategy is to explore the AF2 pocket as an alternative drug target that will help avoid resistance due to altered ER. AF2 is a protein-protein interaction site and is essential for ER transcriptional activity by recruiting co-activators proteins such as SRCs and PELP1. Thus, targeting the AF2 pocket provides potential to not only inhibit wild-type ERα, but also clinically relevant mutant forms of ERα that confer resistance to clinically used aromatase inhibitors and SERMs. The discovery of ERα AF2 inhibitors in this study involved the hit identification, lead optimization and preclinical evaluation. Although the developed lead AF2 inhibitor needs further optimization and preclinical assessment, it has already demonstrated all the desired activity profiles and may serve as a prospective therapeutic for advanced and hormone resistant BCa.

1.10 Thesis layout

Chapter 1 provides the background information on BCa, structure and function of ER, and drug resistance mechanisms. Chapter 2 presents materials and methods developed and applied in the current work. Chapter 3 and 4 summarize results of the research project aimed to develop novel ER AF2 inhibitors which have been published in a research article as indicated in the preface. Chapter 5 includes summary and future directions.

Chapter 2: Materials and Methods

2.1 Cell culture

T47D-KBluc, MDA-MB-453, MDA-MD-231 cell lines were obtained from ATCC, Manassas, VA, USA. MCF7 and HeLa cell lines were a gift from Dr. Sandra Dunn (Division of Hematology and Oncology, Department of Pediatrics, University of British Columbia, Vancouver, Canada). ZR-75-1 cell line was obtained from Dr. Marcel Bally (Department of Experimental therapeutics, BCCA-BCCRC). PC3 cells were obtained from Dr. Paul Rennie (Department of Urologic Sciences, University of British Columbia). Tamoxifen resistant cell lines, TamR3 and TamR6 were kindly provided by Dr. Euphemia Leung (University of Auckland, New Zealand). Cells were cultured at 37°C in humidified incubator with 5% CO2. The cell lines were maintained in the following culture media: MCF7 and ZR-75-1: phenol-red-free RPMI 1640 (Gibco, Life Technologies), supplemented with 10% fetal bovine serum (FBS) (Gibco, Life Technologies); T47D-KBluc: phenol red-free RPMI 1640 containing 4.5 g/liter glucose (Sigma-Aldrich), 10 mMHepes (Sigma-Aldrich), pH 7.5, 1 mM sodium pyruvate (Life Technologies), 0.2 U/ml insulin (Sigma-Aldrich) and 10% FBS; MDA-MB-453, MDA-MB-231, PC3 and Hela: dulbecco's modified eagles medium (DMEM) (Hyclone, Thermo Scientific) supplemented with 10% FBS (Gibco, Life Technologies); TamR3 and TamR6: phenol-red-free RPMI 1640, containing 10% charcoal stripped serum (CSS) (Gibco, Life Technologies) and 1 μM Tamoxifen (Sigma-Aldrich).

2.2 Chemicals and antibodies

17β-Estradiol (E2), 4-HydroxyTamoxifen (OHT) was obtained from Sigma-Aldrich. E2 was dissolved in100% ethanol. OHT, Tamoxifen and test compounds were dissolved in DMSO.

Cold PGC1a (Peroxisome proliferator-activated receptor gamma co-activator 1-alpha) peptide (EAEEPSLLKKLLLAPANTQ) was synthesized from Elim Biopharmaceuticals, Inc. (CA, USA). The rabbit monoclonal anti-pS2 antibody (EPR3972) was obtained from Abcam Inc. the mouse monoclonal anti-CDC2 antibody (JI-04-00640) was purchased from RayBiotech, Inc. The rabbit polyclonal antibody for α-Actin (A2066) and mouse monoclonal anti-Cathepsin-D antibody (C0715) were obtained from Sigma-Aldrich.

2.3 Computational screening pipeline

2.3.1 Protein and ligand preparation

Virtual screening was carried out on the ERα crystal structure [PDB:3UUD] (1.60 Å resolution) [132]. The ZINC database version 8.0 was used for virtual screening against the ERα AF2 site. The compounds were imported into a molecular database using the Molecular Operating Environment (MOE) version 2012.[133] Hydrogen atoms were added after these structures were "washed" (a procedure including salt disconnection, removal of minor components, deprotonation of strong acids, and protonation of strong bases). The following energy minimization was performed with the MMFF94x force field, as implemented by the MOE,[133] and optimized structures were exported into the Maestro suite in SD file format.

2.3.2 Virtual screening, consensus scoring and voting

Initially, ~ 4 million compounds were docked into the AF2 site using Glide SP module[134] (figure 2.1). Next, we re-docked about 2 million molecules, which had a glide score <_5.0, into the same binding cavity using the electronic high-throughput screening (eHiTS) docking module.[135] A total of 5×10^5 structures, which received eHiTS docking scores below the 3.0 threshold, were identified for further *in silico* refinement.

The determined docking poses of the 5×10^5 selected compounds were evaluated by (1) Glide docking score, (2) eHiTS docking score, (3) predicting pKi of protein-ligand binding using MOE SVL script *scoring.svl* to improve accuracy of the prediction of energies of hydrogen bonds and hydrophobic interactions, (4) calculating rigorous docking scores, defined by the Ligand Explorer (LigX) module of the MOE package, which accounts for receptor/ligand flexibility and (5) computing the root mean square deviation (r.m.s.d.) between docking poses generated by Glide and eHiTS programs to quantify their docking consistency. On the basis of these sorted output values from the above four procedures, each molecule would then receive a binary 1.0 vote for every "top 10% appearance". The final cumulative vote (with the maximum possible value of 5) was then used to rank the training set entries. On the basis of the cumulative count, we selected the most highly voted (5×10^3) molecules and subjected their docking poses to visual inspection as shown in figure 2.1.

After this final selection step, we formed a list of 100 compounds that were purchased from commercial vendors and tested in a panel of *in vitro* assays as shown in figure 2.2. From these 100 compounds, 15 were found to be active and demonstrated the ability to displace the coactivator peptide from the target AF2 site. Benzothiophenone analogues were developed based on similarity search as discussed in Chapter 4.

ZINC leadlike database
~ 4 million compounds

~2 million compounds — Glide SP program

500 000 — eHiTS docking

5000 — r.m.s.d. & consensus scoring

100 — Visual inspection

15 Active compounds ← *In vitro* assays
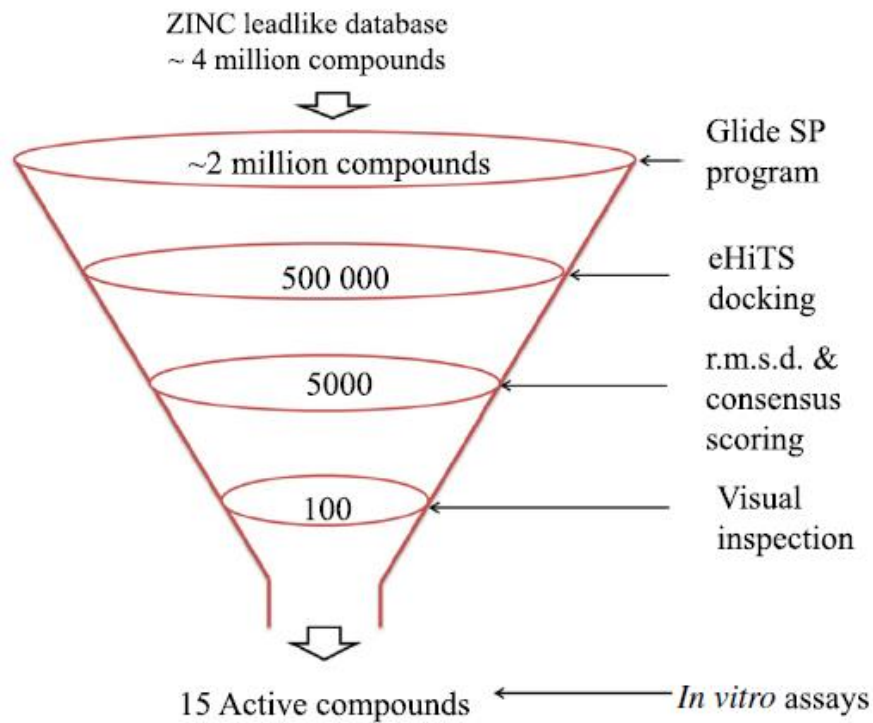
Figure 2.1. Virtual screening protocol used for the discovery of AF2 binders. The numbers indicate compounds obtained after each screening step. (eHiTS, Electronic high-throughput screening; r.m.s.d, Root mean square deviation).
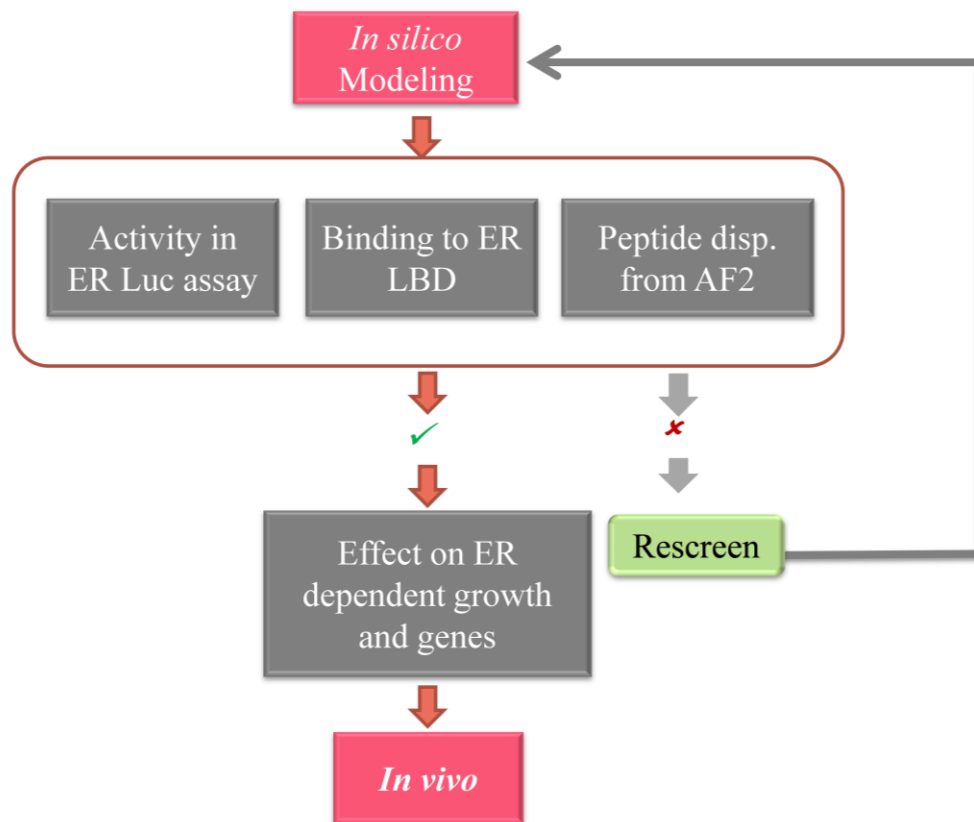
Figure 2.2. Workflow for screening compounds. The most promising compounds were purchased and screened using 3 assays: 1) Luciferase assay to measure the inhibition of ER transcriptional activity, 2) Biolayer interferometry (BLI) assay to measure the binding of compounds to ER, 3) Peptide displacement assay to assess if active compounds prevent protein-protein interactions at AF2 site. If compounds failed at any stage, they were sent back to computational lab to design better derivatives. If compounds were active in these assays, they were further tested in BCa cells. The best compound identified through this screen was tested for *in vivo* activity.

2.4   Luciferase ER-α transcriptional assay

ERα-positive T47D-KBluc human BCa cells were grown in phenol-red-free RPMI 1640 supplemented with 10% CSS for 5 days. The cells were seeded on a 96-well plate ($2x10^4$ cells/well). After 24 h, the cells were treated with either the test compounds or OHT in the presence of 1 nM E2. The test compounds were screened at two concentrations, 12 µM and 30 µM. OHT was added at a final concentration of 5 µM. For generation of dose response curves, the compounds were added at a range of 0.1-50 µM and OHT was added at a range of 0.000006—3 µM. The medium contained 0.1% (v/v) ethanol and 0.1% (v/v) dimethyl sulfoxide (DMSO). 24 h after treatment, the medium was aspirated off and the cells were lysed by adding 50 µL of 1× passive lysis buffer (Promega). The plates were placed on a shaker at room temperature for 15 min and then subjected to two freeze−thaw cycles to help lyse the cells. Then 20 µL of the lysate from each treatment was transferred onto a 96-well white flat-bottom plate (Corning) and the luminescence signal was measured after adding 50 µL of the luciferase assay reagent (Promega) on TECAN M200pro plate reader. Differences in growth were normalized against total protein concentration measured by BCA assay.

To rule out binding at EBS, dose response curves (0.1-50 µM) of test compounds and (0.000095-50 µM) of OHT were generated in the presence of a set of higher concentrations (1,10,50,100 nM) of E2 following the same procedure as described above.

2.5   Transient transfection

For transient transfection pGL2.TATA.Inr.luc plasmid was used which contains three copies of vitellogenin estrogen response element (ERE) upstream of the TATA promoter

(Addgene plasmid 11354). This is the same plasmid used to construct pGL2.TATA.Inr.luc.neo, used to create the stable cell line, T47D-KBluc.

Tamoxifen-resistant cells, TamR3 and TamR6, were grown in phenol-red-free RPMI 1640 supplemented with 10% CSS supplemented with 1μM Tamoxifen. The cells were seeded on a 96-well plate ($2x10^4$ cells/well).After 24 h, the cells were co-transfected with 50 ng each of the ERα responsive luciferase plasmid and a constitutive renilla reporter (to normalize for variations in transfection efficiency) using TransIT-2020 reagent (Mirus). Cells were treated next day with the test compounds in the presence of 1 nM E2. The compounds were added in a 2-fold dilution ranging from 0.1-50 μM. Tamoxifen was added at concentrations ranging from 0.000095-6 μM and fulvestrant was added in the range of 0.000095-50 μM. The medium contained 0.1% (v/v) ethanol and 0.1% (v/v) DMSO. 24 h after treatment, the medium was aspirated off and the cells were lysed by adding 50 μL of 1× passive lysis buffer (Promega). Luciferase activities were assayed using the dual luciferase assay system (Promega).

2.6   TR-FRET ER-α co-activator assay

Peptide displacement was assessed with the LanthaScreen TR-FRET ER-α Co-activator Assay Kit (PV4544, Life Technologies) as per instructions of the manufacturer. The principle of TR-FRET assay is that when a suitable pair of fluorophores is brought within close proximity of one another, excitation of the first fluorophore (the donor) can result in energy transfer to the second fluorophore (the acceptor). This energy transfer is detected by an increase in the fluorescence emission of the acceptor and a decrease in the fluorescence emission of the donor (Figure 2.1).

The compounds were tested in the range of 0.1-50 μM and cold PGC1a was added at 3-fold dilution ranging from 1.8-50 μM. For the peptide competition assay, the compounds were tested in the range of 0.05-400 μM in the presence of three different concentrations (250, 500 and 1000 nM) of Fluorescein-PGC1a peptide and the recommended concentrations of GST tagged ER-LBD (7.25 nM), Trebium labelled anti-GST antibody (5 nM). Briefly, a 2-fold serial dilution of the test compounds was prepared at 100X final concentration in DMSO. The compounds were diluted 50-fold in complete assay buffer (assay buffer containing 5mM Dithiothreitol (DTT)) to get a 2X final concentration and 2% DMSO. The GST tagged ER-LBD was prepared at 4X final concentration in complete assay buffer, 4X Fluorescein-PGC1a/4X Tb anti-GST antibody /4X EC80 E2 mix was prepared separately in complete assay buffer. The EC80 of E2 was determined to be 6.1μM in this assay. 10 μl of the diluted test compounds was added to a black flat bottom 384-well plate followed by addition of 5 μl of the 4X ER-LBD mix. 4X Fluorescein-PGC1a/4X Tb anti-GST antibody/4X EC80 E2 mix was added last. The plate was incubated at room temperature for 2 h and FRET was analysed on Synergy-4 multi-plate reader with the following setting: Excitation: 340 nm, Emission: 495 nm and 520 nm. The emission ratio (520:495) was analysed and plotted.
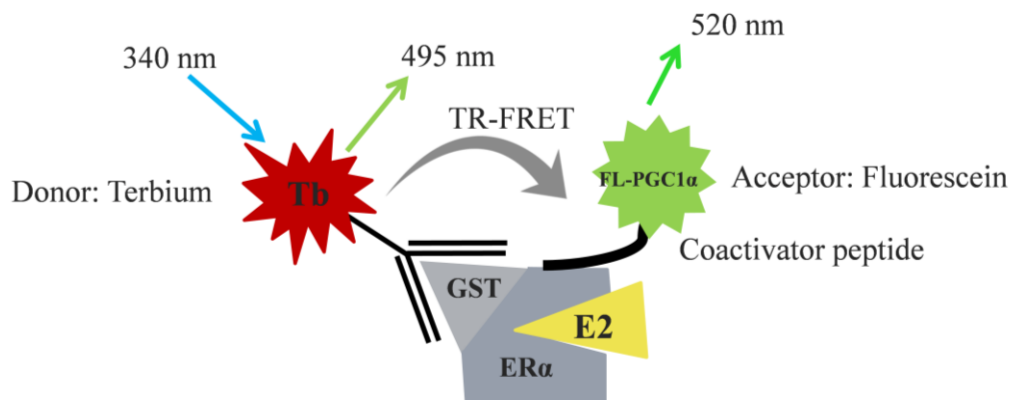
Figure 2.3. TR-FRET Assay. GST tagged ER-LBD is incubated with Terbium labelled anti-GST antibody, Fluorescein labelled coactivator peptide and E2 either alone or in combination with the test compounds. Excitation of the donor at 340 nm leads to emission at 495 nm which causes excitation of the acceptor. The fluorescence emission from the acceptor is detected at 520 nm. Compounds blocking coactivator recruitment show a decrease in the fluorescence emission.

2.7   E2 displacement assay

E2 displacement was assessed with the Polar Screen Estrogen Receptor-α Competitor Green Assay Kit (P2698, Life Technologies) as per the instructions of the manufacturer. For screening purposes, the compounds were tested at 20 μM in the presence of 25nM full length ERα and 4.5nM fluorescein labelled-E2 (Fl-E2). For E2 ligand competition assay, a 2-fold serial dilution of the test compounds was prepared at 100X final concentration in DMSO. The compounds were diluted 50-fold in assay buffer to get a 2X final concentration and 2% DMSO. 50 μl of the diluted test compounds were added to a 50 μl mixture containing 2X full length ERα and Fl-E2 in each well to obtain final concentrations of 3-150 μM of test compound in presence of 25nM full length ERα and 4.5nM Fl-E2. Unlabelled -E2 was tested at concentrations ranging

from (0.01-1000 nM). After 2h incubation, polarization was measured as per instructions of the manufacturer on TecanF500 plate reader.

2.8   Biolayer interferometry assay

The direct reversible interaction between small molecules and the ERα was quantified by BLI using an OctetRED (ForteBio) apparatus. The LDB of the biotinylated ERα (bERα) was produced in situ with AviTag technology (Avidity). The AviTag sequence (GLNDIFEAQKIEWHE) was incorporated at the N terminus of the ERα-LBD (302-552). A six residue histidine tag was incorporated at the C-terminus of the ERα-LBD for purification of the protein. Escherichia coli strain BL21 containing both biotin ligase and ERα-LBD vectors was induced with 0.5 mM isopropyl-β-D-thiogalactopyranoside (IPTG) in the presence of 0.02 mM E2 and 0.15 mM biotin at 16°C overnight. The bacteria were then lysed by sonication, and the resulting lysate was purified by immobilized metal ion affinity chromatography (IMAC) with nickel-agarose beads (GE Healthcare) and cation-exchange chromatography (HiTrap SP). Purified and biotinylated protein (bERα-LBD at 0.05 mg/mL) was bound to the super-streptavidin sensors overnight at 4°C in assay buffer [20 mMTris, pH 7.5, 500 mMNaCl, 0.2 mMtris (2-carboxyethyl) phosphine (TCEP), 0.02 mM E2, 5% glycerol and 5% DMSO]. The compounds were dissolved in the assay buffer in a 2-fold dilution series ranging from 3.1-100 μM. In all experiments, a known AF2-interacting peptide, PGC-1a (Elim Biopharmaceuticals, CA, USA) was used as a control to confirm functionality of the bERα-LBD.

2.9   Cell proliferation assay

Cell proliferation was determined using the MTS assay. Cells were seeded in 96-well plates at a density of 5×10^3 cells/well. MCF7, TamR3, TamR6, MDA-MB-453 and HeLa cells were seeded in their respective media. On the following day, the cells were treated with test compounds (0.2-50 µM) in the presence of 1nM E2 and incubated at 37°C in 5% CO2. After 96 h, 30 µL of MTS reagent (CellTiter 961 Aqueous One Solution Reagent, Promega) was added and incubated for 90 mins at 37°C in 5% CO2. The production of formazan was measured at 490 nm.

2.10   qRT-PCR

mRNA levels were analysed by quantitative real-time reverse transcriptase-polymerase chain reaction (qRT-PCR). For this purpose, serum starved MCF7 cells and TamR3 cells were seeded onto 6 well plates at a density of 6×10^5 cells/well. After 24h, the cells were treated with the either test compounds or OHT in the presence and absence of 1nM E2. RNA was isolated after 24h with TRIzol reagent and purified with the RNAeasy mini-kit (Qiagen). The purified mRNA was quantified using nanodrop. 0.5 µg RNA was reverse transcribed using iScript kit (Biorad). 100 ng cDNA product was added to the primer mix. Final concentration of the primers was 5 pM. The sequences of the primers used in the qRT-PCR were as follows: pS2, forward 5'-TTGTGGTTTTCCTGGTGTCA-3' and reverse 5'-GCAGATCCCTGCAGAAGTGT-3', Cathepsin-D, forward 5'-CAGAAGCTGGTGGACCAGAAC-3' and reverse 5'-TGCGGGTGACATTCAGGTAG-3', CDC2, forward 5'-ACTGGCTGATTTTGGCCTTG-3' and reverse 5'- TTGAGTAACGAGCTGACCCCA-3', GAPDH, forward 5'-TGCACCACCAACTGCTTAGC-3' and reverse 5'-GGCATGGACTGTGGTCATGAG-3'. The

fold change in expression of the gene was calculated using the delta delta Ct method with GAPDH as the internal control.

2.11 Western blotting

MCF7 cells were cultured in phenol red-free RPMI containing 10% CSS for five days. The cells were then seeded onto a 6-well plate at a density of 6×10^5 cells/well and treated the following day with the test compounds in the presence of 1nM E2. After 24h, the medium was aspirated off and the cells were washed with ice-cold phosphate-buffered saline (PBS). Cells were lysed in 1X radioimmunoprecipitation assay (RIPA) buffer containing 1 tablet of protease inhibitor cocktail (Roche). Cell debris was pelleted by centrifugation at 15000g for 10 min at 4ºC. The supernatants were collected and quantified using the BCA assay. In each case, 25 µg of protein was loaded onto 15% (v/v) sodium dodecyl sulphate polyacrylamide gel electrophoresis (SDS-PAGE) gels, separated and transferred to PVDF membrane. Membranes were incubated with pS2, Cathepsin-D and CDC2 antibodies or control alpha-actin antibody. Bound antibodies were detected using horseradish peroxidase-conjugated secondary antibodies. Chemiluminescence was detected with ECL Detection Kit (GE Healthcare) and bands were visualised using the GBox imager (Syngene).

2.12 Mammalian two hybrid assay

The fusion protein constructs were created using vectors from the CheckMate™ Mammalian Two-Hybrid System (Promega). The LBD of ERα was cloned into the pACT vector to produce the ERα-LBD protein fused to the VP16 activation domain. The SRC-3 coactivator peptide (aa 614-698) containing LxxLL motives 1 and 2 was cloned into the pBIND vector to

produce the SRC-3 protein fused to the GAL4-DNA binding domain. MDA-MB-231 cells were seeded on 96-well plates ($2x10^4$ cells/well) in 150 μL medium. The cells were co-transfected with 25 ng each of pACT-ERα-LBD, pBIND-SRC-3, pG5luc and a constitutively active renilla reporter plasmid using TransIT-2020 reagent (Mirus). Cells were treated next day with the test compounds in the presence of 1 nM E2. After 24 h the cells were lysed and luminescence was measured in the same way as for the luciferase transcriptional assay described above.

2.13 Chromatin immunoprecipitation (ChIP)

E2-deprived MCF7 cells were treated for 24 h with DMSO alone, DMSO+E2, or compounds+E2. DNA-protein crosslinking was performed with 1% formaldehyde treatment for 10 min at room temperature and quenched with 125 mM glycine for 5 min. Cell lysates ($1x10^7$ cells/ml) were subjected to sonication with a Thermo Scientific 1/8-inch sonication probe and Sonic Dismembrator 550 instrument to yield DNA fragments of 200–1000 bp in size. Immunoprecipitation of lysates ($3.3x10^6$ cell eq) was performed with 5 μg of anti-ERα antibody or 1 μg of rabbit isotype control IgG (Santa Cruz Biotechnology) using a EZ-ChIP chromatin immunoprecipitation kit (Millipore). Bound DNA was quantified by quantitative PCR (SYBR Green master mix, Invitrogen) using the following primer sets: pS2 enhancer, forward 5′-GTACACGGAGGCCCAGACAGA-3′ and reverse 5′-AGGGCGTGACACCAGGAAA-3′; GAPDH promoter, forward 5-TAC TAG CGG TTT TAC GGG CG and reverse 5-TCG AAC AGG AGC AGA GAG CGA. The quantitative PCR results are presented as fold enrichment of PCR amplification over control IgG antibody and normalized based on the total input (nonprecipitated chromatin). Primers for the GAPDH promoter were used as a negative control lacking any ERE.

40

2.14 Generation of stable MCF7LUC cells

A fragment of DNA encoding firefly luciferase was cloned into pLVX-IRES-Puro (Clontech) at EcoR1 and BamH1 sites as transfer vector. Lenti-X 293T packaging cells (Clontech) were transfected with transfer vector, packaging vector R8.91 and pCMV-VSV-G at the ratio of 2:2:1 with TransIT 2020 (Mirus Bio LLC). 24 h later, culture medium in lenti-X 293T was replaced with fresh DMEM containing low FBS. The supernatant containing lentivirus was harvested 48 h later and filtered through a filter of 0.45 um (Sartorius). To create the stable MCF7LUC cell line, MCF7 cells were exposed to supernatant containing lentivirus overnight and then cultured in fresh medium. Three days after lentiviral transduction, MCF7 cells were cultured in the presence of puromycin (2.5 µg/ml) for seven days to select lentiviral transduced cells which were puromycin-resistant. Before MCF7LUC cells were implanted into nude mice, expression of luciferase by these cells was monitored by detection of luciferase-catalyzed bioluminescent signal with a Xenogen Imaging system (Xenogen). The selected cells exhibited similar growth rates as the parental MCF7 cell line. Additionally MCF7LUC and parental MCF7 were equally sensitive to VPC-16606.

2.15 *In vivo* studies

2.15.1 Tissue culture

Cells were started from frozen vial of lab stock and cultured in phenol red free RPMI1640 medium supplemented with 10% FBS and 2.5µg/mL Puromycin at 37°C in humidified incubator with 5% CO2. The cultures with passage 3 to 10 and 80-90% confluency were harvested for *in vivo* studies.

2.15.2 Harvesting for I.P. inoculation

The cells were briefly rinsed once with Hanks Balanced Salt Solution w/o Ca, Mg. Cells were trypsinized with fresh trypsin/EDTA solution (0.25% trypsin with EDTA 4N) and neutralized with fresh medium once the cells were dispersed. 50 µL of cell suspension was mixed with trypan blue (1:1) and viable cells were counted in a cellometer auto4. Cells were centrifuged at 200g for 7 min and the supernatant aspirated. Cells were re-suspended in HBSS to the appropriate concentration for inoculation. The inoculation volume was 500 µL. The cell viability was re-checked post inoculation by using cellometer.

2.15.3 Tumor cell implantation: MCF7LUC with E2 supplementation (under anaesthesia)

On day -1, mice had 60 day release estradiol pellets (Innovative Research of America; 0.72 mg/pellet) implanted under the skin of the lateral side of the neck. Incisions were closed with sutures. On day 0, 10^7 tumor cells were implanted intraperitoneally into female Rag2 mice in a volume of 500 µL using a 27-gauge needle.

2.15.4 Dose administration

Preparation of VPC-16606 and vehicle solution: The vehicle used for administration was 100% PEG400, pH4.6. VPC-16606 was dissolved in the vehicle to obtain a final concentration of 50 mM.

Filling of Alzet Pumps:

Prime for 48h in saline at 37°C before implantation.

The following steps were performed in a biosafety cabinet using sterile technique:

o   The empty pump together with its flow moderator was weighed.

o Instructions for the mean fill volume for the lot of pumps that were used was checked.

o A filling tube was attached to a syringe and the room temperature solution was drawn out. It is essential that the syringe and attached tube are free of air bubbles. Extra syringe volume was allowed for spillage. With the flow moderator removed, the pump was held in an upright position.

o The filling tube was inserted through the opening at the top of the pump until it could go no further.

o The plunger of the syringe was pushed slowly, holding pump in an upright position. When the solution appeared at the outlet, filling was stopped and the tube carefully removed.

o Excess solution was wiped off and the flow moderator was inserted until the cap or flange was flush with the top of the pump. The flow moderator must be fully inserted into the body of the pump.

o The flow pump was weighed with the flow moderator in place. The difference in the weight obtained in steps 1 and 7 gave the net weight of the solution loaded. The fill volume should be more than 90% of the reservoir volume specified. If so the pump is ready for use. If not, there is some air trapped inside the pump, it must be evacuated and refilled.

Intraperitoneal implantation of Alzet Pump (8 days post inoculation):

o Buprenorphine was administerd at 0.075mg/kg and Metacam at 1mg/kg s.c.

o Mouse was anesthetized with isoflurane

o Eyes were protected with ointment

o For intraperitoneal pump implantation, following steps were performed

• Once the animal was anesthetized, skin over the implantation site was shaved and washed.

43

- A suitable incision was made adjacent to the site chosen for pump placement (i.e. in the skin below the rib cage and another small incision in the abdominal muscle directly under the cutaneous incision).

- The filled pump was inserted, flow moderator first (this minimizes the interaction between the compound delivered and the healing of the incision), into the peritoneal cavity. The muscle incision was closed with sutures and then the skin incision was closed with size 5.0 absorbable suture subcuticular pattern.

2.15.5 Data collection

Luminescence monitoring: Tumor growth of mice was monitored using the IVIS imaging system on the day of cell inoculation and biweekly thereafter for the duration of the study. Imaging was conducted under isoflurane anesthesia. Mice were injected intraperitoneally with 200 µL of 15mg/mL Luciferin 20 minutes prior to imaging. At 10 min prior to imaging mice were placed in the induction chamber for isoflurane anesthesia. Once anaesthetized, a drop of eye gel was placed over reach eye to protect from dehydration during imaging. When mice reached humane endpoint, observation of tumors in abdomen was noted. Following Day 50, mice were closely monitored and the study was terminated at day 60.

2.15.6 Observation of animals

Clinical Observations: All animals were observed post administration, and at least once a day, more if deemed necessary for mortality and morbidity. In particular, signs of ill health were based on body weight loss, change in appetite and behavioral changes such as altered gait,

lethargy and gross manifestations of stress. Animals would be terminated if signs of severe illness were to be observed. Moribund animals were to be terminated for humane reasons.

The methodology described here is within a service oriented Animal Care Protocol that has been reviewed and approved by the Institutional Animal Care Committee (IACC) at UBC-protocol #A14-0290. During the study the care, housing and use of animals was performed in accordance with the Canadian Council on Animal Care Guidelines.

2.16 Statistical analysis

Data was analyzed and dose response curves were generated using GraphPad Prism5. 1-way ANOVA test was used with $P < 0.05$ considered to indicate significance. Student t test (2 sided) was used to evaluate statistically significant differences in all experiments. Results are expressed as mean $\pm$ SE with at least 3 biologic replicates.

Chapter 3: Development of Carbohydrazide Derivatives

3.1 Background

It has been previously demonstrated that it is possible to inhibit ERα transcriptional activity by blocking the recruitment of receptor's co-activators to the AF2 site. Several groups have identified small molecule candidate inhibitors of ERα AF2 functionality (as discussed in section 1.7.4). However, such compounds have not yet been shown to inhibit the growth of cells that developed Tamoxifen-resistance - a major challenging clinical scenario. Moreover, these inhibitors demonstrated only moderate μM potencies against the ERα, and are not yet suitable for clinical application. Hence, in an effort to develop potent AF2 inhibitors, computational chemists under the supervision of Dr. Artem Cherkasov (University of British Columbia) performed a large-scale computational screen. Virtual screening was carried out using the ERα crystal structure, PDB id-3UUD (1.60 Å resolution) [132] using an established computational pipeline.[136-138] Based on *in-house* developed protocols, 100 compounds were selected and purchased for biological testing from commercial chemical vendors. I developed and optimized all the assays required to evaluate these virtual hits. Upon testing, fifteen inhibitors that belong to two chemical classes *i.e.* derivatives of pyrazolidine-3, 5 dione and carbohydrazide were identified. Discovery and activity profile of these compounds has been published in *Breast Cancer Research* journal.[139]

3.2 Results

3.2.1 Lead compounds inhibit ERα transcriptional activity in BCa cell lines
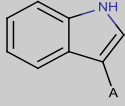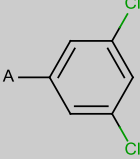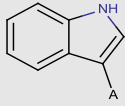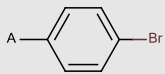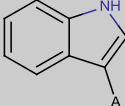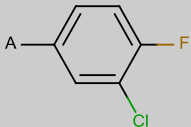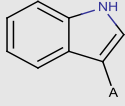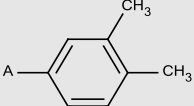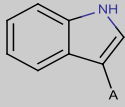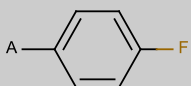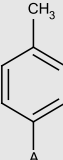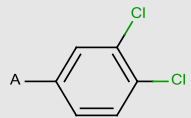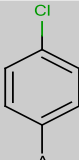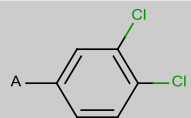
The compounds selected from computational screen were evaluated for their ability to inhibit ERα transcriptional activity using cellular screening assays in ERα-positive T47D-KBluc,

a stable luciferase reporter BCa cell line. In particular, twenty active compounds which inhibited the reporter gene expression by at least 50% at 12 and 30 μM were selected for construction of dose response curves. Among these, 15 compounds demonstrated inhibition of ERα transcriptional activity in a dose dependent manner, with IC_{50} values ranging from 5.8 to 100 μM (Table 3.1 & 3.2). Ten compounds summarized in table 3.1 belong to the chemical class of pyrazolidine-3, 5 diones and five compounds from table 3.2 are derivatives of carbohydrazide. Among these, VPC-13002, VPC-16225 and VPC-16230 demonstrated significant inhibition of the reporter gene expression with IC_{50}'s of 7.6, 8.24 and 5.81 μM respectively (Figure 3.1A). The IC_{50} of OHT in this assay was established as 4.2 nM (Figure 3.1B).

Table 3.1. Structures and measured activities of pyrazolidine-3, 5 dione derivatives.
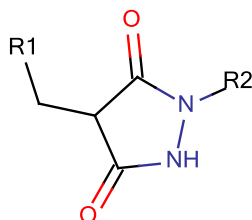
VPC-ID	R1	R2	Peptide Displacement IC_{50} (μM)	ER Inhibition IC_{50} (μM)
13002			2.46	7.60
16019			3.16	9.62

VPC-ID	R1	R2	Peptide Displacement IC$_{50}$ (µM)	ER Inhibition IC$_{50}$ (µM)
16041			4.33	8.24
16046			5.38	16.34
16038			7.98	9.75
16007			11.27	~25
16040			19.54	~35
16003			29.10	> 50
16004			31.98	> 50
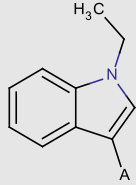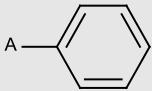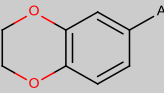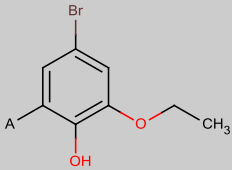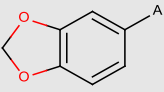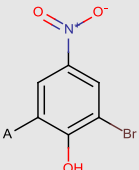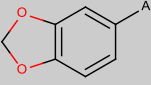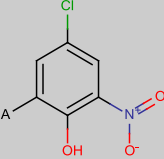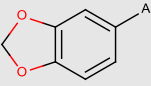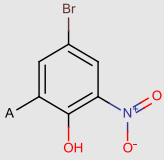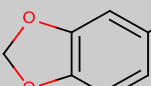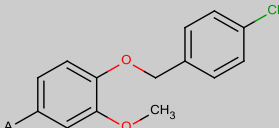
VPC-ID	R1	R2	Peptide Displacement IC$_{50}$ (μM)	ER Inhibition IC$_{50}$ (μM)
16021			>100	> 50

Table 3.2. Structures and measured activities of acetohydrazide derivatives.
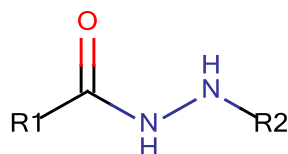
VPC-ID	R1	R2	Peptide Displacement IC$_{50}$ (μM)	ER Inhibition IC$_{50}$ (μM)
16230			2.98	5.81
16225			3.76	8.24

VPC-ID	R1	R2	Peptide Displacement IC$_{50}$ (μM)	ER Inhibition IC$_{50}$ (μM)
16222			8.64	9.32
16223			9.78	10.46
16236			16.27	22.01

3.2.2   Effect of active compounds on co-activator recruitment to the AF2 site

We anticipated that binding of the identified small molecules to the AF2 site should inhibit E2 dependent co-activator peptide recruitment to this site. To test this hypothesis, the AF2 binders were analyzed by using LanthaScreen TR-FRET ERα co-activator assay kit from Life Technologies. Terbium labelled anti-GST antibody indirectly labels the ERα-LBD by binding to a GST tag on the protein. Binding of the agonist, E2 to the ERα causes conformational changes that result in an increase in the affinity of ERα for a fluorescently labeled co-activator peptide, Fluorescein-PGC-1a. PGC-1a has been shown to interact with the AF2 site of ERα in agonist-dependent manner. The close proximity of Fluorescein-PGC-1a to the terbium-labeled antibody causes an increase in the TR-FRET signal. When a compound binds to the AF2 site, the

recruitment of the co-activator peptide is blocked, causing a decrease in the TR-FRET signal, which is measured as a ratio of emission at 520 nm to 495 nm.

Out of 15 chemicals tested, 9 demonstrated effective blocking of AF2/PGC-1a interaction in a concentration-dependent manner and their IC_{50} values were determined to range between 2 and 20µM (Table 3.1&3.2). This suggests that the compounds bind to the AF2 site, thereby inhibiting co-activator recruitment. VPC-13002, VPC-16225 and VPC-16230 that were effective in cellular assays demonstrated IC_{50} values of 2.46, 3.76 and 2.98 µM respectively (Figure 3.1C). The cold PGC1a peptide used as a control in this assay showed a dose-dependent decrease in the FRET signal with increase in concentration (Figure 3.1D).
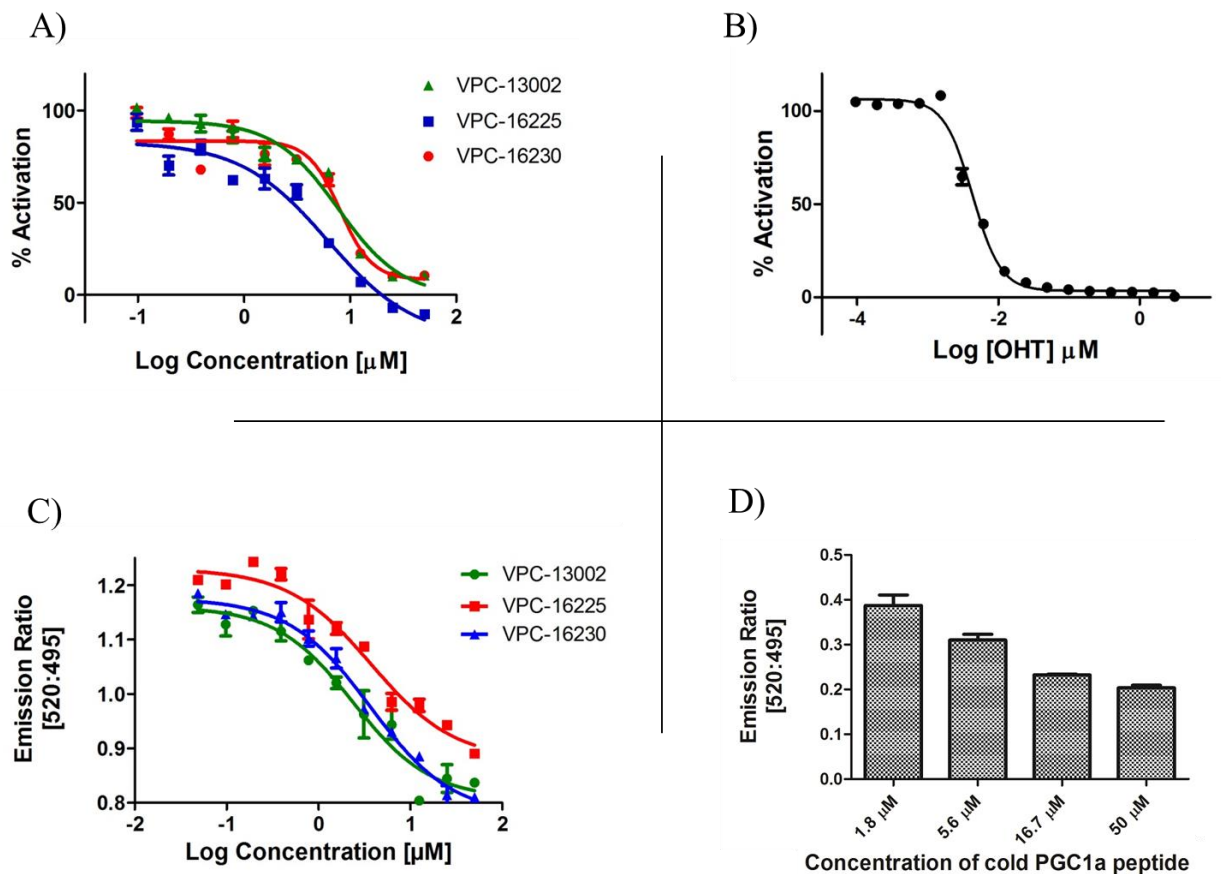
Figure 3.1. The lead compounds inhibit ERα transcriptional activity and co-activator binding at the AF2 site. (A) Dose response curves (0.1-50 μM) of compounds VPC-13002, VPC-16225 and VPC-16230 (IC_{50}: 7.6, 8.24, 5.81 μM respectively) showing inhibition of the ERα transcriptional activity as measured by luciferase reporter assay in T47D KBluc cells. (B)Dose response curve (0.000006-3 μM) of OHT (IC_{50}: 4.2 nM) showing inhibition of the ERα transcriptional activity as measured by luciferase reporter assay in T47D KBluc cells. Data was fitted using log of concentration of the inhibitors Vs % activation with GraphPad Prism 5. (C) Dose response curves (0.1-50 μM) of compounds VPC-13002, VPC-16225 and VPC-16230 (IC_{50}: 2.46, 3.76, 2.98 μM respectively) for displacement of the PGC-1a peptide from the AF2 site as measured by TR-FRET assay. (D) Dose dependent (1.8-50 μM) behavior of Cold PGC1a peptide for displacement of the Fluorescein-PGC-1a peptide from the AF2 site as measured by TR-FRET assay. Data points represent average of three independent experiments performed in triplicates. Error bars indicate standard error of mean (SEM) for N=3 values.

The three compounds were tested for competition with increasing concentrations of Fluorescein-PGC1a (250, 500 and 1000 nM) to confirm their AF2-mediated mode of action. As expected, a right shift in the dose response curves of the compounds was observed in the presence of higher concentrations of Fluorescein-PGC1a (Figure 3.2A-C). This suggests that the compounds bind to the AF2 site.
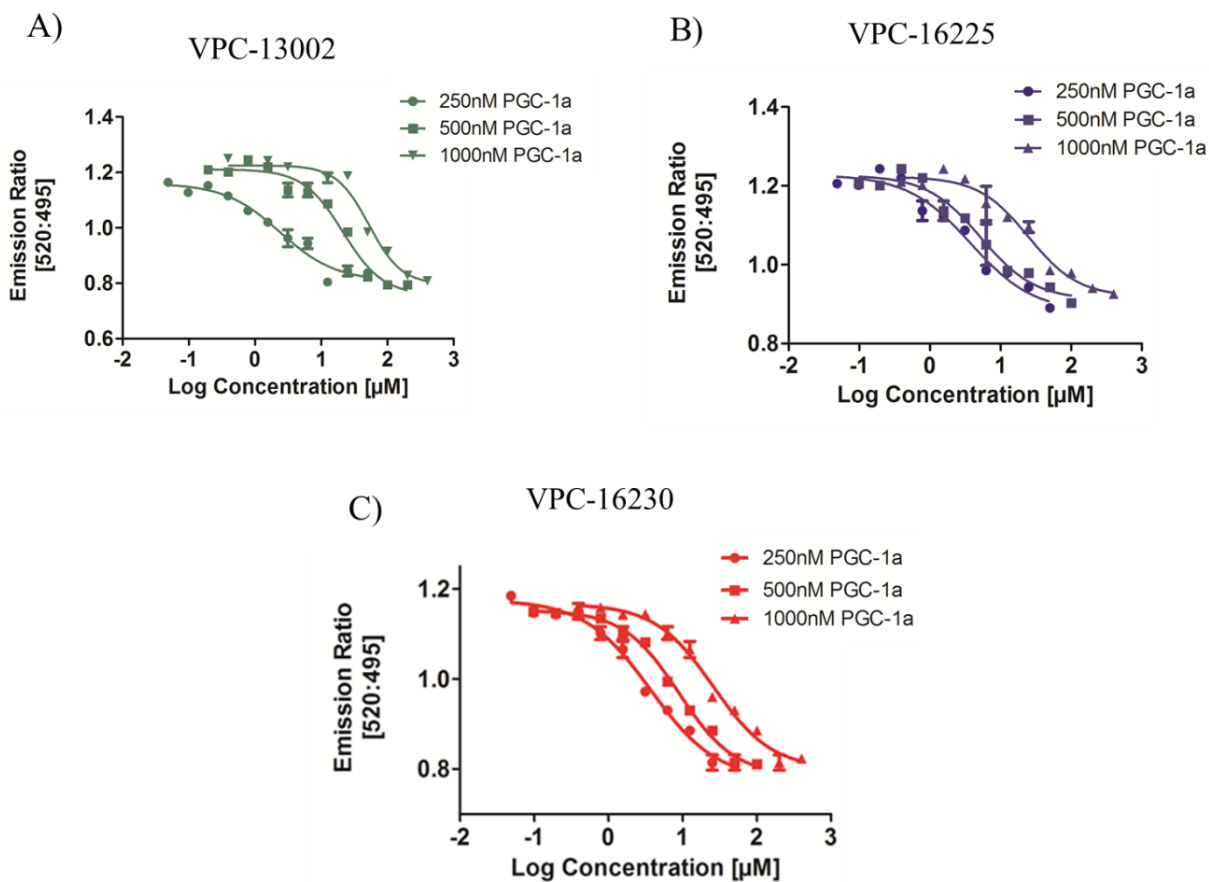
Figure 3.2. The dose response curves of the lead compounds are right-shifted in the presence of higher concentrations of co-activator peptide. Dose response curves (0.05-400 μM) of VPC-13002 (A), VPC-16225 (B) and VPC-16230 (C) showing a right shift with increase in concentrations of Fluorescein-PGC1a generated by the TR-FRET assay. (Error bars indicate standard error of mean (SEM) for N=3 values. Data was fitted using log of concentration of the inhibitors Vs emission ratio with GraphPad Prism 5.

3.2.3   Active compounds do not bind to the ERα-EBS

For the compounds to be deemed AF2 specific, it is important to confirm that they do not bind to the EBS part of the receptor. To rule out interaction with the EBS, our most active compounds were tested for E2 displacement using PolarScreen™ ERα Competitor Assay kit

from Life Technologies. Nine compounds which effectively inhibited co-activator recruitment were tested for E2 displacement at 20 μM. Out of the nine compounds tested, six (including VPC-13002, VPC-16225 and VPC-16230) did not exhibit any detectible E2 displacement when tested at 20 μM. It should be noted that the Kd of Fl-E2 with full length ERα in this assay is reported by the manufacturer as 18 ± 9 nM. Fl-E2 was used at the recommended concentration of 4.5 nM in order to ensure that the lack of competition observed at 20 μM was not due to the presence of an excess of Fl-E2 ligand. To further confirm that the active compounds do not compete with E2 for binding at the EBS, an E2 ligand competition assay was performed. Results from this experiment demonstrate that these compounds did not displace Fl-E2 even at the highest concentrations tested (3-150 μM) (Figure 3.3A-C), whereas the IC$_{50}$ of unlabeled-E2 for displacement of Fl-E2 from the EBS in this assay is 4.2 nM (Figure 3.3D), which suggests that the estimated cellular IC$_{50}$'s do not reflect binding to the EBS.

54
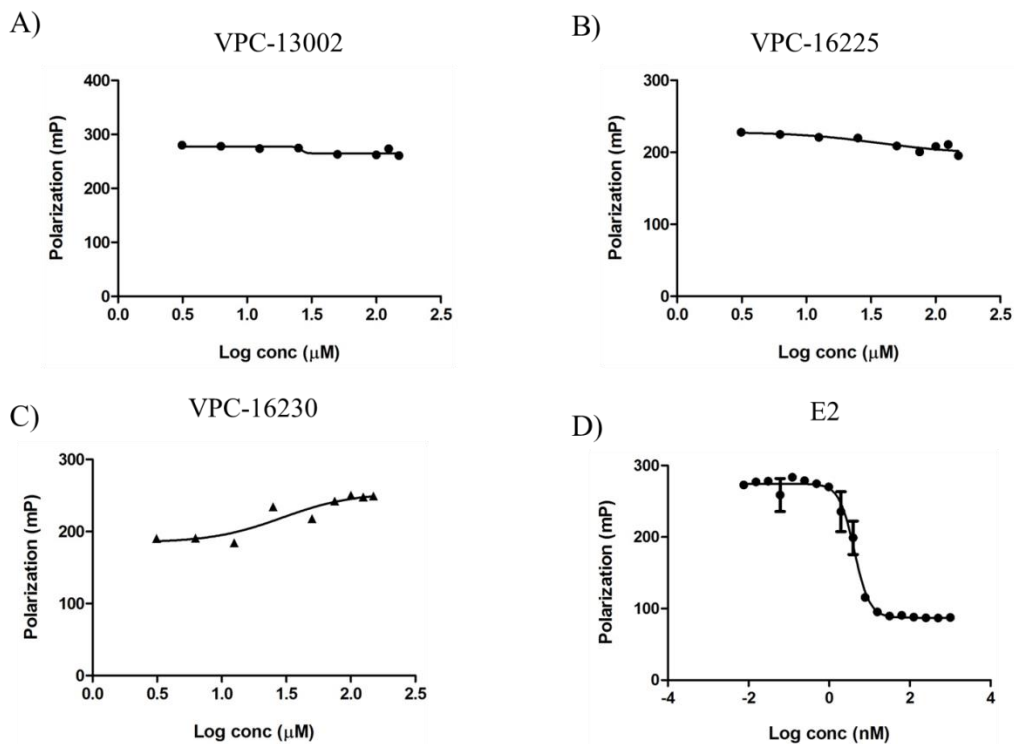
Figure 3.3. The lead compounds do not displace E2 from EBS of ERα. Dose response curve (3-150 µM) of VPC-13002 (A), VPC-16225 (B), VPC-16230 (C) and E2 (0.01-1000 nM; IC_{50}: 4.2 nM) (D) for displacement of Fl-E2 in fluorescence polarization assay. Data was fitted using log of concentration of the inhibitors Vs polarization with GraphPad Prism 5.

A second confirmation that the compounds do not bind to EBS was obtained by measuring IC_{50}'s of the developed inhibitors in the presence of higher concentrations of E2 (luciferase assay on T47D-KBluc cell line). Since OHT (used as a positive control) competes with E2 for binding at the EBS, we observed a right-shift in the IC_{50} curve of OHT that was proportional to the fold increase in E2 (Figure 3.4A). On the contrary, IC_{50} curves of VPC-16225 and VPC-16230 compounds did not show any significant shift (Figure 3.4B, C). This confirmed that the compounds do not bind to the EBS.

A) OHT   B) VPC-16225   C) VPC-16230

E2 Conc (nM)	OHT IC_{50} (µM)
1	.004
10	.05
50	.2
100	.55

E2 Conc (nM)	16225 IC_{50} (µM)
1	7.6
10	12.02
50	12.06
100	15.2

E2 Conc (nM)	16230 IC_{50} (µM)
1	6.1
10	5.7
50	5.6
100	6.5
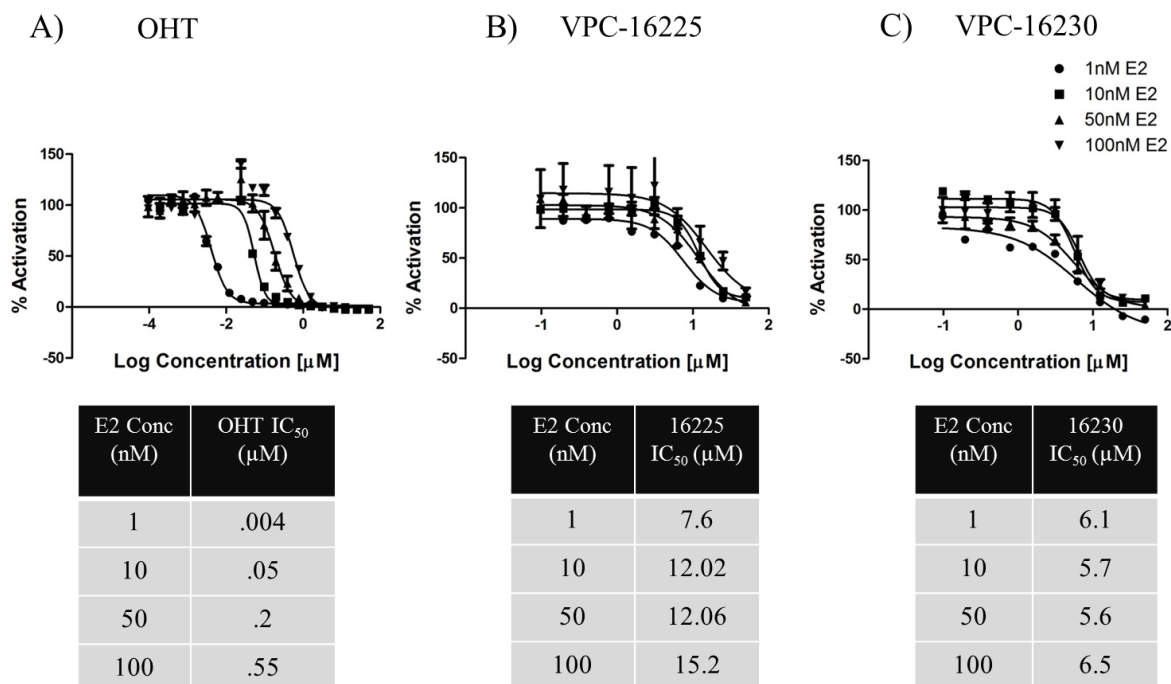
Figure 3.4. The dose response curves of the lead compounds do not shift in the presence of higher concentrations of E2. (A) Dose response curves (0.000095–50 μM) of OHT showing a right shift proportional to the fold increase in concentrations of E2 generated by the luciferase assay in T47D-KBluc cell line. (B) Dose response curves (0.1-50 μM) of VPC-16225 and VPC-16230 (C) showing no significant right shift in the presence of higher concentrations of E2 as measured by luciferase assay in T47D-KBluc cell line. Error bars indicate standard error of mean (SEM) for N=3 values. Data was fitted using log of concentration of the inhibitors Vs % activation with GraphPad Prism 5.

3.2.4 Active compounds show direct binding to the ERα-LBD

To confirm that the identified inhibitors directly bind to the ERα, the ERα-LBD in fusion with an avi-tag at the N-terminus and a six residue histidine tag at the C-terminus was cloned and purified. The ERα-LBD was biotinylated on the avi-tag by a biotin ligase expressed by the bacterial cells co-transformed with the biotin ligase plasmid pBirACm. The bERα-LBD was purified by Ni-affinity chromatography and immobilized on streptavidin biosensor tip. The interaction between small molecule and protein is measured in real time as a shift in the interference pattern of the incident light. A response profile is generated on the Octet system.

The binding of the identified 6 most potent lead compounds was confirmed using this assay. Figure 3.5A-D features the BLI data obtained for the most potent compounds, VPC-13002, VPC-16225 and VPC-16230 along with the PGC-1a peptide used as a control, demonstrating their direct and reversible interaction with ERα. Importantly, it should be noted that the binding curves of these compounds could fit with a simple 1:1 model even at higher concentration, suggesting their single-site ER binding.
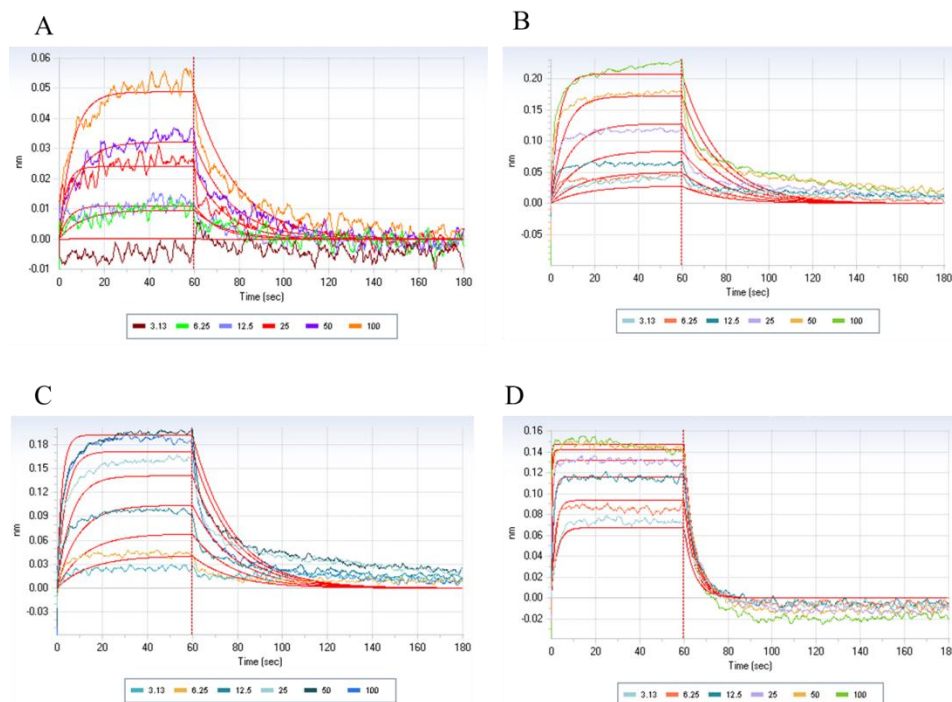
Figure 3.5. The lead compounds show direct reversible binding to the ERα-LBD. BLI dose response curves (3-100 μM) reflecting the binding of the compounds (A) VPC-13002 (B) VPC-16225 (C) and (D) VPC-16230 to ERα-LBD in a dose dependent manner. PGC-1a co-activator peptide is used as a positive control.

3.2.5 VPC-16225 and 16230 reduce the growth of MCF7 cells including TamR cells

The main objective of the current study was to inhibit the growth of BCa cells by designing small molecules that specifically block the ERα co-regulator interaction. To ascertain the growth inhibitory potential of VPC-13002, VPC-16225 and VPC-16230, we evaluated their ability to inhibit the E2 stimulated growth of ERα-positive, MCF7, TamR3 and TamR6 BCa cells in MTS assays. Cell viability was assessed after 96 h of incubation with each compound. General cell toxicity was assessed by measuring inhibition of growth in ERα-negative MDA-MB-453 and HeLa cell lines. The VPC-13002 molecule is a derivative of pyrazolidine-3, 5 dione that demonstrated certain toxicity in ERα-negative cells; hence, the growth inhibitory effect of

this compound was not considered to be ERα-mediated (Figure 3.6A) and the molecule was eliminated from further analysis. Figures 3.6B and C show that carbohydrazide derivatives (VPC-16225 and VPC-16230) exhibited growth inhibition of MCF7 cells in a concentration dependent manner confirming their ERα-specific effect. Next, we tested VPC-16225 and VPC-16230 in TamR3 and TamR6. These cell lines were derived from parental MCF7 cells upon prolonged treatment with Tamoxifen and retained expression of ERα. Compared to controls, both VPC-16225 and VPC-16230 inhibited the proliferation of these cell lines in a dose dependent manner at the concentrations tested. The IC_{50} values for VPC-16225 are 3.1 μM and 4.1 μM in TamR3 and TamR6 respectively. VPC-16230 had IC_{50} values of 3.4 μM and 6.3 μM in TamR3 and TamR6 respectively. It may be noted that due to the development of resistance, the growth of the TamR3 and TamR6 cell lines is not affected by the presence of 1 μM Tamoxifen in the medium.
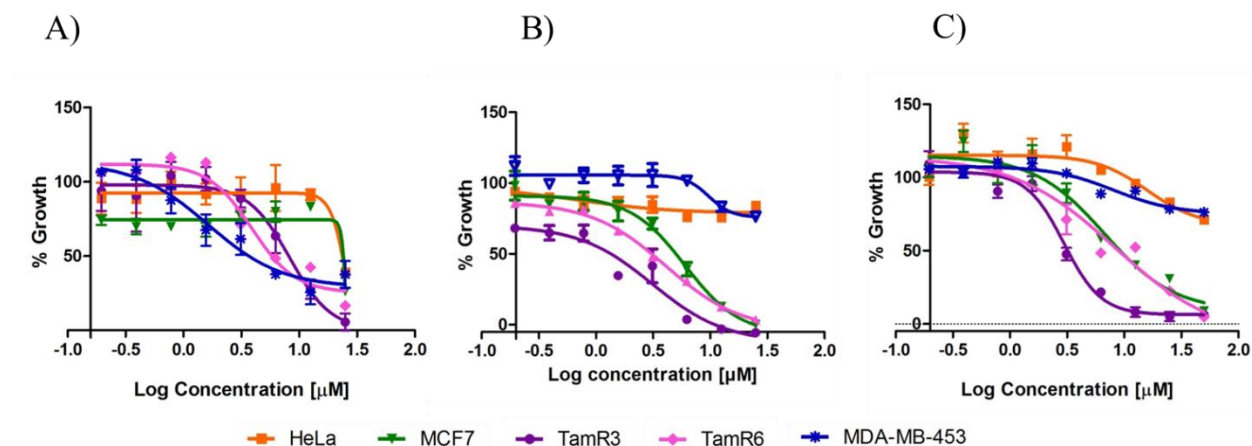
Figure 3.6. The lead compounds affect the viability of ERα-positive cells. Dose response curves (0.2-50 μM) of the lead compounds showing decrease in cell viability as assessed by the MTS assay. The compounds, VPC-13002 (A), VPC-16225 (B) and VPC-16230 (C) inhibit the growth of ERα-positive MCF7 and Tamoxifen resistant cells (TamR3 and TamR6) with very little effect on ERα-negative MDA-

MB-453 and HeLa cells except VPC-13002, which is toxic in both the control cell lines. Data points represent average of two independent experiments performed in triplicates. Error bars indicate standard error of mean (SEM) for N=3 values. Data was fitted using log of concentration of the inhibitors Vs % growth with GraphPad Prism 5

3.2.6 VPC-16225 and VPC-16230 inhibit ERα in Tamoxifen-resistant cells

To confirm that the growth inhibition of Tamoxifen-resistant cell lines, TamR3 and TamR6 was through inhibition of ERα activity, we assessed the ability of VPC-16225 and VPC-16230 to inhibit the expression of an estrogen responsive luciferase reporter gene. TamR3 and TamR6 cells were transiently transfected with the luciferase plasmid (3X ERE TATA luc) and then treated the following day with compounds at concentrations ranging from 0.1 to 50 μM, all in the presence of 1 nM E2. Both compounds showed significant inhibition of E2-stimulated ERα transcriptional activity in the two cell lines as measured by the luminescence signal (Figure 3.7A-D). Fulvestrant, which was used as a positive control in these cells, yielded IC_{50} values of 0.09 and 0.04 μM in TamR3 and TamR6 systems respectively. As expected, OHT was ineffective in inhibiting the transcriptional activity of ERα in these cells.
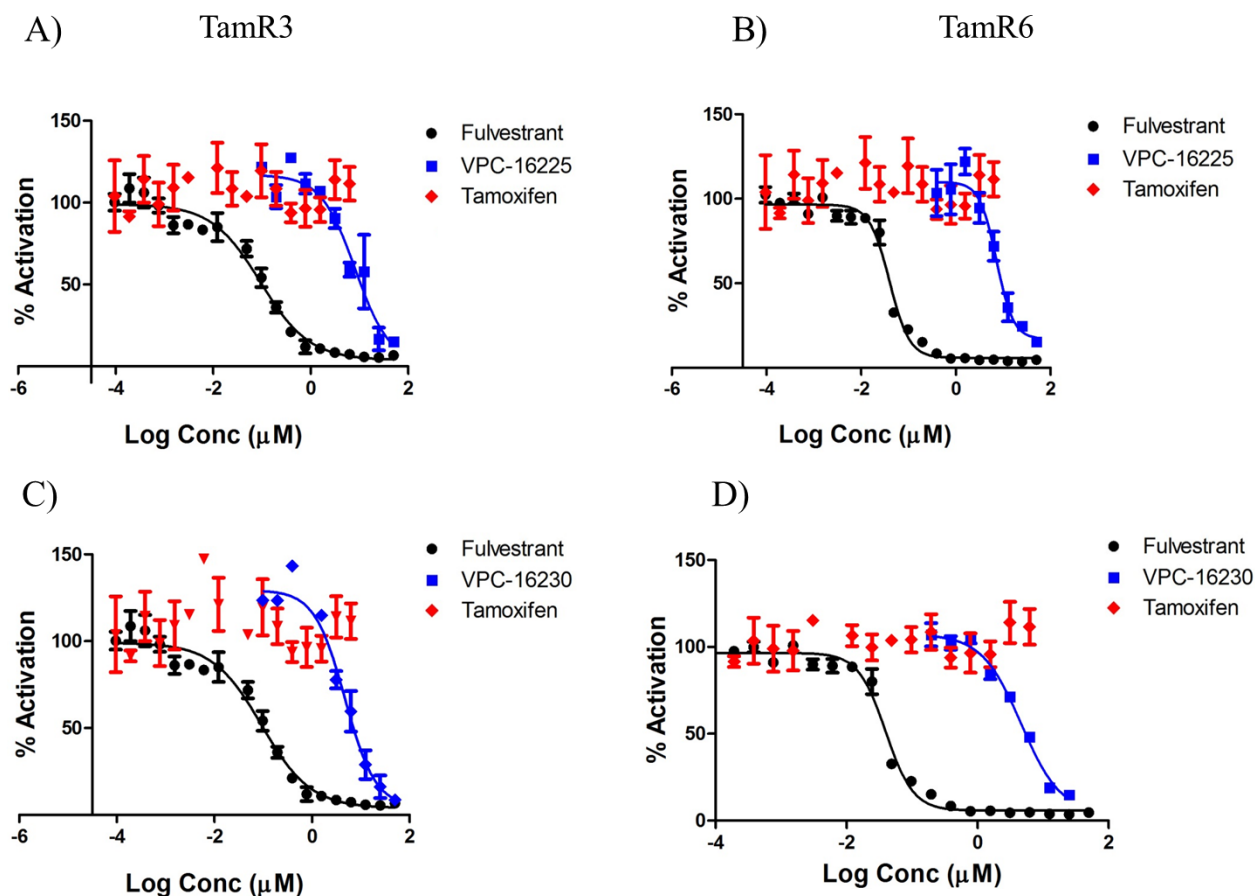
Figure 3.7. VPC-16230 and VPC-16225 inhibit ERα transcriptional activity in Tamoxifen resistant cells. Dose response curves (0.1-50 μM) of compound VPC-16225 for transcriptional inhibition of transiently transfected E2-responsive luciferase reporter in Tamoxifen resistant cells TamR3, IC_{50}: 8.2 μM (A) and TamR6, IC_{50}: 7.2 μM (B). VPC-16230 inhibits ERα transcriptional activity in a dose dependent manner in TamR3, IC_{50}: 4.7 μM (C) and TamR6, IC_{50}: 4.7 μM (D). Dose response curves (0.000095–50 μM) of Fulvestrant (IC_{50} in TamR3: 0.09 μM; IC_{50} in TamR6: 0.04 μM) and Tamoxifen (0.000095-6 μM) have been shown for comparison. Data points represent average of three independent experiments performed in triplicates. Error bars indicate standard error of mean (SEM) for N=3 values. Data was fitted using log of concentration of the inhibitors Vs % activation with GraphPad Prism 5.

3.2.7   VPC-16230 inhibits expression of ERα driven genes in MCF7 cells

VPC-16225 and VPC-16230 were measured for their effect on the mRNA expression levels of the estrogen responsive genes, pS2, Cathepsin-D and CDC2. MCF7 cells were treated with the test compounds for 24 h following which the mRNA was isolated and qRT-PCR analyses performed. While VPC-16225 did not show any significant effect (Figure 3.8D), VPC-16230 considerably reduced mRNA levels of these genes in a dose dependent manner (Figure 3.8A). However, when treated in the absence of E2, VPC-16230 did not significantly inhibit gene expression compared to the vehicle control (Figure 3.8B). The inhibition of gene expression in the presence of E2 was also observed at the protein level (Figure 3.8C).
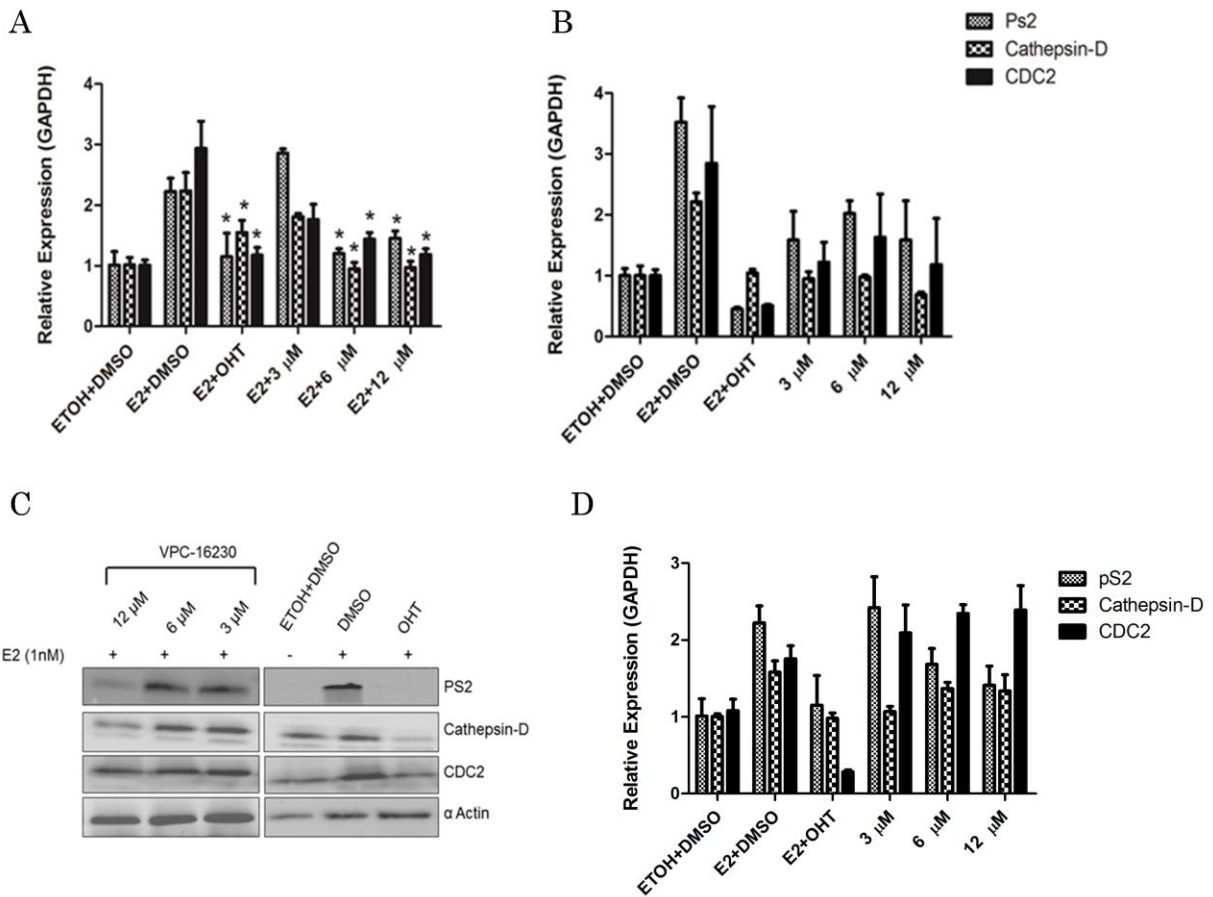
Figure 3.8. The lead compounds inhibit mRNA and protein expression levels of ERα dependent genes: (A) VPC-16230 significantly decreases mRNA levels of pS2, Cathepsin-D and CDC2 at 12 and 6 μM in the presence of 1nM E2 in MCF7 cells. Data points represent average of three independent experiments performed in triplicates. Error bars indicate standard error of mean (SEM) for N=3 values. A p value <0.05 was considered significant (*) compared to E2+DMSO control. (B) VPC-16230 does not significantly decrease mRNA levels of pS2, Cathepsin-D and CDC2 at 12, 6 and 3 μM in the absence of 1nM E2. (C) VPC-16230 decreases protein levels of pS2, Cathepsin-D and CDC2 at 12 and 6 μM in MCF7 cells as observed by western blot. (D) VPC-16225 had some effect on pS2 gene expression at high concentration but overall it did not significantly reduce the expression level of other genes in the presence of 1 nM E2 in MCF7 cells.

3.3   Discussion

With the use of in silico modeling, we have identified 15 structures that offer two novel classes of molecular scaffolds capable of inhibiting ERα-coactivator interaction at the AF2 site. These identified AF2 binders belong to two distinctive types: derivatives of pyrazolidine-3, 5 dione (Table 3.1) and carbohydrazide (Table 3.2). Molecular docking studies performed on the lead inhibitor, VPC-16230 suggested that the compound is likely to be anchored by three hydrogen bonds with the Lys362 and Gln375. In addition, 5-bromo-3-ethoxy-2-hydroxyphenyl and benzodioxene moieties of the VPC-16230 form strong hydrophobic contacts with Val368, Ile358, Leu372 and V376 (Figure 3.9).
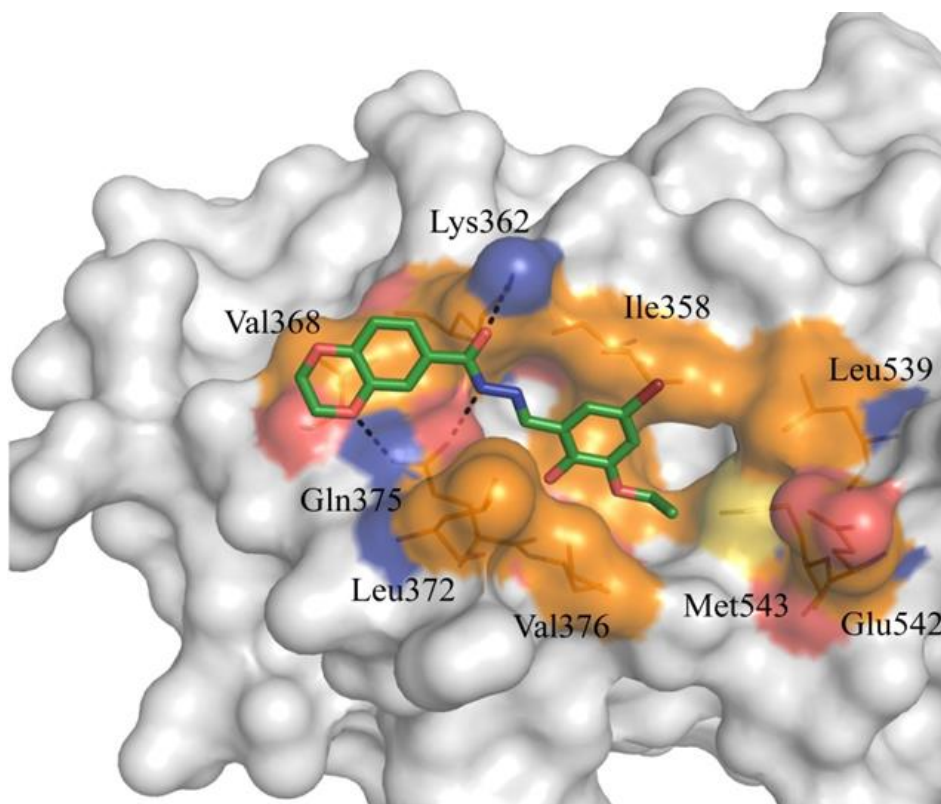
Figure 3.9. Predicted binding orientation of VPC-16230 inside the ER AF2 site. Hydrogen bond is shown in black. Hydrophobic residues are in brown, positive charged residues in blue and negative charged residues are in red.

VPC-13002, VPC-16225 and VPC-16230 appeared to be promising inhibitors of ERα transcriptional activation in cells and AF2 co-activator binding *in vitro*, demonstrating explicit dose response behaviour. These compounds show a right shift in their dose response curves upon increasing the concentration of the co-activator peptide as shown in figure 3.2A-C. This confirms that the compounds are in fact binding at the AF2 site. Further investigation of these molecules

using BLI binding assessment, E2 displacement assay and qRT-PCR experiments allowed characterizing VPC-16230 as the most promising ERα AF2 binder.

In luciferase assays the IC_{50} of VPC-16230 was established as 5.8 µM (in the presence of 1 nM E2). If we assume that this activity is due to the binding to EBS part of the receptor, then the binding affinity of the compound is $1/5800^{th}$ that of E2. This means that in direct ligand competition assay with Fl-E2, the compound should be able to compete with the fluorescently labelled E2 and its binding affinity should be close to $1/5800^{th}$ that of E2. However, when tested in the presence of 4.5 nM Fl-E2, the compound failed to displace the fluorescently labelled ligand even at concentrations as high as 150 µM (binding affinity ~ $1/30,000^{th}$ that of E2). The EC_{50} of unlabelled E2 for displacement of FL-E2 was established at 4.2 nM in this assay. Moreover, if VPC-16230 bound to the EBS, we would observe a shift in its IC_{50} values in the presence of higher concentrations of E2. This was not the case in T47D-KBluc cells where the inhibition by the compound was tested in the luciferase reporter assay in the presence of 1, 10, 50 and 100 nM E2. The dose response curve of the compound did not shift significantly with the IC_{50} varying only from 6.1 µM to 6.5 µM with 100 fold increase in E2 concentration. However, OHT presented a right shift of IC_{50} values from 0.004 to 0.5 µM, in proportion to a 100 fold increase in E2 concentration. Taken together, these observations confirm that the mechanism of action of VPC-16230 is not related to EBS binding and is likely to be through AF2 interaction.

Tamoxifen resistance remains a fundamental cause of therapeutic failure in BCa therapy. This creates a challenge for researchers in the field of BCa drug discovery. Studies have shown that the majority of resistant tumors retain dependence on ERα and E2 for survival. In this scenario, AF2 directed compounds could prove critical in suppressing tumor growth. To test this hypothesis we began by evaluating our compounds in two MCF7 derived Tamoxifen resistant

cell lines, TamR3 and TamR6. Results from the E2 dose response experiments with a reporter assay confirmed that these cell lines retain a functionally active ER. The E2 responsiveness suggests that ligand dependent co-activator recruitment at the AF2 site remains functional in TamR3 and TamR6 cells. Since our lead compounds VPC-16225 and VPC-16230 showed promising inhibition of ER transcriptional activity in an AF2-specific manner, we anticipated that these compounds should also be able to reduce the growth of these resistant cells. When tested in MTS assays, VPC-16225 and VPC-16230 demonstrated promising anti-proliferative effects in MCF7, TamR3 and TamR6 with no effect on ER independent MDA-MB-453 and HeLa cells. This is the first evidence of AF2 directed molecules with an inhibitory effect on Tamoxifen resistant cells. The tested compounds significantly inhibited the expression of a transiently transfected E2-responsive luciferase reporter in both TamR3 and TamR6, further confirming that the reduction in the growth of TamR3 and TamR6 is via ERα inhibition through AF2-directed action.

A comparison of the binding modes of AF2 ligands and Tamoxifen (Figure 3.9) revealed distinct differences in the structural conformation of ER. Tamoxifen allosterically affects co-activator recruitment by competitively inhibiting association between E2 and ERα EBS. This causes conformational changes in the receptor which eventually lead to movement of helix12 in such a way that it prevents the formation of the AF2 site. Since E2 continues to activate ERα, it means that the AF2 site is still accessible and the compounds can bind the pocket and inhibit the receptor in TamR3 and TamR6 cells. This provides a possible explanation why AF2 inhibitors are effective in these cells as observed in our assays.
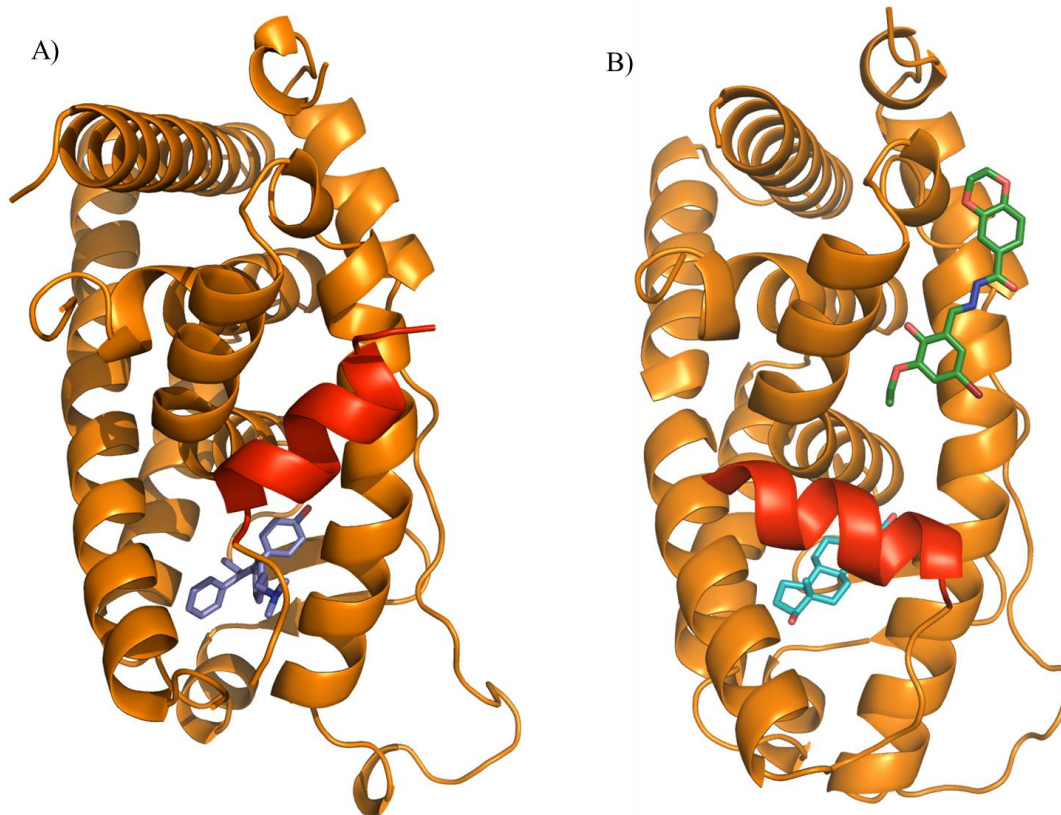
Figure 3.10. Antagonist and agonist models of estrogen receptor-α: (A) Binding of Tamoxifen (shown in purple color) to ER-α leads to an antagonist conformation, which results in repositioning of alpha helix-12 (show in red color) and prevents AF2 formation. (B) Binding of E2 (shown in cyan color) causes the movement of alpha helix-12 such that it opens up the AF2 pocket. In this scenario, AF2 inhibitor (shown in green) directly prevents interaction between co-activators and the receptor.

The downstream effect of ERα inhibition should be reflected as down regulation of its target genes. Out of the two compounds tested, VPC-16230 could significantly decrease E2 stimulated mRNA expression levels of ERα target genes such as pS2, cathepsin-D and CDC2 in MCF7 cells. However when treated in the absence of E2, the compound did not show any significant effect on the expression levels of these genes; this was expected since E2 is required

for the AF2 pocket to be formed and in its absence the compounds will not bind to the AF2 site and therefore will not show any effect. It is well established that E2 stimulates the proliferation of MCF7 cells, and it was observed that CDC2, a cell cycle associated gene whose expression was increased 3-fold upon E2 stimulation, was significantly reduced by VPC-16230. This observation correlates with the inhibition of proliferation by VPC-16230 of MCF7 cells in MTS assays. Since these genes are ERα-dependent, their inhibition corroborates the idea that blocking co-activator binding is a promising approach to inhibit ER activity in BCa cells. Since VPC-16225 did not significantly downregulate ER dependent gene expression, it was eliminated form further analysis.

Overall, these results indicate that targeting the AF2 site with small molecules represents a feasible therapeutic approach that allows successful inhibition of growth of Tamoxifen-resistant BCa cells. The only limitation of the study was we did not achieve great potency. Nonetheless, these derivatives were promising enough to carry out further hit-to-lead optimization efforts.

Chapter 4: Development of Benzothiophenone-Based Derivatives

4.1 Background

Although, the AF2 inhibitors reported[139] and discussed in chapter 3 demonstrated promising *in vitro* activity profile there was room for improvement in potency. Hence the current study was initiated to identify different chemical series using the carbohydrazide moiety of VPC-16230 as the chemical template for further drug optimization. As a result, benzothiophenone chemicals were identified with enhanced potency. The AF2 mediated mode of action was confirmed through *in vitro* assays. Moreover, mammalian two hybrid assay was developed to study effect on ERα-co-activator interaction in the cellular environment. Further, the compounds effectively blocked recruitment of a panel of co-activators as tested in TR-FRET and MARCoNI assays. The mechanism of action was probed using ChiP assay which indicated reduced binding of ERα on ERE in the presence of the compounds. This study showed that disruption of coactivator binding on AF2 destabilizes the ERα thereby preventing formation of transcription complex required for the functionality of the receptor. In preclinical studies, the lead AF2 inhbitor reduced tumor burden in an intraperitoneal model of MCF7LUC breast cancer. Overall this study was successful in exploring mechanism of action of AF2 inhibitors and their preclinical applications.

4.2 Results

4.2.1 Identification of VPC-16230 analogues using *in silico* modeling methods

Based on VPC-16230, a chemical template was designed (Figure 4.1) and a molecular similarity search was performed to identify the analogous compounds with different substitutions

around this template. Instant JChem, a 2D similarity searching tool from ChemAxon,[140] was employed to search through ZINC database.[141] As a result, a total of 2000 compounds were obtained for further analysis.

Using our *in-house* drug discovery pipeline, a total of 2000 compounds were virtually tested and selected. A previous study indicated that amino acids Lys362, Gln375, Val355, Ile358 and Leu379 are critical for protein-ligand coordination.[139] Therefore, the corresponding hydrophobic constraints were applied during *in silico* experiments. Based on the computational protocols described,[139] compounds belonging to benzothiophenone were purchased from chemical vendors and tested for their biological activity (Table 4.1).
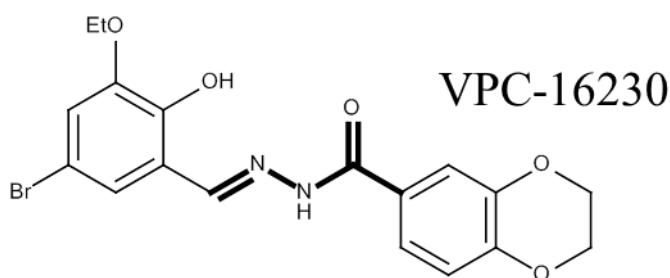
Figure 4.1. Chemical template input (highlighted in bold) derived based on VPC-16230.

Table 4.1. Structures and measured activities of the identified ER AF2 inhibitors.
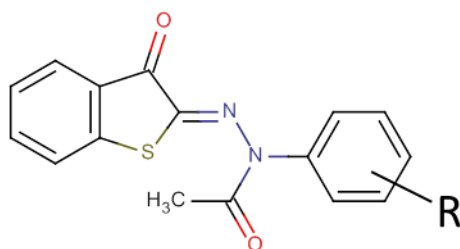
VPC-ID	R	IC$_{50}$ (µM)
16457	3-Me	3.78
16464	**2-Cl**	**2.7**
16487	2-F	4.643
16484	3,4-Me	9.833
16475	4-Me	12.25

4.2.2 Activity profile of VPC-16464

All of the purchased compounds were tested for their ability to inhibit ERα activity using the luciferase reporter assay.[139] These compounds exhibited activity in the range of 2-13 µM. VPC-16464 showed dose dependent inhibition of ERα driven luciferase gene expression with an IC$_{50}$ of 2.7 µM (Figure 4.2A). Furthermore, BLI studies demonstrated a direct, reversible and dose-dependent interaction between the ligand and the ERα LBD (Figure 4.2B).
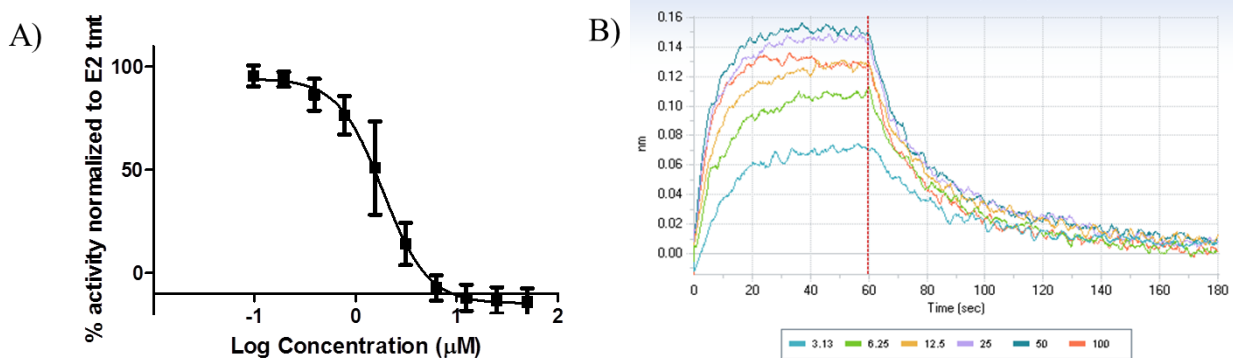
Figure 4.2. Activity Profile of Compound VPC-16464 (A) Dose-response curve illustrating the inhibiting effect of VPC-16464 (IC_{50} = 2.7μM) on ERα transcriptional activity in T47D cells. Data points represent the mean of two independent experiments performed in triplicate. Error bars represent the SEM for N = 3 values. Data were fitted using log of concentration of the inhibitors versus percent activation with GraphPad Prism 6. (B) BLI dose-response curves (3–100 μM) reflecting the direct binding of VPC-16464.

4.2.3 VPC-16464 stably binds to AF2 site during molecular dynamics simulations

Experimental outcomes like binding affinity are directly associated to microscopic behavior of the of the protein-ligand atoms. Since VPC-16464 demonstrated promising activity and binding, it was investigated how this compound exactly fits into the AF2 site. To understand this, molecular dynamics (MD) simulations, a computational method that calculates the time dependent behavior of a molecular system,[142] was performed. In MD simulations, the atoms and molecules are allowed to interact for a certain period of time, giving a view of the motion of the protein-ligand atoms.
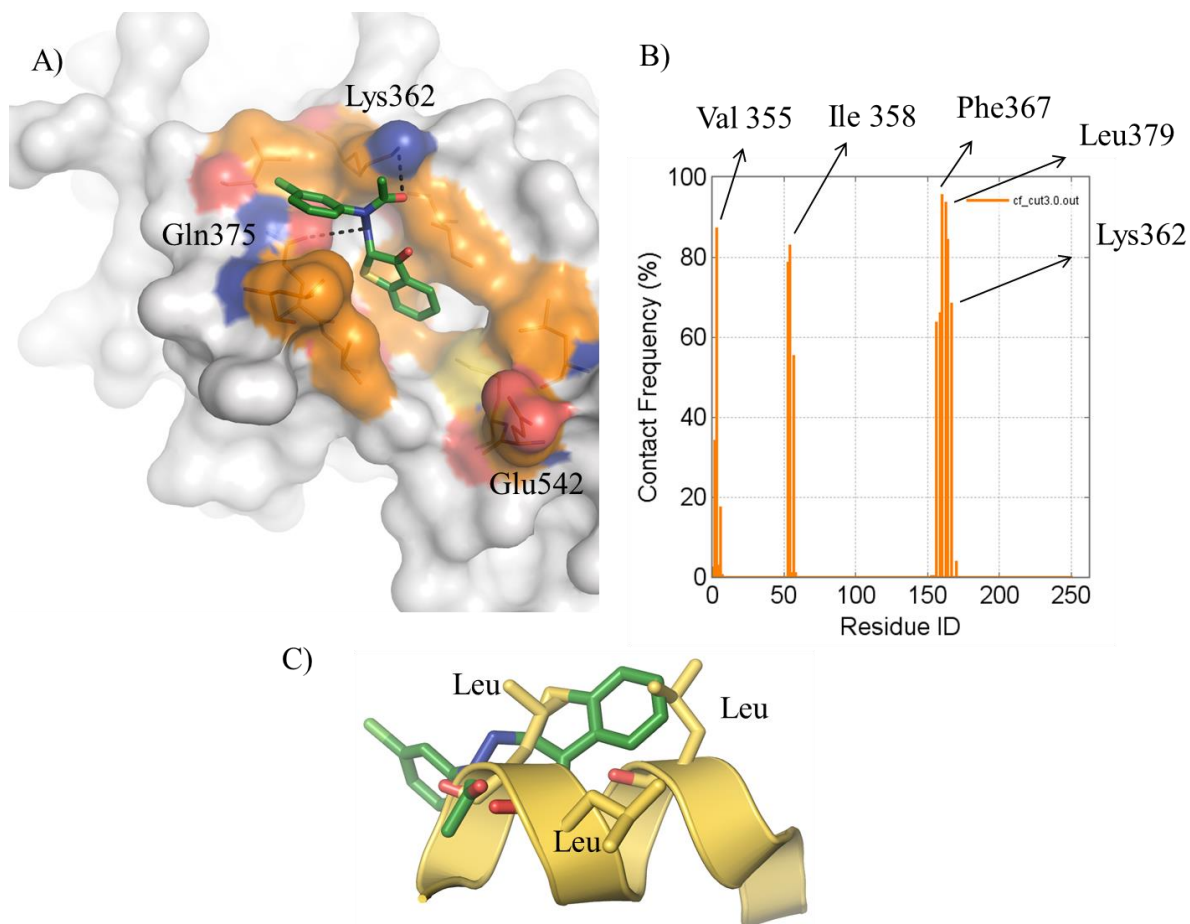
Figure 4.3. The analysis of MD simulations performed on ER AF2-VPC-16464 complex. (A) The most stable conformation of VPC-16464 obtained from MD simulations (green). H-bond interactions are shown in black dotted lines. (B) List of AF2 residues that are in close contact with the ligand during MD simulations. (C) Overlay of the compound VPC-16464 binding pose (green) over the α-helical LxxLL motif (yellow). Benzothiophenone group of VPC-16464 overlaps with the Leu of the LxxLL motif of the co-activator.

During 30ns-MD simulations it was observed that the compound was tightly bound to the AF2 site throughout the simulation period. Based on the binding free energy calculations, the most stable binding conformation of the VPC-16464 was identified (Figure 4.3A). Figure 4.3B

shows the AF2 residues having frequent contacts with the ligand during the MD simulations. For example, Val355, Ile358, Lys362, Phe367 and Leu379 had contact with VPC-16464 over 60% of the total MD simulation time. The benzothiophenone moiety forms strong H-bond interactions with Lys362 and Gln375 (Figure 4.3A). In addition, Ile358, Lys362, Val368 and Leu372 residues make strong hydrophobic contacts with the chemical core. Since MD simulations suggested VPC-16464 is a stable AF2 binder, a series of experiments were performed to evaluate its ability to displace co-activators from the AF2 site.

4.2.4   VPC-16464 blocks the interactions between co-activators and ERα AF2

Mammalian two-hybrid assay: The direct effect of VPC-16464 on ERα-co-activator interaction was assessed by mammalian two-hybrid system (Promega). ERα-LBD was cloned into pACT vector to produce ERα-LBD protein fused to the VP16 activation domain. The SRC-3 co-activator peptide (aa 614-698) containing LxxLL motives 1 and 2 was cloned into pBIND vector to produce SRC-3 protein fused to GAL4-DBD. MDA-MB-231 cells were transfected with pACT-ERα-LBD, pBIND-SRC-3, a luciferase reporter plasmid containing a GAL4 recognition sequence and a constitutively active renilla reporter plasmid. The cells were treated with VPC-16464 at 6 concentrations with a two-fold dilution starting from 50 µM. The compound significantly inhibited the interaction between ERα and SRC-3 in a dose dependent manner (Figure 4.4A). This provides direct evidence that the compound shows AF2 mediated activity.

TR-FRET assay: In this assay, a 3-fold dilution range of VPC-16464 starting at 50 µM was tested. It successfully displaced the Fluorescein-PGC-1a and SRC-2-3 co-activator peptides in a dose dependent manner (Figure 4.4B).

73
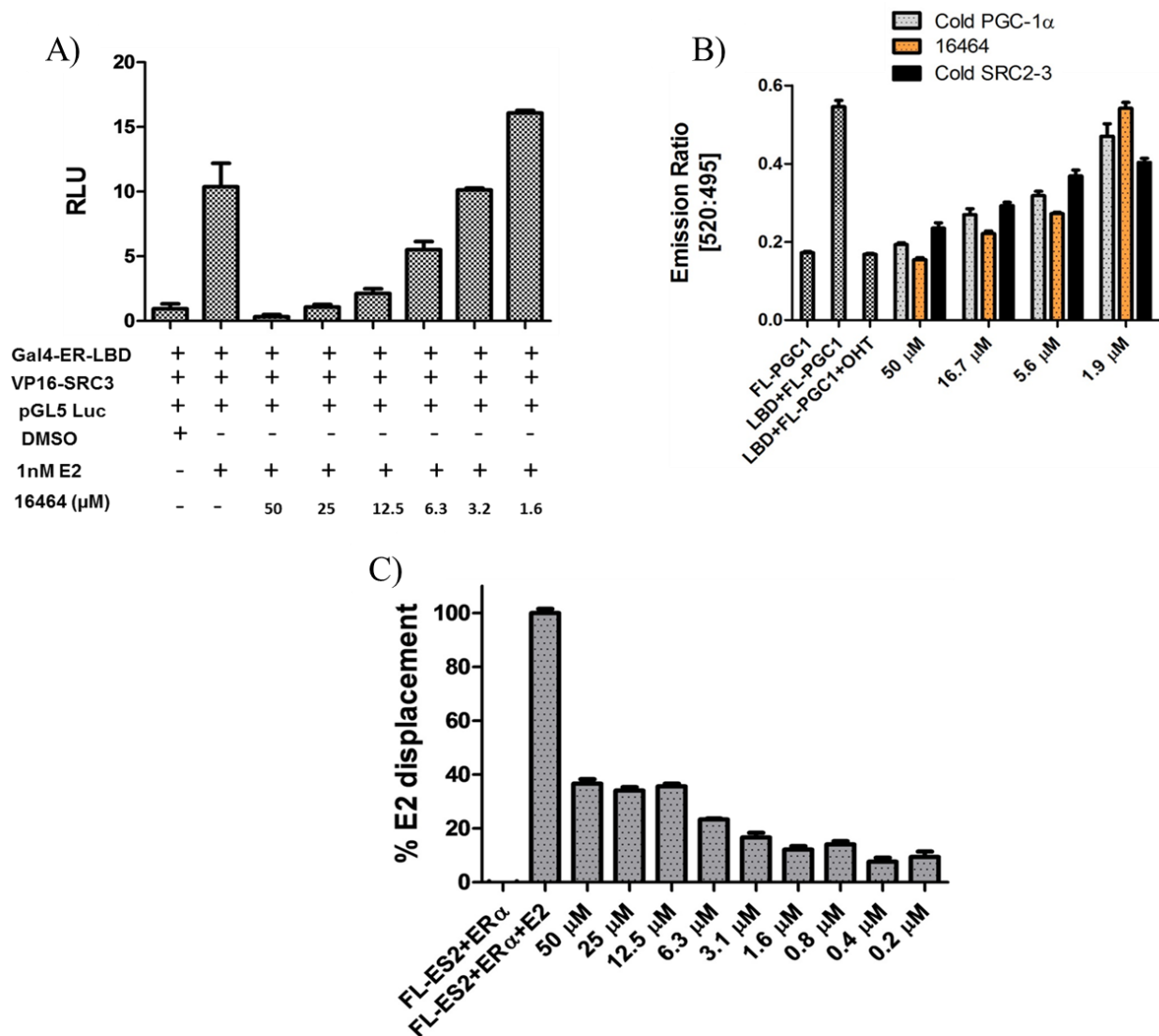
Figure 4.4. Further characterization of VPC-16464. (A) Mammalian two-hybrid system. MDA-MB-231 cells were transfected with the plasmids along with a constitutively active renilla reporter plasmid and treated for 24 h with 2-fold dilution series of VPC-16464 starting at 50 µM. The compound inhibited ERα-LBD interaction with the SRC-3 peptide in a dose dependent manner. (B) Peptide displacement was assessed with TR-FRET assay. Dose response curves were generated with 3-fold dilution series of test compound starting at 50 µM. (C) E2 displacement was measured by fluorescence polarization assay. VPC-16464 showed < 50% displacement of fluorescently labelled E2 (FL-ES2) at the highest

concentration of 50 µM. Non-labelled E2 was added as control. Error bars indicate standard error of mean (SEM) for N=3 values.

SERMs like Tamoxifen displace co-activators allosterically *i.e.* by binding to EBS. In order to confirm VPC-16464 is not an EBS binder like Tamoxifen, E2 displacement was assessed with the Polar Screen Estrogen Receptor-α Competitor Green Assay Kit (P2698, Life Technologies). The compound showed less than 40% inhibition at 50 µM (Figure 4.4C) confirming that it is a true AF2 binder.

4.2.5   VPC-16464 prevents interactions with several LxxLL motif containing peptides

In the cellular environment different types of co-activators can be recruited to the AF2 site. Therefore it was interesting to expand the study to a panel of co-activators expressed in the cell. In order to test this, Microarray Assay for Real time Co-regulator Nuclear receptor Interaction (MARCoNI) assay was used. This is a commercial service provided by Pamgene Inc., Netherlands. Basically, there are number of wells and each well contains a different type of co-activator peptide immobilized onto a matrix. The protein, detection antibody and test compound solution are continuously circulated through the matrix to form a homogenous environment. Binding of ERα to the peptide is detected and quantified through sensors (Figure 4.5).
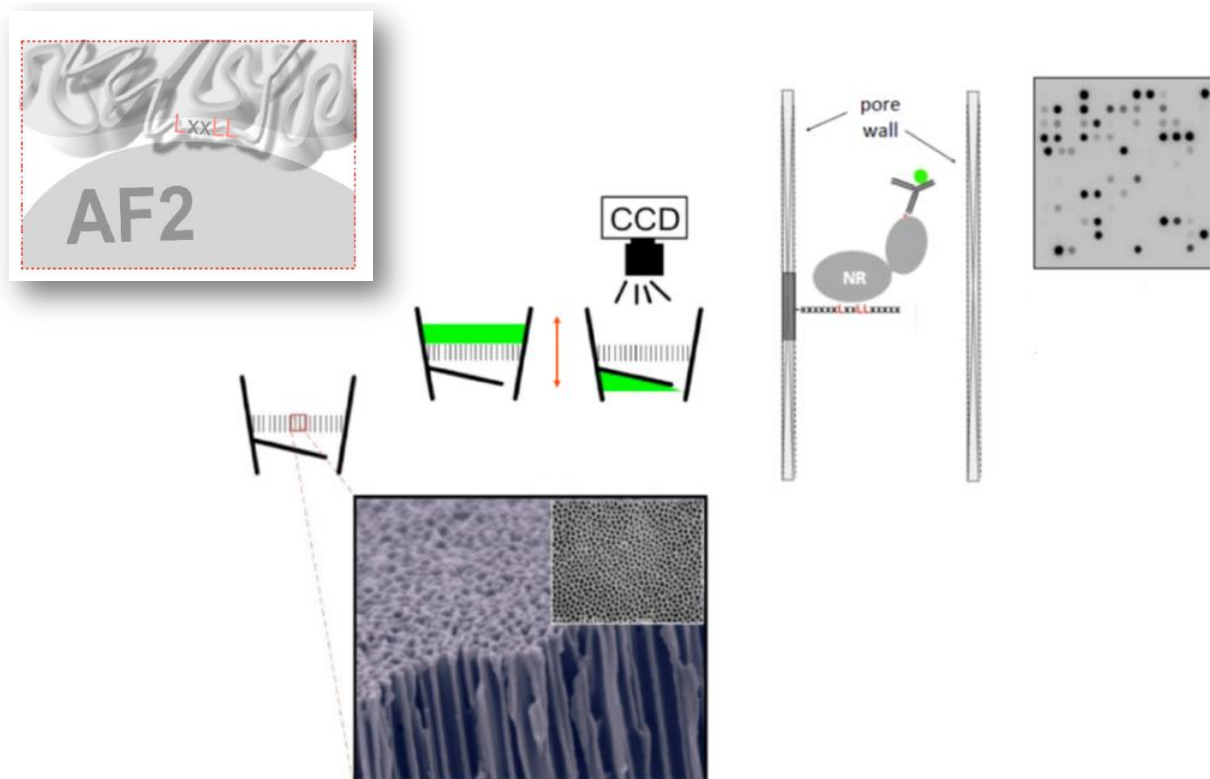
Figure 4.5. MARCoNI assay © (Pamgene Inc.) co-activator peptides are immobilized onto a matrix. Each well contains a different co-activator peptide. The binding of fluorescently labelled antibody bound ERα protein to co-activator is detected by sensors.

VPC-16464 was tested in this assay at the highest soluble concentration of 50 μM. The compound blocked the binding of ERα to five different types of co-activators with similar effect as the control peptide, PGC1 (Figure 4.6A). Looking closely into the sequence of these co-activators revealed that they all contained the LxxLL motif for binding to AF2 site (Figure 4.6B). These results were encouraging as they provided further proof that the compound works against not only SRC family but a variety of co-activators. Superimposing the compound structure onto the LxxLL motif of the peptide revealed that the compound has structural features that closely

resemble the key Leucine residues on this motif and therefore competes with peptide for binding (Figure 4.3C).

A)

B)

```
sp|Q8IZL8|PELP1_HUMAN     GASGEAL LTHLLSDISPPA
sp|Q05086|UBE3A_HUMAN     --SSELT LQELLGEERR--
sp|A5YKK6|CNOT1_HUMAN     --FIKQK LPDLLRSYIDA-
sp|P16455|MGMT_HUMAN      --FTRQV LWKLLKVVKFG-
sp|Q08999|RBL2_HUMAN      --MMDRH LDQLLMCAIY--
                                *  . **
```
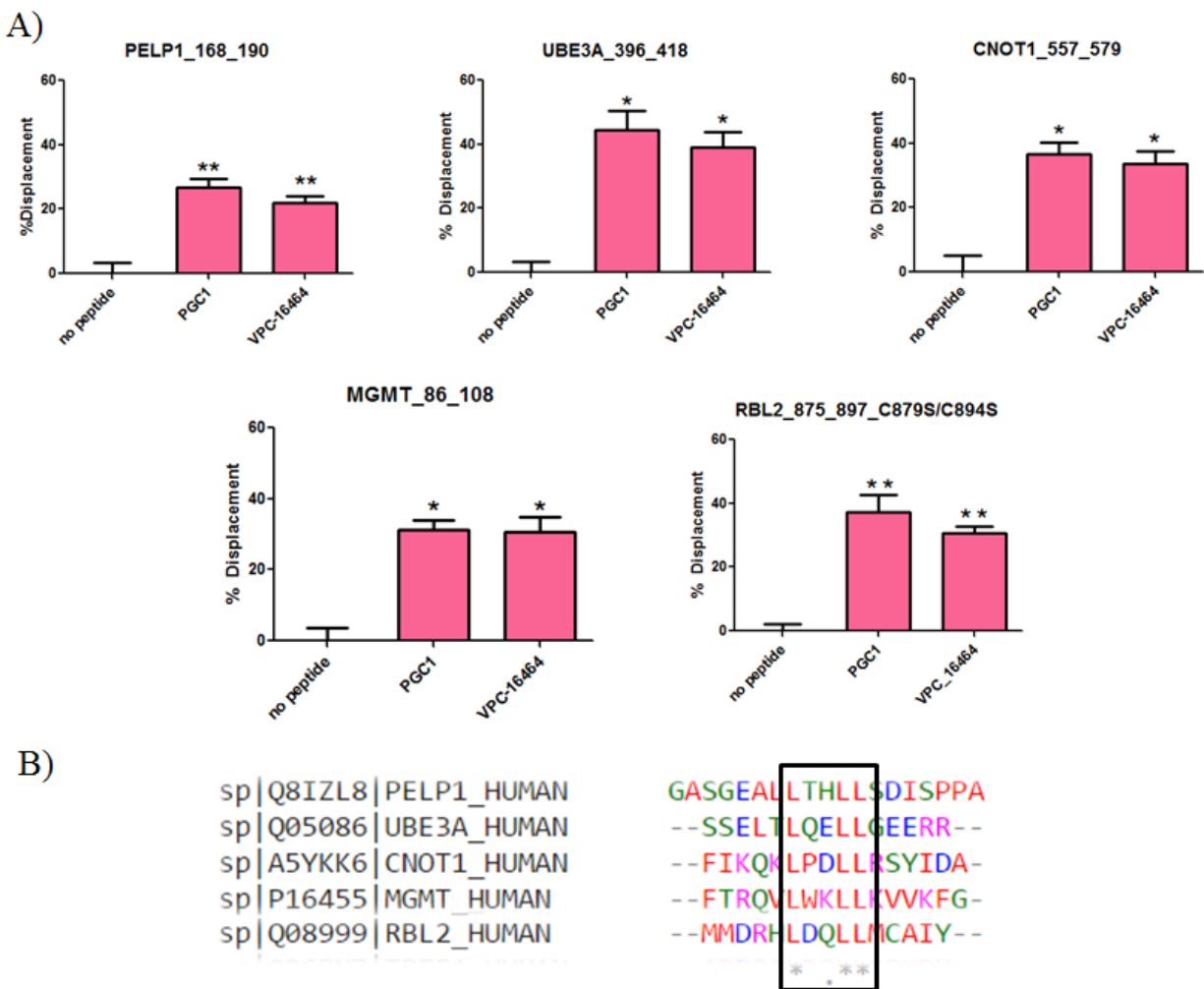
Figure 4.6. Effect of VPC-16464 on ERα-co-activator complexes. (A) VPC-16464 was tested on a panel of co-activators in the MARCoNI assay. Each graph panel represents a different co-activator. The pink bar in the middle is the positive control peptide, PGC1 and the bar on extreme right is the test compound VPC-16464. The compound could successfully inhibit binding of all these co-activator peptides to ER in a similar fashion as the control peptide. % displacement from control peptide and compound tested condition (ERα antibody) was statistically compared against no peptide condition with a two-tailed t test

(paired): *, p value < 0.05; **, p value < 0.01. (B) Sequence alignment of tested co-activators showing highly conserved LxxLL residues.

4.2.6   VPC-16464 inhibits the growth of ERα+ and TamR BCa cells

Presto Blue cell viability assay was used to assess the growth inhibitory potential of VPC-16464 on MCF7 and T47D and TamR3 cells. They were treated for 96 h with 2-fold dilution range of the compound starting at 50 µM. ERα negative MDA-MB-453 cells were used as a negative control. The compound significantly reduced the growth of the three cell lines without any effect on triple negative cells (Figure 4.7), which makes any off target effect on growth less likely.
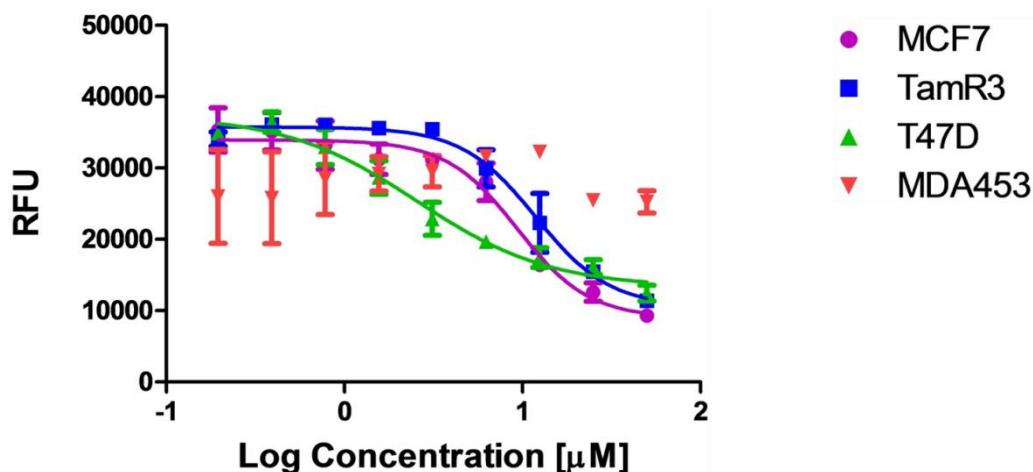
Figure 4.7. Dose-response curves of VPC-16464 showing decrease in cell viability as assessed by the Presto Blue viability assay. The cells were treated with the test compound for 96 h in the presence of 1nM E2 for MCF7 and 1nME2 + 1µM OHT for TamR3 cells. The compounds inhibit the growth of ERα-positive MCF7 and Tamoxifen resistant, TamR3 cells with very little effect on ERα-negative MDA-MB-453 cells. Error bars indicate standard error of mean (SEM) for N=3 values.

4.2.7 VPC-16464 down-regulates ER target genes in MCF7 and TamR3 cells

To further investigate the effect of inhibition of ER transcriptional activity by VPC-16464 expression levels of ER-regulated genes, PR, Ps2 and CDC2 in MCF7 and TamR3 cells were tested. VPC-16464 significantly down-regulated the expression of PR, Ps2 and CDC-2 mRNA at all the concentrations tested in those two cell lines (Figure 4.8A-D).
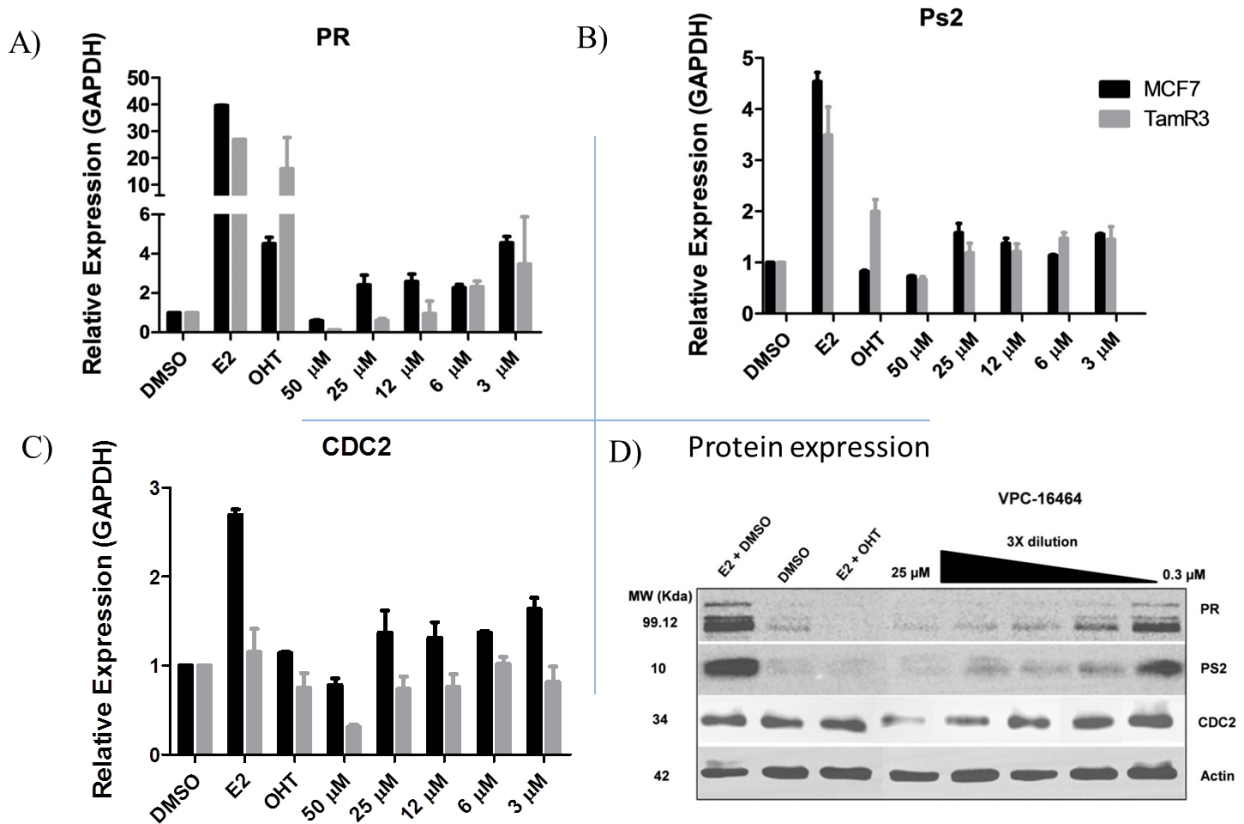
Figure 4.8. Effect of VPC-16464 on ER dependent genes. (A-C) VPC-16464 significantly decreased mRNA levels of ERα dependent genes PR, pS2 and CDC2 in MCF7 and TamR3 cells. Cells were treated with the test compound for 24 h in the presence of 1 nM E2. OHT was used as control. Error bars indicate standard error of mean (SEM) for N=3 values. (D) Effect of VPC-16464 on protein expression levels.

4.2.8 Lead optimization of VPC-16464

Based on MD simulations performed on ERα-16464 complex, the most stable binding orientation of VPC-16464 was identified as shown in figure 4.3A. Hence, a lead optimization based on this pose was initiated to enhance the potency as shown in figure 4.9. Derivatives where the S group was replaced with C or O were inactive, highlighting the importance of this group for activity. It should be observed that benzothiophenone moiety of VPC-16464 buried deeply into the AF2 site. Hence addition of a small hydrophobic group such as methyl group may favour the potency. Two more analogues were designed (VPC-16606 and 16607) with methyl and fluorine, respectively. As anticipated, 16606 demonstrated 10-fold increase in potency (Figure 4.10A) due to stronger van der Waals contacts with nearby residues.
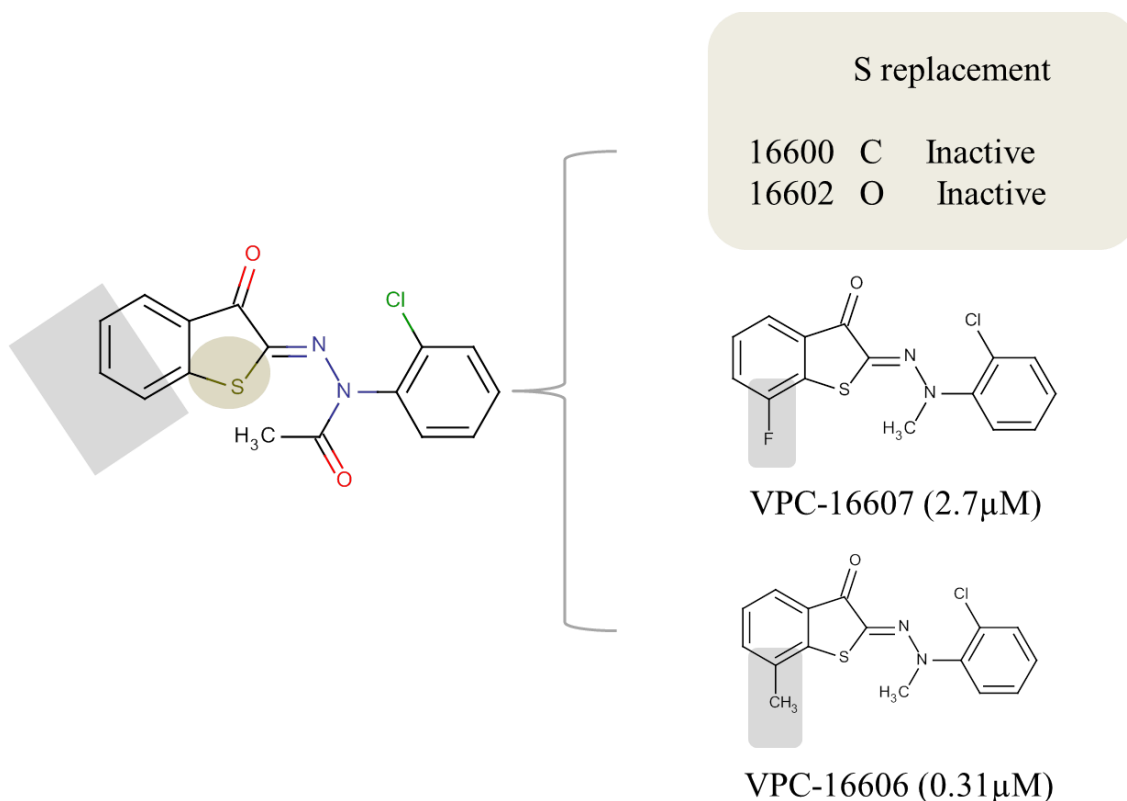
Figure 4.9. Design and development of benzothiophene derivatives.

Earlier analysis of ER AF2-16464 complex revealed the mechanism behind the possible displacement of peptides containing LxxLL motif from the AF2 site. The Leu residues of LxxLL motif make strong H-bond interactions with charge clamp residues. Due to the presence 7-methyl benzothiophenone in 16606, the compound binds more tightly at the binding pocket and disrupts H-bond interactions between Lys362 and AF2 residues. Moreover, 7-methyl benzothiophenone competes strongly with Leu of LxxLL motif in comparison with benzothiophenone of VPC-16464. Hence, greater free energy of binding for VPC-16606 was observed compared to VPC-16464. This explains why VPC-16606 exhibits stronger inhibition and displacement of co-activators of ER compared to its parental compound (2.7µM versus 0.31µM).
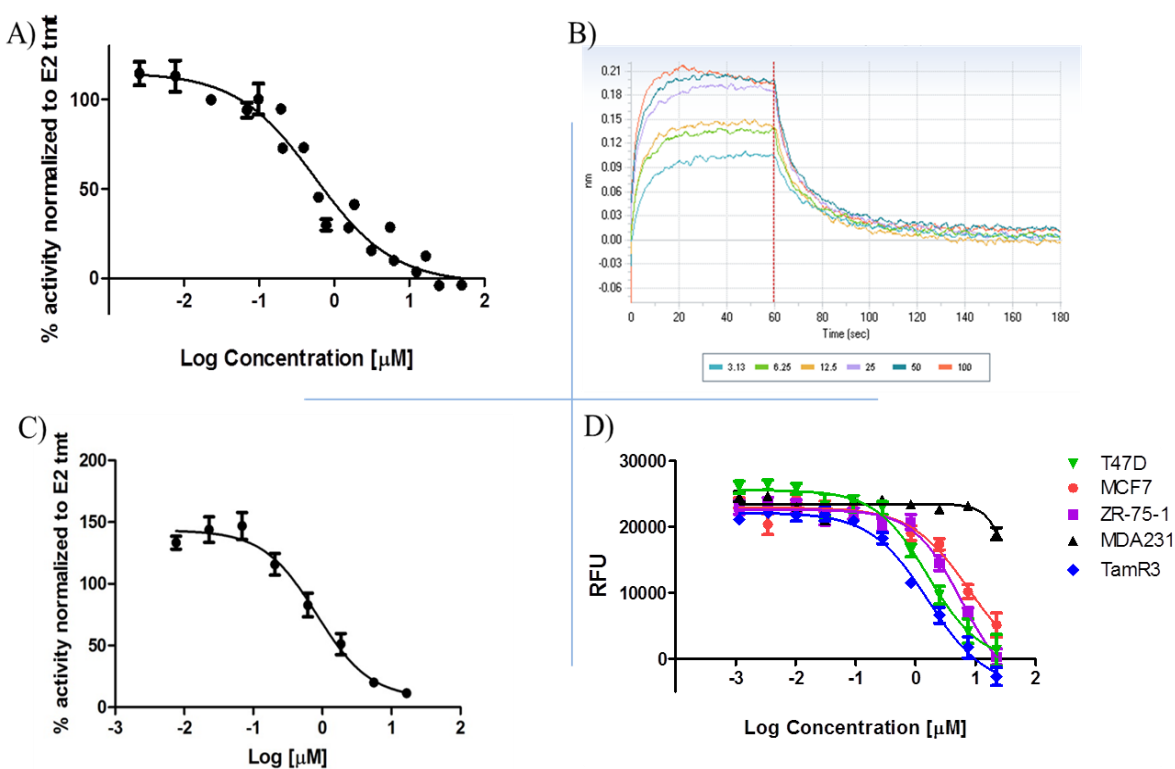
Figure 4.10. Activity profile of VPC-16606 (A) Dose-response curve illustrating the inhibiting effect of compound VPC-16606 (IC$_{50}$ = 0.31µM) on the ER transcriptional activity in T47D cells. (B) BLI dose-

response curves (3–100 μM) reflecting the direct binding of VPC-16606. (C) VPC-16606 inhibited ERα-LBD interaction with the SRC-3 peptide in a dose dependent manner in mammalian two-hybrid system. (D) Dose-response curves of VPC-16606 showing decrease in cell viability as assessed by the Presto Blue viability assay. Error bars indicate standard error of mean (SEM) for N=3 values.

4.2.9   Activity profile of VPC-16606

As shown in figure 4.10A the compound resulted in IC_{50} values of 0.31μM for its anti-ER activity in T47D cells and exhibited direct reversible interaction with ER LBD (Figure 4.10B). Importantly, the compound blocked the interaction between ER AF2 site and its co-activator effectively in mammalian two-hybrid system (Figure 4.10C). VPC-16606 was effective in reducing the growth of T47D, MCF7, ZR75-1 and TamR3 with no effect on ER-independent MDA 231 cells, confirming its ER-specific action (Figure 4.10D). Furthermore, VPC-16606 down-regulates Ps2, PR, Cyclin D1 and CDC2 in MCF7 and TamR3 cells (Figure 4.11).
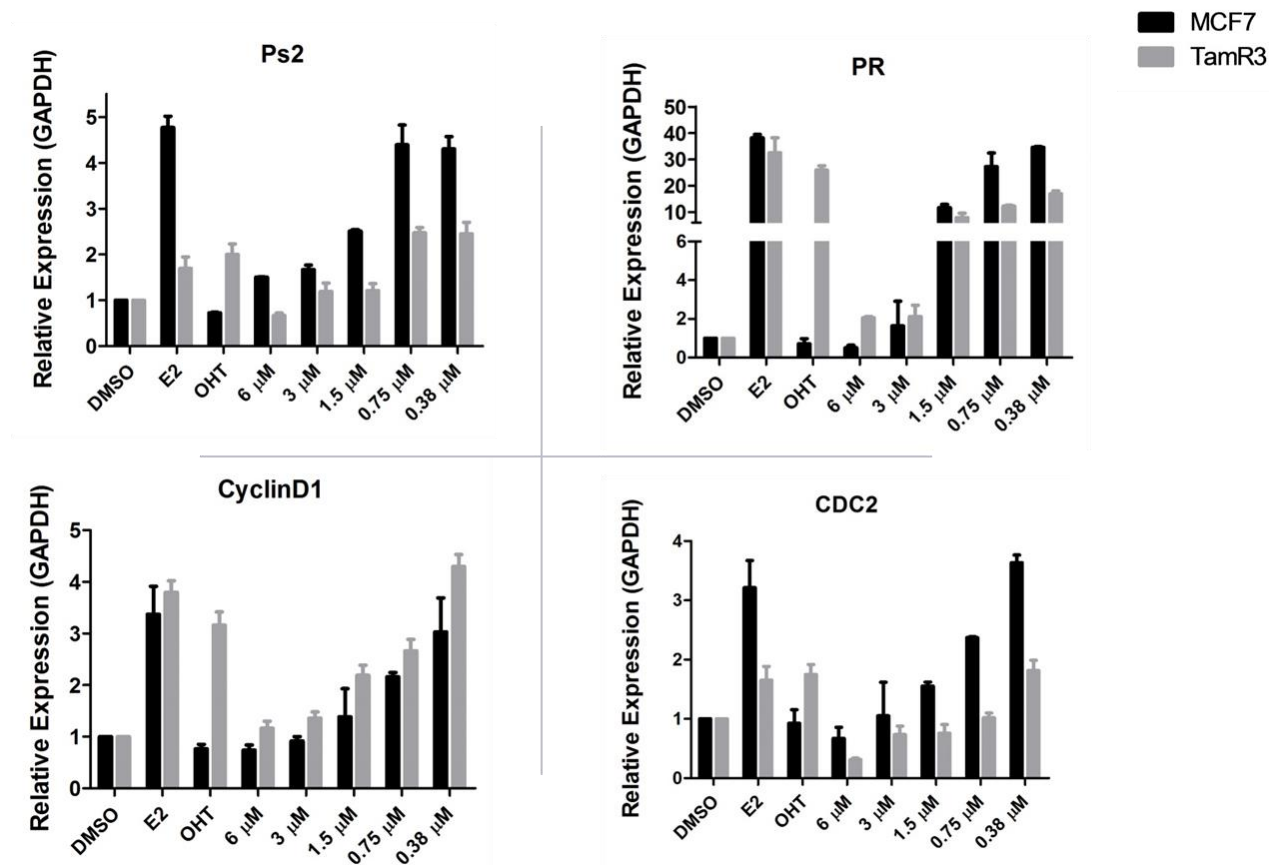
Figure 4.11. VPC-16606 significantly decreased mRNA levels of ER dependent genes, pS2, PR, CyclinD1 and CDC2 in MCF7 and TamR3 cells. Cells were treated with the test compound for 24 h in the presence of 1nM E2. OHT was used as control. Error bars indicate standard error of mean (SEM) for N=3 values.

4.2.10 VPC-16606 diminishes ERα binding on ERE

Binding of co-activators to the AF2 site is crucial for formation of the transcription complex. The SRC family of co-activators, such as SRC-1 aid the transcription process by interacting with hormone bound ERα to recruit other components of the large co-activator complex to the ERE of the target gene. They do so by interacting with the histone acetyltransferases CBP and p300 through their activation domain 1 AD1, with the histone

methyltransferases CARM1 and PRMT1 through their AD2 and with SWI/SNF (an ATP-dependent chromatin remodeling complex) through their AD3. The formation of such a co-activator complex results in chromatin remodeling and bridges the hormone-activated ERα with the general transcription machinery for transcriptional activation of its specific target genes.[143] Therefore the binding of SRC-1 to ERα is the first crucial step in initiation of transcription. Since the developed ERα inhibitors are designed to inhibit co-activator interaction with the receptor, it was important to evaluate whether this would affect ERα binding to the EREs of estrogen-regulated genes.

To test this ChIP assay was performed in MCF7 cells. The cells were treated for 24h with vehicle and estradiol either alone or in combination with VPC-16606. OHT was used as a positive control. The analysis of chromatin showed that VPC-16606 significantly reduced ERα pull down of the promoter of ER regulated gene, Ps2 compared to estradiol treatment alone. Control experiments revealed no pull down of the enhancers in the absence of E2, after OHT treatment or under any condition with the GAPDH promoter negative control (Figure 4.12). These results provide an explanation for the transcriptional inhibition of ERα observed in the luciferase and qRT PCR analyses. These results strongly suggest that blocking co-activator recruitment at the AF2 site prevents formation of transcription complex and therefore destabilizes binding of ERα on ERE.
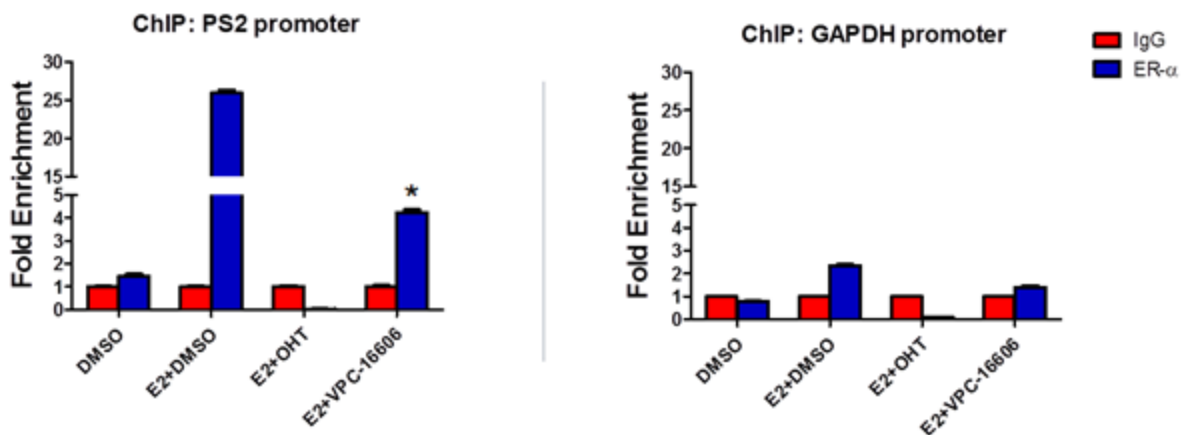
Figure 4.12. Effect of VPC-16606 on ERα-DNA complex. ChIP analysis of ER binding to the Ps2 enhancer, or the GAPDH promoter, in MCF7 cells. Where indicated, ERα was stimulated with 1 nM E2 (or DMSO only), and compound was administered at 10 μM concentration. Sheared chromatin-protein complexes were precipitated with the ERα antibody, reverse cross-linked, and analyzed by quantitative PCR. The results are normalized as fold enrichment over precipitation with a rabbit isotype control IgG antibody for each condition tested. Error bars indicate standard error of mean (SEM) for N=3 values. Fold enrichment from the compound tested condition (ERα antibody) was statistically compared against DMSO + E2 with a two-tailed t test (paired): *, p value < 0.05.

4.2.11   VPC-16606 is specific to ERα

The selectivity of VPC-16606 towards ERα was tested using a luciferase assay. Figure 4.13 demonstrates that VPC-16606 does not have a significant effect on androgen receptor (AR), glucocorticoid receptor (GR) and progesterone receptor (PR). The compound did not exhibit any significant effect on AR and PR. However, it showed some effect at 50μM on GR. But the dose at which the effect was observed is much higher than the effective dose on ER. Since there are similarities between the receptors as they belong to the same nuclear receptor superfamily, at high doses some effect could be observed but the rational design of these inhibitors exploits the

subtle differences between the amino acid residues among these receptors which allow room for specificity.
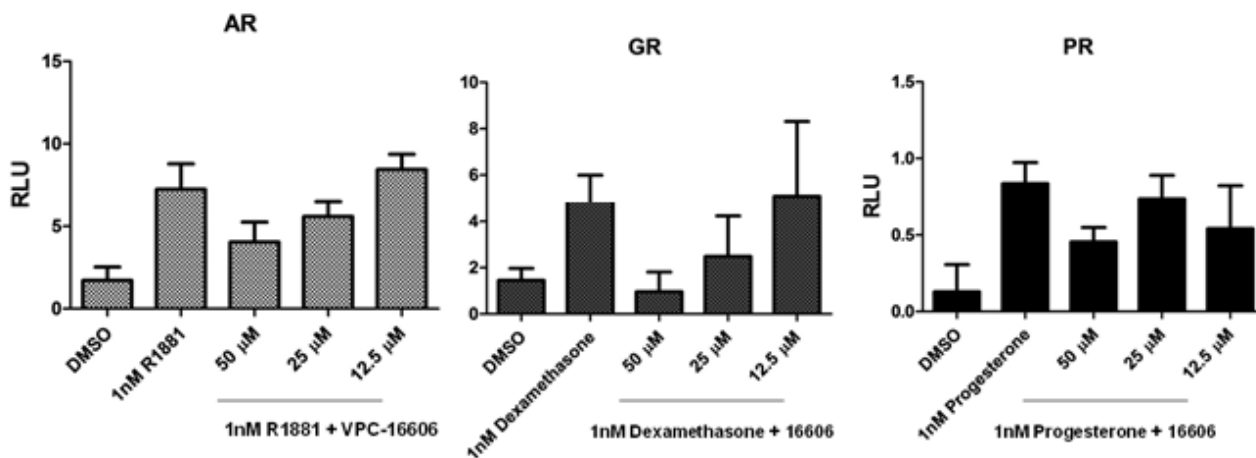
Figure 4.13. Specificity of VPC-16606 was evaluated in luciferase reporter assay. PC3 cells were transfected with plasmids expressing AR, PR or GR along with their responsive luciferase reporter constructs bearing ARE, PRE and GRE respectively. The cells were treated for 24 h followed by lysis and measurement of luciferase signal. Error bars indicate standard error of mean (SEM) for N=3 values.

4.2.12 VPC-16606 inhibits clinically relevant mutant forms of ERα

ESR1 mutations have long been speculated to play a role in endocrine therapy resistance but have been rarely detected.[126-128] However, various studies utilizing next-generation sequencing on ER+ metastatic clinical samples have revealed that recurrent *ESR1* mutations are far more frequent than previously thought and play an important role in acquired endocrine therapy resistance. The Y537S mutant has been shown by different groups to be constitutively active. The location of this residue outside the AF2 pocket is advantageous as the binding of VPC-16606 should not be affected by this mutation.

In order to study the structural effects of Y537S form of ERα in comparison with wild type (WT) to decipher the molecular mechanisms responsible for the hormone-independent activities of the mutant form, a molecular dynamic study was conducted. Computational modeling on Y537S form (in the absence of E2) revealed that mutated S537, located on H12, forms an additional H-bond interaction with neighboring D351 (Figure 4.14A). This causes the receptor to be in a constitutively open conformation causing it to recruit co-activators independent of E2 activation. It should be noted that this particular scenario does not occur in WT (Figure 4.14A).
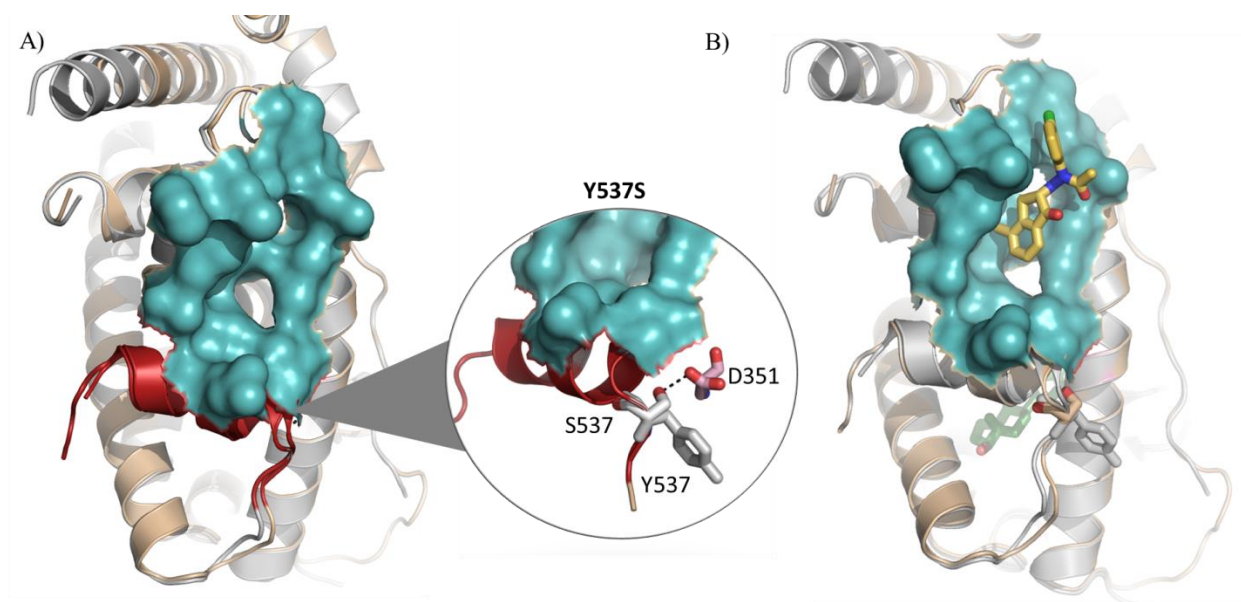
Figure 4.14. Graphical representation of WT ERα and its mutant form. (A) MD simulated structures of WT-type and Y537S form of ERα superimposed on each other. Wild-type is shown in grey whereas mutant form is shown in light brown color. Additional hydrogen bond formed between S537 and D351 of mutant form is shown in a circle. (B) Binding pose of VPC-16606 in WT and mutant form (yellow).

Next, the effect of VPC-16606 binding on both WT and Y537S forms was investigated. It was observed that there is no difference in compound orientation as topology and features of AF2 site in mutant form are highly similar to WT (Figure 4.14B). Moreover, the binding energies are similar for WT and mutant forms. Based on these observations it can be anticipated that VPC-16606 should exert similar activity on these two forms of ERα.

To test this hypothesis, all the clinically reported mutants (L536Q, Y537S, Y537C, Y537N, D538G, Y537S/D538G, S463P/Y537N) were synthesized using site-directed mutagenesis on WT-ERα. As shown in Figure 4.15A these mutants were constitutively active and unlike WT, showed stimulation independent of E2. Next, MDA-MB-231 cells were transfected with plasmids encoding either WT or mutant ER along with an estrogen responsive luciferase reporter plasmid and a constitutively active renilla reporter plasmid. The cells were treated with VPC-16606 with 2-fold dilution concentrations starting from 50 µM. As expected, the compound successfully inhibited all the mutant forms in the range of 0.5-1µM (Figure 4.15B). The expression levels of ERα from corresponding treatments were analyzed by western blot to confirm that the observed effect was not due to lower levels of the transfected receptor. The overall study is particularly important because it corroborates the idea that such clinically relevant mutant forms of the receptor which cause receptor to be E2 independent can be inhibited by targeting an alternative site on the receptor.
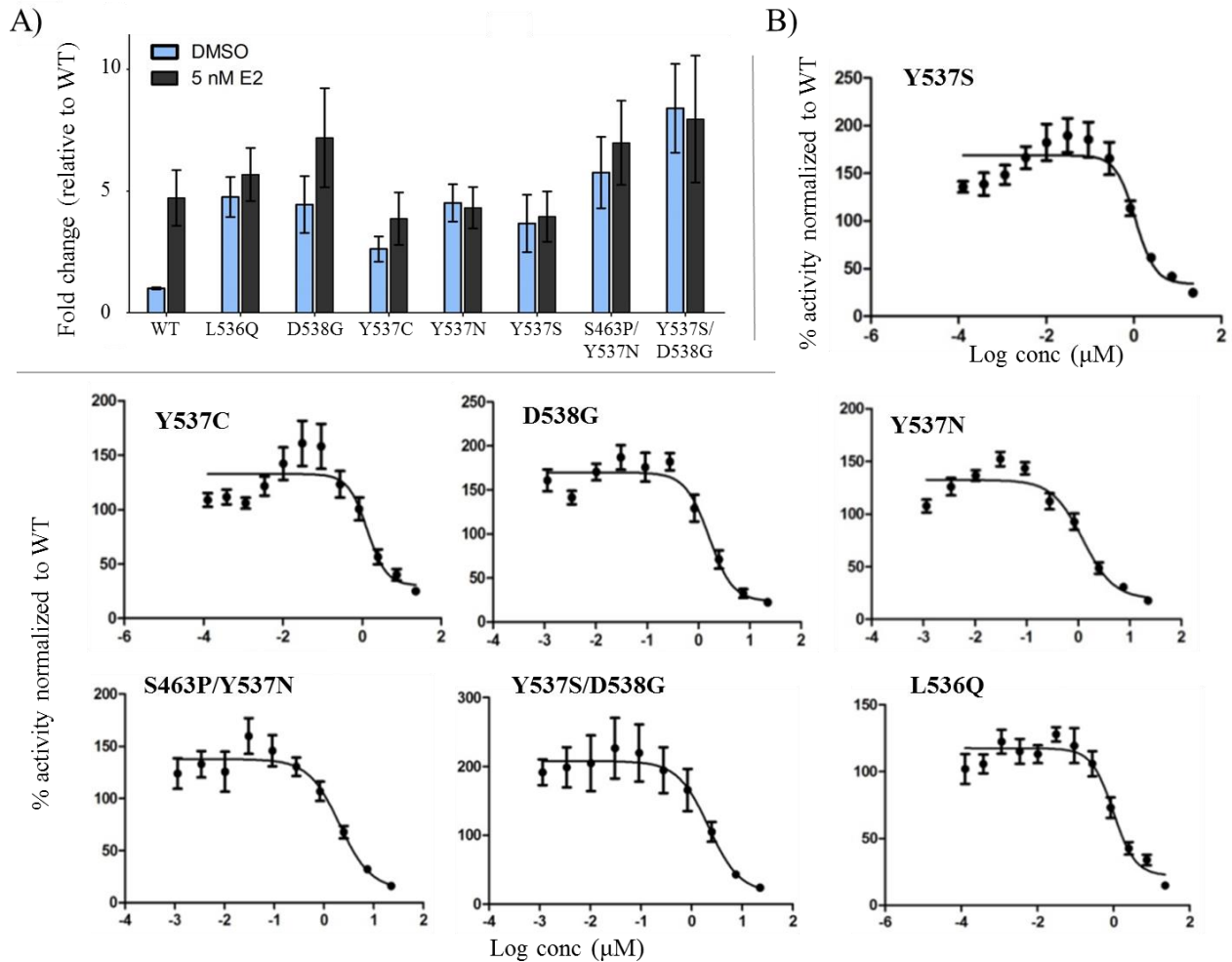
Figure 4.15. Effect of VPC-16606 on ER mutants. (A) E2 responsiveness of the synthesized mutants (B) pSG5 plasmid encoding either the full length WT or mutant forms of ERα was transfected into MDA-MB-231 cells along with the 3X-ERE-TATA luciferase reporter plasmid. The cells were treated with 2-fold dilution of VPC-16606 starting at 50 μM in the presence of 1 nM E2. The compound successfully inhibited the constitutively active mutant forms of the receptor in a dose dependent manner. Error bars indicate standard error of mean (SEM) for N=3 values.

4.2.13   VPC-16606 reduces tumor burden in mice

The next step towards developing a potential ER AF2 inhibitor is to test it in preclinical mouse models. The activity profile of VPC-16606 presented thus far indicates that this compound should reduce tumor burden in mice. This part of the study determined whether the favorable growth inhibition of BCa cells observed *in vitro* could be recapitulated *in vivo*. MCF7, a classic ERα-positive BCa cell line was chosen for tumor development. The cell line was luciferase modified to generate MCF7LUC to image and assess growth or possibly metastases with an *in vivo* imaging system. The intraperitoneal model of mice was chosen considering the fact that the peritoneal cavity is a site, albeit uncommon, of metastasis in BCa patients. In a comprehensive study of 21 (0.9% of the cohort) BCa patients with peritoneal metastases, 38.1% of the patients were luminal A and 23.8% were luminal B and only 9.5% were triple negative.[144] Therefore it was interesting to see if the compound could reduce tumor burden in this metastatic site. Moreover, with limited quantities of the drug available for the study the therapeutic activity could be best assessed by delivering the drug to the same site intraperitoneally.

VPC-16606 was used to treat mice with established MCF7LUC tumors. 10-12 weeks old female rag2 mice (n=6, per treatment group) were randomized for treatment with vehicle control or VPC-16606 (51 mg; administered through Alzet pump). The highest soluble concentration of the compound was used for treatment. Tumor growth was monitored using the non-invasive IVIS 200 imaging system to image luciferase expressing MCF7LUC cells. Tumors in animals treated with VPC-16606 exhibited reduced total light emission (luciferase expression) 60 days post-cell injection when compared with vehicle treated control mice (Figure 4.16A). Qualitatively analysis demonstrated tumor burden was less in mice that had received the compound treatment as compared with mice treated with the vehicle control.

The Kaplan-Meier survival analysis (Figure 4.16B) based on survival endpoints showed that the median survival time was 53 days for untreated mice and 60 days for mice treated with VPC-16606. It should be noted that all the mice in the latter group had scheduled euthanasia and survived to day 61 (end of the study) while only 3 of the 6 mice in the vehicle treated group were still alive at day 61 and the rest had been terminated due to tumor burden.
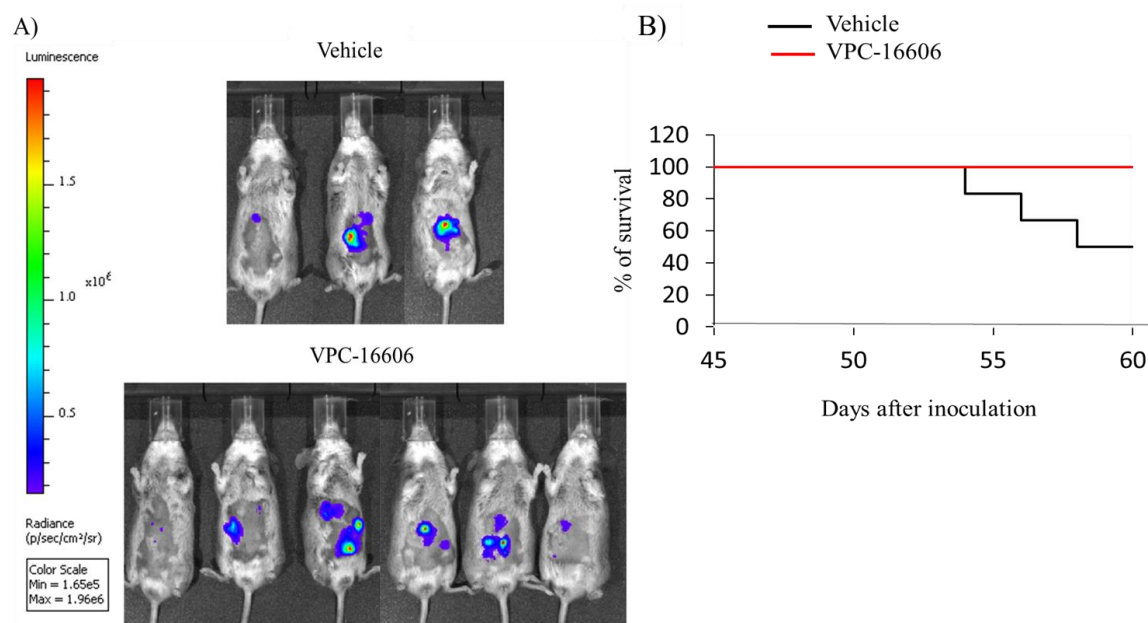
Figure 4.16. *In vivo* efficacy of VPC-16606. (A) VPC-16606 showed reduction of tumor burden in an intraperitoneal model of MCF7LUC BCa as measured by decrease in fluorescence in IVIS imaging. (B) Kaplan-Meier survival curve showing 100% survival at the end of the study in compound treated group.

4.3   Discussion

In this chapter, a systematic computer-guided lead optimization was performed on a derived carbohydrazide scaffold. Experimental screening of several derivatives led to the

identification of VPC-16464 bearing the benzothiophenone chemical moiety. This compound demonstrated an IC_{50} of 2.7 µM in the transcriptional assay and effectively displaced co-activator peptides from the AF2 site in i) *in vitro* TR-FRET assays ii) cell based two mammalian hybrid assay and iii) the MARCoNI assay developed at PamGene Inc., Netherlands. The most stable conformation of the VPC-16464 identified using MD simulation analysis (Figure 4.3) enabled to perform structure-based lead optimization to enhance the potency of the benzothiophenone chemicals (Figure 4.19). Replacing the S group of VPC-16464 with either C or O completely obliterated its activity highlighting its importance in compound binding. Adding Fluorine to the benzothiophenone core did not alter the potency since Fluorine does not facilitate non-polar interactions whereas addition of a methyl group resulted in 10-fold improvement in potency (VPC-16606) with an IC_{50} of 0.31 µM. Computational modeling of ER-16606 complex revealed that the presence of methyl group in ligand results in formation of additional van der Waals interactions with neighboring AF2 residues.

It has been further established that VPC-16606 did not displace estrogen but blocked ERα-co-activator interaction as measured by TR-FRET assays and a cell based mammalian two-hybrid assay, thereby confirming its AF2 specific inhibition of ERα (Figure 4.10). VPC-16606 exhibited strong anti-proliferative effect against a panel of ERα+ cell lines (MCF7, ZR-75-1, T47D) with no effect on ERα negative MDA-MB-453 cells, confirming its ER dependent activity (Figure 4.10). Inhibition of ERα activity by blocking co-activator recruitment resulted in down-regulation of ERα regulated genes, Ps2, PR and CDC2 both at mRNA and protein levels (Figure 4.11). Since the ultimate goal of developing new AF2 inhibitors is to target endocrine and Tamoxifen resistant BCa, VPC-16606 was tested against TamR cells. The compound showed significant reduction in the growth of TamR3 cells.

Computer modeling of the structural effects of the WT and Y537S ERα helped to decipher the molecular mechanisms responsible for the hormone-independent activities of the ER mutant forms. MD stimulations of the Y537S mutant bound to LxxLL peptide showed that Y537S form favors formation of the agonist conformation similar to WT ERα as shown in figure 4.15. During simulations, an additional hydrogen bond was observed in mutant form between S537 of helix 12 and D351. It should be noted that Y537 does not form any interaction with D351 in WT receptor. Furthermore, this stimulation is in agreement with the activity levels of the Y537S mutant, suggesting that the hydrogen bond stabilizes the agonist conformation, especially for the co-activator recruiting H12 helix and its surroundings and may contribute to the elevated activity of the mutant.

One of the critical applications of the developed AF2 inhibitor is its effectiveness on clinically reported ER mutants which cause resistance to existing anti-aromatase and anti-ER therapies. When VPC-16606 was tested against 5 single and 2 double constitutively active mutant forms of ER, it successfully inhibited the transcriptional activity of these mutants with similar efficacy as with the WT receptor (0.5 to 1µM versus 0.31µM; Figure 4.15). It should be noted that this offers a great advantage over the applicability of conventional hormone therapies as they require significantly higher doses. But due to dual agonist/antagonist activity of SERMs such an approach increases the risk developing endometrial cancer. *In vivo* efficacy of VPC-16606 was evaluated in an intraperitoneal model of MCF7-Luc BCa. The choice of intraperitoneal model over other popular models of BCa was mainly driven by the fact that the compound had poor microsomal stability. Female rag2 mice implanted with 1×10^6 MCF7-Luc cells were randomized for treatment with 50mg/kg of compound or vehicle and tumor growth was monitored using the IVIS imaging system. At the end of the study, all mice in VPC-16606

treated group had survived whereas only 50% mice survived in the vehicle treated group (Figure 4.16). Results from this study provide an indication of the potential value of this type of compound in reducing tumor burden.

Together, these studies helped to identify a novel class of ER AF2 inhibitors which have the potential to effectively inhibit ER activity by a unique mechanism and circumvent the issue of hormone resistance in BCa patients. This would likely decrease the time to cancer remission in those patients and eventually having a substantial impact on patient survival.

Chapter 5: Conclusion

5.1   Summary of the study

Several studies have previously confirmed that ERα signaling continues to play an important role even after the development of resistance to existing hormonal therapies. There are numerous mechanisms involved in the development of such resistance including point mutations in ERα. Moreover, conventional and clinically used anti-ERα agents share a similar chemical scaffold and act by direct binding to the receptor's EBS and, hence, are vulnerable to mutations (such as Y537S) arising around the EBS which can confer resistance.[145-147] Moreover, cross-talk between ERα and activated growth factor receptor pathways[148] as well as notch signaling pathways[149] have been shown to play a major role in activating ERα even in the absence of its native ligand, E2. Thus, drugs that target ERα EBS can become ineffective with time. Therefore, there is an urgent need to develop alternative therapeutic strategies. This thesis work addresses the problem by using the combined power of computer modeling, biological screening and medicinal chemistry to develop an entirely novel class of cancer drugs that directly target the AF2 site without any cross-reactivity toward the EBS.

Since the AF2 pocket plays a pivotal role in mediating ERα function, targeting this site offers a rich opportunity for the discovery of a whole new class of anti-BCa drugs. Inhibiting ERα in this manner offers several advantages over conventional anti-estrogens for the treatment of Tamoxifen-resistant and metastatic BCa. First, by targeting a different site from the EBS, AF2 inhibitors should be effective against hormone resistant BCa, since mutations around the EBS should have no effect on the efficacy of AF2 binders. Furthermore, since all conventional anti-estrogens bind to the EBS, they cannot be used therapeutically in combinations. By targeting a different site on the ERα, a given AF2 inhibitor could be added to the repertoire of available

antiestrogens as another option for patients who have relapsed on current therapy, thereby significantly increasing relapse free interval and more importantly increasing survival rate of breast cancer patients. Moreover since they directly bind to the AF2 site, they would be highly beneficial against the constitutively active ER mutations developed in metastatic patients who have progressed on aromatase inhibitors.

Our group has previously utilized the power of virtual screening combined with experimental evaluations to discover a number of small-molecules that effectively target other therapeutic targets.[136-138, 150] Therefore, taking the advantage of the crystallographic structure of ERα (pdb id-3UUD), millions of compounds were screened virtually. My role as a PhD student was to develop and optimize the entire experimental pipeline required to evaluate these virtual hits developed for BCa project.

In the first part of this study, compounds belonging to pyrazolidine-3, 5 dione and carbohydrazide scaffold (as discussed in Chapter 3) were identified. From these chemicals, VPC-16230 was used as an input template to search for further analogues using high-powered computational modeling methods as described briefly in Chapter 4. Consequently, VPC-16464 bearing the thiobenzimidazole moiety was developed with a much improved activity profile against ERα with an IC_{50} of 2.7 µM in ERα transcriptional assay. Upon testing, it effectively blocked the binding of a panel of different co-activators at AF2 site in both *in vitro* and cell based assays without any cross reactivity with EBS. In addition, this compound competes with several LxxLL co-activator peptides and prevents their interaction with ERα in MARCoNI assays (Pamgene Inc., Netherlands). These outcomes confirm that VPC-16464 is a true AF2 binder.

MD simulations performed on the ERα-16464 complex system showed that VPC-16464 stably binds to the AF2 site through the entire simulation time of 30 ns. Moreover, this study helped to elucidate the most stable binding orientation of the ligand which consequently helped to guide further medicinal chemistry optimization. As a result, four derivatives of VPC-16464 were rationally designed and synthesized to enhance potency. Among the developed synthetic derivatives, VPC-16606 demonstrated a 10-fold increment in anti-ER activity compared to its parental molecule (2.7 μM vs 0.31μM). Such an improvement in potency can be explained by computational modeling. MD simulations analysis suggested that the presence of a 7-methyl group on benzothiophenone of VPC-16606 forms additional hydrophobic interactions in the AF2 pocket leading to stronger binding and inhibition. As anticipated, VPC-16606 demonstrated excellent activity profile in further assays tested. Importantly, it effectively reduced the growth of a panel of ERα positive breast cancer cell lines including Tamoxifen resistant cells.

The developed ER AF2 inhibitor VPC-16606 prevented co-activator binding in a dose dependent manner in cell based mammalian two hybrid assay and down-regulated the expression of ERα regulated genes in ERα positive and Tamoxifen-resistant cells. In ChIP assays, VPC-16606 blocked co-activator recruitment and inhibited the formation of co-activator complexes which eventually destabilized ERα binding on EREs of target genes. This could explain mechanism of action of the AF2 compound. However a ChIP-Seq analysis would be useful to provide a better picture of how coactivators are globally affected due to the compound. VPC-16606 demonstrated specificity towards ER which is a crucial feature for a potential drug candidate. It does not bind to the conventional EBS thereby highlighting its unique mechanism of action.

Recently, Toy *et al* and Robinson *et al* performed two independent studies and both groups identified recurrent mutations affecting the EBS of *ESR1* gene that were not observed in unselected or untreated populations. They confirmed that ERα mutants are constitutively active (even in the absence of its natural ligand, E2) and promote hormone-independent tumor growth after estrogen deprivation *in vivo*. Therefore, the most important and clearly the most significant relevance of our developed AF2 inhibitor is its effectiveness on clinically reported ER mutants which cause resistance to current therapies. Computational modeling efforts revealed that such mutations cause the receptor to adopt an agonist conformation in which Helix 12 is oriented in such a way that the AF2 pocket remains open even in the absence of hormone, leading to constitutive activity of the receptor. This is exactly the scenario in which an AF2 inhibitor, as an alternative therapeutic strategy to inhibit ER signaling, should provide a significant benefit over conventional and currently available hormone therapies. Upon testing the effect of VPC-16606 on all the clinically reported ER mutants it was found that indeed our AF2 ligand inhibits mutant forms with similar potency as with WT ER. Hence this type of drug would provide another treatment option to BCa patients who have relapsed on traditional drugs thereby significantly extending their life.

Finally, since VPC-16606 showed promising profile in cell based assays, it was tested in an intraperitoneal model of MCF7LUC breast cancer. The compound was administered through Alzet pumps and the effect of this compound on tumor burden was assessed as a decrease in fluorescence signal. At the end of the study, the compound treated group showed 100% survival compared to the vehicle group with only 50% survival rate. The outcome of this study provides proof of principle that although, shallow surface exposed pockets such as AF2 are very

challenging to work on, small molecule inhibitors targeting this site have the potential to be developed as alternative therapeutics for treatment of breast cancer.

5.2 Future directions

Although the current thesis work has successfully identified AF2 inhibitors as promising drug proto-types, however, in retrospect several improvements are feasible for future studies.

1.   A key component in drug discovery is the process of achieving the optimum combination of potency and stability of a drug-like candidate. Though VPC-16606 was confirmed to be very potent, its potential to become a drug candidate is restricted by its poor microsomal stability. There is scope for further optimization of the scaffold to enhance its pharmacokinetic profile. This would enable lower and less frequent dosing and oral route of administration.

2.   Potential toxic effects of VPC-16606 in *in vivo* studies could be identified by examining the internal organs (liver, gall bladder, spleen, lung, kidney and heart) of the mice used in the study.

3.   The efficacy of improved AF2 inhibitors could be further evaluated in *in vivo* model of TamR cells and patient derived models of clinically relevant ERα mutant forms.

4.   A major clinical impact of the AF2 inhibitors would be if they may be used in combination with other clinical agents such as Everolimus (mTOR inhibitor) to possibly avoid or delay progression to resistance.

Bibliography

1.   Horoszewicz, J. S.; Leong, S. S.; Chu, T. M.; Wajsman, Z. L.; Friedman, M.; Papsidero, L.; Kim, U.; Chai, L. S.; Kakati, S.; Arya, S. K.; Sandberg, A. A. The LNCaP cell line--a new model for studies on human prostatic carcinoma. *Progress in clinical and biological research* **1980,** 37, 115-32.
2.   Sorlie, T.; Tibshirani, R.; Parker, J.; Hastie, T.; Marron, J. S.; Nobel, A.; Deng, S.; Johnsen, H.; Pesich, R.; Geisler, S.; Demeter, J.; Perou, C. M.; Lonning, P. E.; Brown, P. O.; Borresen-Dale, A. L.; Botstein, D. Repeated observation of breast tumor subtypes in independent gene expression data sets. *Proc Natl Acad Sci U S A* **2003,** 100, 8418-23.
3.   Szakacs, G.; Paterson, J. K.; Ludwig, J. A.; Booth-Genthe, C.; Gottesman, M. M. Targeting multidrug resistance in cancer. *Nature Reviews Drug Discovery* **2006,** 5, 219-34.
4.   Thomas, C.; Gustafsson, J. A. The different roles of ER subtypes in cancer biology and therapy. *Nat Rev Cancer* **2011,** 11, 597-608.
5.   Hewitt, S. C.; Couse, J. F.; Korach, K. S. Estrogen receptor transcription and transactivation Estrogen receptor knockout mice: what their phenotypes reveal about mechanisms of estrogen action. *Breast Cancer Res* **2000,** 2, 345-52.
6.   Niemeier, L. A.; Dabbs, D. J.; Beriwal, S.; Striebel, J. M.; Bhargava, R. Androgen receptor in breast cancer: expression in estrogen receptor-positive tumors and in estrogen receptor-negative tumors with apocrine differentiation. *Modern Pathol* **2010,** 23, 205-12.
7.   Lewis-Wambi, J.; et al. Treatment of Postmenopausal Breast Cancer with Selective Estrogen Receptor Modulators (SERMs). *Breast Dis* **2005,** 24, 93-105.
8.   EBCTCG. Effects of chemotherapy and hormonal therapy for early breast cancer on recurrence and 15-year survival: an overview of the randomised trials. *Lancet* **2005,** 365, 1687-717.
9.   Johnston, S.; et al. Changes in estrogen erceptor, progesterone receptor and ps2 experssion in tamoxifen resistant human breast cancer. *Cancer Res* **1995,** 55, 3331-8.
10.   Harrell, J.; et al. Estrogen receptor positive breast cancer metastasis: Altered hormonal sensitivity and tumor aggressiveness in lymphatic vessels and lymph nodes. *Cancer Res* **2006,** 66, 9308-15.
11.   Shang, Y. F. Hormones and cancer. *Cell Res* **2007,** 17, 277-9.
12.   Koos, R. D. Minireview: Putting physiology back into estrogens' mechanism of action. *Endocrinol* **2011,** 152, 4481-8.
13.   Liang, J.; Shang, Y. F. Estrogen and Cancer. In *Annual Review of Physiology, Vol 75*, Julius, D., Ed. 2013; Vol. 75, pp 225-40.
14.   Miller, W. L.; Auchus, R. J. The molecular biology, biochemistry, and physiology of human steroidogenesis and its disorders. *Endocrine Rev* **2011,** 32, 81-151.
15.   Cleary, M. P.; Grossmann, M. E. Obesity and Breast Cancer: The Estrogen Connection. *Endocrinol* **2009,** 150, 2537-42.
16.   Nilsson, S.; Koehler, K. F.; Gustafsson, J. A. Development of subtype-selective oestrogen receptor-based therapeutics. *Nat Rev Drug Discovery* **2011,** 10, 778-92.
17.   Kuiper, G.; Enmark, E.; PeltoHuikko, M.; Nilsson, S.; Gustafsson, J. A. Cloning of a novel estrogen receptor expressed in rat prostate and ovary. *Proc Natl Acad Sci U S A* **1996,** 93, 5925-30.

18.   Dupont, S.; Krust, A.; Gansmuller, A.; Dierich, A.; Chambon, P.; Mark, M. Effect of single and compound knockouts of estrogen receptors alpha (ER alpha) and beta (ER beta) on mouse reproductive phenotypes. *Development* **2000,** 127, 4277-91.

19.   Imamov, O.; Lopatkin, N. A.; Gustafsson, J. A. Estrogen receptor beta in prostate cancer. *N Eng J Med* **2004,** 351, 2773-4.

20.   Fliss, A. E.; Benzeno, S.; Rao, J.; Caplan, A. J. Control of estrogen receptor ligand binding by Hsp90. *J Steroid Biochem Mol Biol* **2000,** 72, 223-30.

21.   Knoblauch, R.; Garabedian, M. J. Role for Hsp90-associated cochaperone p23 in estrogen receptor signal transduction. *Mol Cell Biol* **1999,** 19, 3748-59.

22.   Pratt, W. B.; Toft, D. O. Steroid receptor interactions with heat shock protein and immunophilin chaperones. *Endocrine Rev* **1997,** 18, 306-60.

23.   Pratt, W. B.; Galigniana, M. D.; Morishima, Y.; Murphy, P. J. M. Role of molecular chaperones in steroid receptor action. *Essays in Biochemistry: Nuclear Receptor Superfamily* **2004,** 40, 41-58.

24.   Smith, C. L.; O'Malley, B. W. Coregulator function: A key to understanding tissue specificity of selective receptor modulators. *Endocrine Rev* **2004,** 25, 45-71.

25.   Le Romancer, M.; Poulard, C.; Cohen, P.; Sentis, S.; Renoir, J. M.; Corbo, L. Cracking the estrogen receptor's posttranslational code in breast tumors. *Endocrine Rev* **2011,** 32, 597-622.

26.   Bain, D. L.; Heneghan, A. F.; Connaghan-Jones, K. D.; Miura, M. T. Nuclear receptor structure: Implications for function. In *Annual Review of Physiology*, 2007; Vol. 69, pp 201-20.

27.   Warnmark, A.; Wikstrom, A.; Wright, A. P. H.; Gustafsson, J. A.; Hard, T. The N-terminal regions of estrogen receptor alpha and beta are unstructured in vitro and show different TBP binding properties. *J Biol Chem* **2001,** 276, 45939-44.

28.   Kumar, R.; Thompson, E. B. Transactivation functions of the N-terminal domains of nuclear hormone receptors: Protein folding and coactivator interactions. *Mol Endocrinol* **2003,** 17, 1-10.

29.   Dahlmanwright, K.; Baumann, H.; McEwan, I. J.; Almlof, T.; Wright, A. P. H.; Gustafsson, J. A.; Hard, T. Structural characterization of a minimal functional transactivation domain from the human glucocorticoid receptor. *Proc Natl Acad Sci U S A* **1995,** 92, 1699-703.

30.   Dyson, H. J.; Wright, P. E. Coupling of folding and binding for unstructured proteins. *Curr Opin Struct Biol* **2002,** 12, 54-60.

31.   Garza, A. M. S.; Khan, S. H.; Kumar, R. Site-specific phosphorylation induces functionally active conformation in the intrinsically disordered N-terminal activation function (AF1) domain of the glucocorticoid receptor. *Mol Cell Biol* **2010,** 30, 220-30.

32.   Combet, C.; Blanchet, C.; Geourjon, C.; Deleage, G. NPS@: Network Protein Sequence Analysis. *Trends in Biochem Sci* **2000,** 25, 147-50.

33.   McInerney, E. M.; Weis, K. E.; Sun, J.; Mosselman, S.; Katzenellenbogen, B. S. Transcription activation by the human estrogen receptor subtype beta (ER beta) studied with ER beta and ER alpha receptor chimeras. *Endocrinol* **1998,** 139, 4513-22.

34.   Onate, S. A.; Boonyaratanakornkit, V.; Spencer, T. E.; Tsai, S. Y.; Tsai, M. J.; Edwards, D. P.; O'Malley, B. W. The steroid receptor coactivator-1 contains multiple receptor interacting and activation domains that cooperatively enhance the activation function 1 (AF1) and AF2 domains of steroid receptors. *J Biol Chem* **1998,** 273, 12101-8.

35.   Webb, P.; Nguyen, P.; Shinsako, J.; Anderson, C.; Feng, W. J.; Nguyen, M. P.; Chen, D. G.; Huang, S. M.; Subramanian, S.; McKinerney, E.; Katzenellenbogen, B. S.; Stallcup, M. R.;

Kushner, P. J. Estrogen receptor activation function 1 works by binding p160 coactivator proteins. *Mol Endocrinol* **1998,** 12, 1605-18.

36. McInerney, E. M.; Katzenellenbogen, B. S. Different regions in activation function-1 of the human estrogen receptor required for antiestrogen- and estradiol-dependent transcription activation. *J Biol Chem* **1996,** 271, 24172-8.

37. Nilsson, S.; Makela, S.; Treuter, E.; Tujague, M.; Thomsen, J.; Andersson, G.; Enmark, E.; Pettersson, K.; Warner, M.; Gustafsson, J. A. Mechanisms of estrogen action. *Physiological Rev* **2001,** 81, 1535-65.

38. Kumar, R.; Thompson, E. B. The structure of the nuclear hormone receptors. *Steroids* **1999,** 64, 310-9.

39. Danielian, P. S.; White, R.; Lees, J. A.; Parker, M. G. Identification of a conserved region required for hormone dependent transcriptional activation by steroid hormone receptors. *EMBO J* **1992,** 11, 1025-33.

40. Tasset, D.; Tora, L.; Fromental, C.; Scheer, E.; Chambon, P. Distinct classes of transcriptional activating domains function by different mechanisms. *Cell* **1990,** 62, 1177-87.

41. Kraus, W. L.; McInerney, E. M.; Katzenellenbogen, B. S. Ligand-dependent, transcriptionally productive association of the amino- and carboxyl-terminal regions of a steroid hormone nuclear receptor. *Proc Natl Acad Sci U S A* **1995,** 92, 12314-8.

42. Kleinhitpass, L.; Tsai, S. Y.; Greene, G. L.; Clark, J. H.; Tsai, M. J.; Omalley, B. W. Specific binding of estrogen-receptor to the estrogen response element. *Mol Cell Biol* **1989,** 9, 43-9.

43. Wood, J. R.; Likhite, V. S.; Loven, M. A.; Nardulli, A. M. Allosteric modulation of estrogen receptor conformation by different estrogen response elements. *Mol Endocrinol* **2001,** 15, 1114-26.

44. Glass, C. K.; Rosenfeld, M. G. The coregulator exchange in transcriptional functions of nuclear receptors. *Genes & Develop* **2000,** 14, 121-41.

45. Brown, M.; Sharp, P. A. Human estrogen receptor forms multiple protein-DNA complexes. *J Biol Chem* **1990,** 265, 11238-43.

46. Schwabe, J. W. R.; Chapman, L.; Finch, J. T.; Rhodes, D. The crystal-structure of the estrogen-receptor DNA-binding domain bound to DNA - how receptors discriminate between their response elements. *Cell* **1993,** 75, 567-78.

47. Schwabe, J. W. R.; Neuhaus, D.; Rhodes, D. Solution structure of the DNA-binding domain of the estrogen-receptor. *Nature* **1990,** 348, 458-61.

48. Schwabe, J. W. R.; Chapman, L.; Rhodes, D. The estrogen-receptor recognizes an imperfectly palindromic response element through an alternative side-chain conformation. *Structure* **1995,** 3, 201-13.

49. Montano, M. M.; Muller, V.; Trobaugh, A.; Katzenellenbogen, B. S. The carboxy-terminal f-domain of the human estrogen-receptor - role in the transcriptional activity of the receptor and the effectiveness of antiestrogens as estrogen antagonists. *Mol Endocrinol* **1995,** 9, 814-25.

50. Koide, A.; Zhao, C. Q.; Naganuma, M.; Abrams, J.; Deighton-Collins, S.; Skafar, D. F.; Koide, S. Identification of regions within the F domain of the human estrogen receptor alpha that are important for modulating transactivation and protein-protein interactions. *Mol Endocrinol* **2007,** 21, 829-42.

51.   Webb, P.; Nguyen, P.; Valentine, C.; Lopez, G. N.; Kwok, G. R.; McInerney, E.; Katzenellenbogen, B. S.; Enmark, E.; Gustafsson, J. A.; Nilsson, S.; Kushner, P. J. The estrogen receptor enhances AP-1 activity by two distinct mechanisms with different requirements for receptor transactivation functions. *Mol Endocrinol* **1999,** 13, 1672-85.

52.   Johnston, S. R. D.; Lu, B.; Scott, G. K.; Kushner, P. J.; Smith, I. E.; Dowsett, M.; Benz, C. C. Increased activator protein-1 DNA binding and c-Jun NH2-terminal kinase activity in human breast tumors with acquired tamoxifen resistance. *Clin Cancer Res* **1999,** 5, 251-6.

53.   Sentis, S.; Le Romancer, M.; Bianchin, C.; Rostan, M. C.; Corbo, L. Sumoylation of the estrogen receptor alpha hinge region regulates its transcriptional activity. *Mol Endocrinol* **2005,** 19, 2671-84.

54.   Wang, C. G.; Fu, M. F.; Angeletti, R. H.; Siconolfi-Baez, L.; Reutens, A. T.; Albanese, C.; Lisanti, M. P.; Katzenellenbogen, B. S.; Kato, S.; Hopp, T.; Fuqua, S. A. W.; Lopez, G. N.; Kushner, P. J.; Pestell, R. G. Direct acetylation of the estrogen receptor alpha hinge region by p300 regulates transactivation and hormone sensitivity. *J Biol Chem* **2001,** 276, 18375-83.

55.   Greene, G. L.; Press, M. F. Structure and dynamics of the estrogen-receptor. *J Steroid Biochem Mol Biol* **1986,** 24, 1-7.

56.   Tsai, M. J.; Omalley, B. W. Molecular mechanisms of action of steroid/thyroid receptor superfamily members. *Annual Rev Biochem* **1994,** 63, 451-86.

57.   Brzozowski, A. M.; Pike, A. C. W.; Dauter, Z.; Hubbard, R. E.; Bonn, T.; Engstrom, O.; Ohman, L.; Greene, G. L.; Gustafsson, J. A.; Carlquist, M. Molecular basis of agonism and antagonism in the oestrogen receptor. *Nature* **1997,** 389, 753-8.

58.   Wurtz, J. M.; Bourguet, W.; Renaud, J. P.; Vivat, V.; Chambon, P.; Moras, D.; Gronemeyer, H. A canonical structure for the ligand-binding domain of nuclear receptors. *Nat Struct Biol* **1996,** 3, 87-94.

59.   Shiau, A. K.; Barstad, D.; Loria, P. M.; Cheng, L.; Kushner, P. J.; Agard, D. A.; Greene, G. L. The structural basis of estrogen receptor/coactivator recognition and the antagonism of this interaction by tamoxifen. *Cell* **1998,** 95, 927-37.

60.   Sever, R.; Glass, C. K. Signaling by nuclear receptors. *Cold Spring Harbor Perspectives in Biology* **2013,** 5.

61.   Hong, H.; Kohli, K.; Trivedi, A.; Johnson, D. L.; Stallcup, M. R. GRIP1, a novel mouse protein that serves as a transcriptional coactivator in yeast for the hormone binding domains of steroid receptors. *Proc Natl Acad Sci U S A* **1996,** 93, 4948-52.

62.   Onate, S. A.; Tsai, S. Y.; Tsai, M. J.; Omalley, B. W. Sequence and characterization of a coactivator for the steroid-hormone receptor superfamily. *Science* **1995,** 270, 1354-7.

63.   Li, H.; Gomes, P. J.; Chen, J. D. RAC3, a steroid/nuclear receptor-associated coactivator that is related to SRC-1 and TIF2. *Proc Natl Acad Sci U S A* **1997,** 94, 8479-84.

64.   Pike, A. C. W.; Brzozowski, A. M.; Hubbard, R. E.; Bonn, T.; Thorsell, A. G.; Engstrom, O.; Ljunggren, J.; Gustafsson, J. K.; Carlquist, M. Structure of the ligand-binding domain of oestrogen receptor beta in the presence of a partial agonist and a full antagonist. *EMBO J* **1999,** 18, 4608-18.

65.   Paech, K.; Webb, P.; Kuiper, G.; Nilsson, S.; Gustafsson, J. A.; Kushner, P. J.; Scanlan, T. S. Differential ligand activation of estrogen receptors ER alpha and ER beta at AP1 sites. *Science* **1997,** 277, 1508-10.

66.	McDonnell, D. P.; Clemm, D. L.; Hermann, T.; Goldman, M. E.; Pike, J. W. Analysis of estrogen-receptor function in-vitro reveals 3 distinct classes of antiestrogens. *Mol Endocrinol* **1995,** 9, 659-69.

67.	Gojis, O.; Rudraraju, B.; Gudi, M.; Hogben, K.; Sousha, S.; Coombes, C. R.; Cleator, S.; Palmieri, C. The role of SRC-3 in human breast cancer (vol 7, pg 83, 2010). *Nature Reviews Clinical Oncology* **2010,** 7, 122-.

68.	Hao, L.; Rizzo, P.; Osipo, C.; Pannuti, A.; Wyatt, D.; Cheung, L. W. K.; Sonenshein, G.; Osborne, B. A.; Miele, L. Notch-1 activates estrogen receptor-alpha-dependent transcription via IKK alpha in breast cancer cells. *Oncogene* **2010,** 29, 201-13.

69.	Habashy, H. O.; Powe, D. G.; Rakha, E. A.; Ball, G.; Macmillan, R. D.; Green, A. R.; Ellis, I. O. The prognostic significance of PELP1 expression in invasive breast cancer with emphasis on the ER-positive luminal-like subtype. *Breast Cancer Res Treat* **2010,** 120, 603-12.

70.	McGuire, W. L.; Chamness, G. C.; Fuqua, S. A. W. Estrogen-receptor variants in clinical breast-cancer. *Mol Endocrinol* **1991,** 5, 1571-7.

71.	Leygue, E.; Huang, A. H.; Murphy, L. C.; Watson, P. H. Prevalence of estrogen receptor variant messenger RNAs in human breast cancer. *Cancer Res* **1996,** 56, 4324-7.

72.	Herynk, M. H.; Fuqua, S. A. W. Estrogen receptor mutations in human disease. *Endocrine Rev* **2004,** 25, 869-98.

73.	Wang, Z. Y.; Zhang, X. T.; Shen, P.; Loggie, B. W.; Chang, Y. C.; Deuel, T. F. Identification, cloning, and expression of human estrogen receptor-alpha 36, a novel variant of human estrogen receptor-alpha 66. *Biochem Biophys Res Comm* **2005,** 336, 1023-7.

74.	Figtree, G. A.; McDonald, D.; Watkins, H.; Channon, K. M. Truncated estrogen receptor alpha 46-kDa isoform in human endothelial cells - Relationship to acute activation of nitric oxide synthase. *Circulation* **2003,** 107, 120-6.

75.	Poola, I.; Koduri, S.; Chatra, S.; Clarke, R. Identification of twenty alternatively spliced estrogen receptor alpha mRNAs in breast cancer cell lines and tumors using splice targeted primer approach. *J Steroid Biochem Mol Biol* **2000,** 72, 249-58.

76.	Penot, G.; Le Peron, C.; Merot, Y.; Grimaud-Fanouillere, E.; Ferriere, F.; Boujrad, N.; Kah, O.; Saligaut, C.; Ducouret, B.; Metivier, R.; Flouriot, G. The human estrogen receptor-alpha isoform hER alpha 46 antagonizes the proliferative influence of hER alpha 66 in MCF7 breast cancer cells. *Endocrinol* **2005,** 146, 5474-84.

77.	Denger, S.; Reid, G.; Kos, M.; Flouriot, G.; Parsch, D.; Brand, H.; Korach, K. S.; Sonntag-Buck, V.; Gannon, F. ER alpha gene expression in human primary osteoblasts: Evidence for the expression of two receptor proteins. *Mol Endocrinol* **2001,** 15, 2064-77.

78.	Wang, Z. Y.; Zhang, X. T.; Shen, P.; Loggie, B. W.; Chang, Y.; Deuel, T. F. A variant of estrogen receptor-alpha, hER-alpha 36: Transduction of estrogen- and antiestrogen-dependent membrane-initiated mitogenic signaling. *Proc Natl Acad Sci U S A* **2006,** 103, 9063-8.

79.	Pink, J. J.; Wu, S. Q.; Wolf, D. M.; Bilimoria, M. M.; Jordan, V. C. A novel 80 kDa human estrogen receptor containing a duplication of exons 6 and 7. *Nucleic Acids Res* **1996,** 24, 962-9.

80.	Zhang, Q. X.; Borg, A.; Fuqua, S. A. W. An exon-5 deletion variant of the estrogen-receptor frequently coexpressed with wild-type estrogen-receptor in human breast-cancer. *Cancer Res* **1993,** 53, 5882-4.

81.   Jordan, V. C. Fourteenth Gaddum Memorial Lecture - University of Cambridge - January 1993 - A current view of tamoxifen for the treatment and prevention of breast cancer. *British J Pharmacol* **2000,** 131, 221-31.

82.   Powles, T.; Hickish, T.; Kanis, J. A.; Tidy, A.; Ashley, S. Effect of tamoxifen on bone mineral density measured by dual-energy x-ray absorptiometry in healthy premenopausal and postmenopausal women. *J Clin Oncol* **1996,** 14, 78-84.

83.   Mitlak, B. H.; Cohen, F. J. In search of optimal long-term female hormone replacement: The potential of selective estrogen receptor modulators. *Hormone Res* **1997,** 48, 155-63.

84.   Cosman, F.; Lindsay, R. Selective estrogen receptor modulators: Clinical spectrum. *Endocrine Rev* **1999,** 20, 418-34.

85.   Howell, S. J.; Johnston, S. R. D.; Howell, A. The use of selective estrogen receptor modulators and selective estrogen receptor down-regulators in breast cancer. *Best Pract Res Clin Endocrinol Metab* **2004,** 18, 47-66.

86.   Berry, N. B.; Fan, M.; Nephew, K. P. Estrogen receptor-alpha hinge-region lysines 302 and 303 regulate receptor degradation by the proteasome. *Mol Endocrinol* **2008,** 22, 1535-51.

87.   Wijayaratne, A. L.; McDonnell, D. P. The human estrogen receptor-alpha is a ubiquitinated protein whose stability is affected differentially by agonists, antagonists, and selective estrogen receptor modulators. *J Biol Chem* **2001,** 276, 35684-92.

88.   Defriend, D. J.; Howell, A.; Nicholson, R. I.; Anderson, E.; Dowsett, M.; Mansel, R. E.; Blamey, R. W.; Bundred, N. J.; Robertson, J. F.; Saunders, C.; Baum, M.; Walton, P.; Sutcliffe, F.; Wakeling, A. E. Investigation of a new pure antiestrogen (ici-182780) in women with primary breast-cancer. *Cancer Res* **1994,** 54, 408-14.

89.   Robertson, J. F. R. Fulvestrant (Faslodex (R)) - How to make a good drug better. *Oncologist* **2007,** 12, 774-84.

90.   Lai, A.; Kahraman, M.; Govek, S.; Nagasawa, J.; Bonnefous, C.; Julien, J.; Douglas, K.; et al. Identification of GDC-0810 (ARN-810), an orally bioavailable selective estrogen receptor degrader (SERD) that demonstrates robust activity in tamoxifen-resistant breast cancer xenografts. *J Med Chem* **2015,** 58, 4888-904.

91.   Punchihewa, C.; De Alba, A.; Sidell, N.; Yang, D. Z. XR5944: A potent inhibitor of estrogen receptors. *Mol Cancer Ther* **2007,** 6, 213-9.

92.   Wang, L. H.; Yang, X. Y.; Zhang, X. H.; Mihalic, K.; Fan, Y. X.; Xiao, W. H.; Howard, O. M. Z.; Appella, E.; Maynard, A. T.; Farrar, W. L. Suppression of breast cancer by chemical modulation of vulnerable zinc fingers in estrogen receptor. *Nat Med* **2004,** 10, 40-7.

93.   Wang, L. H.; Yang, X. Y.; Zhang, X. H.; An, P.; Kim, H. J.; Huang, J. Q.; Clarke, R.; Osborne, C. K.; Inman, J. K.; Appella, E.; Farrar, W. L. Disruption of estrogen receptor DNA-binding domain and related intramolecular communication restores tamoxifen sensitivity in resistant breast cancer. *Cancer Cell* **2006,** 10, 487-99.

94.   Mao, C.; Patterson, N. M.; Cherian, M. T.; Aninye, I. O.; Zhang, C.; Montoya, J. B.; Cheng, J.; Putt, K. S.; Hergenrother, P. J.; Wilson, E. M.; Nardulli, A. M.; Nordeen, S. K.; Shapiro, D. J. A new small molecule inhibitor of estrogen receptor alpha binding to estrogen response elements blocks estrogen-dependent growth of cancer cells. *J Biol Chem* **2008,** 283, 12819-30.

95.   Rodriguez, A. L.; Tamrazi, A.; Collins, M. L.; Katzenellenbogen, J. A. Design, synthesis, and in vitro biological evaluation of small molecule inhibitors of estrogen receptor a coactivator binding. *J Med Chem* **2004,** 47, 600-11.

96.   Parent, A. A.; Gunther, J. R.; Katzenellenbogen, J. A. Blocking estrogen signaling after the hormone: pyrimidine-core inhibitors of estrogen receptor-coactivator binding. *J Med Chem* **2008,** 51, 6512-30.

97.   Gunther, J. R.; Moore, T. W.; Cottins, M. L.; Katzenettenbogen, J. A. Amphipathic benzenes are designed inhibitors of the estrogen receptor alpha/steroid receptor coactivator interaction. *ACS Chem Biol* **2008,** 3, 282-6.

98.   Shao, D. L.; Berrodin, T. J.; Manas, E.; Hauze, D.; Powers, R.; Bapat, A.; Gonder, D. I.; Winneker, R. C.; Frail, D. E. Identification of novel estrogen receptor alpha antagonists. *J Steroid Biochem Mol Biol* **2004,** 88, 351-60.

99.   LaFrate, A. L.; Gunther, J. R.; Carlson, K. E.; Katzenellenbogen, J. A. Synthesis and biological evaluation of guanylhydrazone coactivator binding inhibitors for the estrogen receptor. *Bioorg Med Chem* **2008,** 16, 10075-84.

100.   Chang, C. Y.; Norris, J. D.; Gron, H.; Paige, L. A.; Hamilton, P. T.; Kenan, D. J.; Fowlkes, D.; McDonnell, D. P. Dissection of the LXXLL nuclear receptor-coactivator interaction motif using combinatorial peptide libraries: Discovery of peptide antagonists of estrogen receptors alpha and beta. *Mol Cell Biol* **1999,** 19, 8226-39.

101.   Northrop, J. P.; Nguyen, D.; Piplani, S.; Olivan, S. E.; Kwan, S. T. S.; Go, N. F.; Hart, C. P.; Schatz, P. J. Selection of estrogen receptor beta- and thyroid hormone receptor beta-specific coactivator-mimetic peptides using recombinant peptide libraries. *Mol Endocrinol* **2000,** 14, 605-22.

102.   Phan, T.; Nguyen, H. D.; Goksel, H.; Mocklinghoff, S.; Brunsveld, L. Phage display selection of miniprotein binders of the Estrogen Receptor. *Chem Commun* **2010,** 46, 8207-9.

103.   Lu, Y. J.; Yang, J.; Sega, E. Issues related to targeted delivery of proteins and peptides. *AAPS J* **2006,** 8, E466-E78.

104.   Schafer, J. M.; Liu, H.; Bentrem, D. J.; Zapf, J. W.; Jordan, V. C. Allosteric silencing of activating function 1 in the 4-hydroxytamoxifen estrogen receptor complex is induced by substituting glycine for aspartate at amino acid 351. *Cancer Res* **2000,** 60, 5097-105.

105.   Vandenberg, H. W.; Lynch, M.; Martin, J.; Nelson, J.; Dickson, G. R.; Crockard, A. D. Characterization of a tamoxifen-resistant variant of the ZR-75-1 human-breast cancer cell-line (ZR-75-9A1) and stability of the resistant phenotype. *Brit J Cancer* **1989,** 59, 522-6.

106.   Graham, M. L.; Smith, J. A.; Jewett, P. B.; Horwitz, K. B. Heterogeneity of progesterone receptor content and remodeling by tamoxifen characterize subpopulations of cultured human breast cancer cells: analysis by quantitative dual parameter flow cytometry. *Cancer Res* **1992,** 52, 593-602.

107.   Yang, X. W.; Phillips, D. L.; Ferguson, A. T.; Nelson, W. G.; Herman, J. G.; Davidson, N. E. Synergistic activation of functional estrogen receptor (ER)-alpha by DNA methyltransferase and histone deacetylase inhibition in human ER-alpha-negative breast cancer cells. *Cancer Res* **2001,** 61, 7025-9.

108.   Parl, F. F. Multiple mechanisms of estrogen receptor gene repression contribute to ER-negative breast cancer. *Pharmacogenomics J* **2003,** 3, 251-3.

109.   Ottaviano, Y. L.; Issa, J. P.; Parl, F. F.; Smith, H. S.; Baylin, S. B.; Davidson, N. E. Methylation of the estrogen-receptor gene CPG island marks loss of estrogen-receptor expression in human breast-cancer cells. *Cancer Res* **1994,** 54, 2552-5.

110.   Kressler, D.; Hock, M. B.; Kralli, A. Coactivators PGC-1 beta and SRC-1 interact functionally to promote the agonist activity of the selective estrogen receptor modulator tamoxifen. *J Biol Chem* **2007,** 282, 26897-907.

111.   Fuqua, S. A. W.; Schiff, R.; Parra, I.; Moore, J. T.; Mohsin, S. K.; Osborne, C. K.; Clark, G. M.; Allred, D. C. Estrogen receptor beta protein in human breast cancer: Correlation with clinical tumor parameters. *Cancer Res* **2003,** 63, 2434-9.

112.   Kurokawa, H.; Lenferink, A. E. G.; Simpson, J. F.; Pisacane, P. I.; Sliwkowski, M. X.; Forbes, J. T.; Arteaga, C. L. Inhibition of HER2/neu (erbB-2) and mitogen-activated protein kinases enhances tamoxifen action against HER2-ovorexpresessed tamoxifen-resistant breast cancer cells. *Cancer Res* **2000,** 60, 5887-94.

113.   Riggins, R. B.; Schrecengost, R. S.; Guerrero, M. S.; Bouton, A. H. Pathways to tamoxifen resistance. *Cancer Lett* **2007,** 256, 1-24.

114.   Chan, K. C.; Knox, W. F.; Gee, J. M.; Morris, J.; Nicholson, R. I.; Potten, C. S.; Bundred, N. J. Effect of epidermal growth factor receptor tyrosine kinase inhibition on epithelial proliferation in normal and premalignant breast. *Cancer Res* **2002,** 62, 122-8.

115.   Shou, J.; Massarweh, S.; Osborne, C. K.; Wakeling, A. E.; Ali, S.; Weiss, H.; Schiff, R. Mechanisms of tamoxifen resistance: Increased estrogen receptor-HER2/neu cross-talk in ER/HER2-positive breast cancer. *J Natl Cancer Inst* **2004,** 96, 926-35.

116.   Turner, N.; Pearson, A.; Sharpe, R.; Lambros, M.; Geyer, F.; et al. FGFR1 amplification drives endocrine therapy resistance and is a therapeutic target in breast cancer. *Cancer Res* **2010,** 70, 2085-94.

117.   Miller, T. W.; Hennessy, B. T.; Gonzalez-Angulo, A. M.; Fox, E. M.; Mills, G. B.; Chen, H. D.; Higham, C.; Garcia-Echeverria, C.; Shyr, Y.; Arteaga, C. L. Hyperactivation of phosphatidylinositol-3 kinase promotes escape from hormone dependence in estrogen receptor-positive human breast cancer. *J Clin Invest* **2010,** 120, 2406-13.

118.   Zwijsen, R. M. L.; Wientjens, E.; Klompmaker, R.; vanderSman, J.; Bernards, R.; Michalides, R. CDK-independent activation of estrogen receptor by cyclin D1. *Cell* **1997,** 88, 405-15.

119.   Wilcken, N. R. C.; Prall, O. W. J.; Musgrove, E. A.; Sutherland, R. L. Inducible overexpression of cyclin D1 in breast cancer cells reverses the growth-inhibitory effects of antiestrogens. *Clin Cancer Res* **1997,** 3, 849-54.

120.   Rudas, M.; Lehnert, M.; Huynh, A.; Jakesz, R.; Singer, C.; Lax, S.; Schippinger, W.; Dietze, O.; Greil, R.; Stigibauer, W.; Kwasny, W.; Grill, R.; Stierer, M.; Gnant, M. F. X.; Filipits, M.; Austrian Breast Colorectal, C. Cyclin D1 expression in breast cancer patients receiving adjuvant tamoxifen-based therapy. *Clin Cancer Res* **2008,** 14, 1767-74.

121.   Stendahl, M.; Kronblad, A.; Ryden, L.; Emdin, S.; Bengtsson, N. O.; Landberg, G. Cyclin DI overexpression is a negative predictive factor for tamoxifen response in postmenopausal breast cancer patients. *British J Cancer* **2004,** 90, 1942-8.

122.   Gonzalez-Angulo, A. M.; Morales-Vasquez, F.; Hortobagyi, G. N. Overview of resistance to systemic therapy in patients with breast cancer. *Breast Cancer Chemosensitivity* **2007,** 608, 1-22.

123.   Johnston, S. R. D.; Haynes, B. P.; Smith, I. E.; Jarman, M.; Sacks, N. P. M.; Ebbs, S. R.; Dowsett, M. Acquired tamoxifen resistance in human breast-cancer and reduced intra-tumoral drug concentration. *Lancet* **1993,** 342, 1521-2.

124.   Katzenellenbogen, B. S.; Miller, M. A.; Mullick, A.; Sheen, Y. Y. Antiestrogen action in breast cancer cells: modulation of proliferation and protein synthesis, and interaction with estrogen receptors and additional antiestrogen binding sites. *Breast Cancer Res Treat* **1985,** 5, 231-43.

125.   Denton, K. M.; Shweta, A.; Anderson, W. P. Preglomerular and postglomerular resistance responses to different levels of sympathetic activation by hypoxia. *J Am Soc Nephrol* **2002,** 13, 27-34.

126.   Jeselsohn, R.; Yelensky, R.; Buchwalter, G.; Frampton, G.; Meric-Bernstam, F.; et al. Emergence of constitutively active estrogen receptor-α mutations in pretreated advanced estrogen receptor-positive breast cancer. *Clinical Cancer Res* **2014,** 20, 1757-67.

127.   Robinson, D. R.; Wu, Y. M.; Vats, P.; Su, F. Y.; Lonigro, R. J.; Cao, X. H.; Kalyana-Sundaram, S.; Wang, R.; Ning, Y.; et al. Activating ESR1 mutations in hormone-resistant metastatic breast cancer. *Nat Gen* **2013,** 45, 1446-U197.

128.   Toy, W.; Shen, Y.; Won, H.; Green, B.; Sakr, R. A.; Will, M.; Li, Z. Q.; et al. ESR1 ligand-binding domain mutations in hormone-resistant breast cancer. *Nat Gen* **2013,** 45, 1439-U189.

129.   Zhang, Q. X.; Borg, A.; Wolf, D. M.; Oesterreich, S.; Fuqua, S. A. W. An estrogen receptor mutant with strong hormone-independent activity from a metastatic breast cancer. *Cancer Res* **1997,** 57, 1244-9.

130.   Carlson, K. E.; Choi, I.; Gee, A.; Katzenellenbogen, B. S.; Katzenellenbogen, J. A. Altered ligand binding properties and enhanced stability of a constitutively active estrogen receptor: Evidence that an open pocket conformation is required for ligand interaction. *Biochemistry* **1997,** 36, 14897-905.

131.   Li, S. Q.; Shen, D.; Shao, J. Y.; Crowder, R.; Liu, W. B.; Prat, A.; al., e. Endocrine-therapy-resistant ESR1 variants revealed by genomic characterization of breast-cancer-derived xenografts. *Cell Rep* **2013,** 4, 1116-30.

132.   Delfosse, V.; Grimaldi, M.; Pons, J.-L.; Boulahtouf, A.; le Maire, A.; Cavailles, V.; Labesse, G.; Bourguet, W.; Balaguer, P. Structural and mechanistic insights into bisphenols action provide guidelines for risk assessment and discovery of bisphenol A substitutes. *Proceedings of the National Academy of Sciences of the United States of America* **2012,** 109, 14930-5.

133.   Chemical Computing Group Inc. Molecular Operating Environment (MOE); Montreal, Quebec, Canada, 2008; . www. chemcomp.com.

134.   Friesner, R. A.; Banks, J. L.; Murphy, R. B.; Halgren, T. A.; Klicic, J. J.; Mainz, D. T.; Repasky, M. P.; Knoll, E. H.; Shelley, M.; Perry, J. K.; Shaw, D. E.; Francis, P.; Shenkin, P. S. Glide: A new approach for rapid, accurate docking and scoring. 1. Method and assessment of docking accuracy. *Journal of Medicinal Chemistry* **2004,** 47, 1739-49.

135.   Zsoldos, Z.; Reid, D.; Simon, A.; Sadjad, S. B.; Johnson, A. P. eHiTS: A new fast, exhaustive flexible ligand docking system. *Journal of Molecular Graphics & Modelling* **2007,** 26, 198-212.

136.   Axerio-Cilies, P.; Lack, N. A.; Nayana, M. R. S.; Chan, K. H.; Yeung, A.; Leblanc, E.; Guns, E. S. T.; Rennie, P. S.; Cherkasov, A. Inhibitors of androgen receptor activation function-2 (AF2) site identified through virtual screening. *J Med Chem* **2011,** 54, 6197-205.

137.   Munuganti, R.; Hassona, M.; Leblanc, E.; Frewin, K.; Singh, K.; Ma, D.; Ban, F.; Hsing, M.; Adomat, H.; Lallous, N.; Andre, C.; Jonadass, J.; Zoubeidi, A.; Young, R.; Guns, E.; Rennie,

P.; Cherkasov, A. Targeting the Binding Function 3 (BF3) Site of the Androgen Receptor Through Virtual Screening. 2. Development of 2-((2-phenoxyethyl) thio)-1H-benzimidazole Derivatives. *J Med Chem* **2013,** 56, 1136-48.

138.   Munuganti, R. S. N.; Hassona, M. D. H.; Leblanc, E.; Frewin, K.; Singh, K.; Ma, D.; Ban, F. Q.; Hsing, M.; Adomat, H.; Lallous, N.; Andre, C.; Jonadass, J. P. S.; Zoubeidi, A.; Young, R. N.; Guns, E. T.; Rennie, P. S.; Cherkasov, A. Identification of a potent antiandrogen that targets the BF3 site of the androgen receptor and inhibits enzalutamide-resistant prostate cancer. *Chem Biol* **2014,** 21, 1476-85.

139.   Singh, K.; Munuganti, R. S. N.; Leblanc, E.; Lin, Y. L.; Leung, E.; Lallous, N.; Butler, M.; Cherkasov, A.; Rennie, P. S. In silico discovery and validation of potent small-molecule inhibitors targeting the activation function 2 site of human oestrogen receptor alpha. *Breast Cancer Res* **2015,** 17.

140.   Cherian, M. T.; Wilson, E. M.; Shapiro, D. J. A Competitive Inhibitor That Reduces Recruitment of Androgen Receptor to Androgen-responsive Genes. *Journal of Biological Chemistry* **2012,** 287, 23368-80.

141.   Irwin, J. J.; Sterling, T.; Mysinger, M. M.; Bolstad, E. S.; Coleman, R. G. ZINC: A free tool to discover chemistry for biology. *J Chem Inf Model* **2012,** 52, 1757-68.

142.   Karplus, M.; McCammon, J. A. Molecular dynamics simulations of biomolecules. *Nat Struct Biol* **2002,** 9, 788-.

143.   Walsh, C. A.; Qin, L.; Tien, J. C. Y.; Young, L. S.; Xu, J. M. The function of steroid receptor coactivator-1 in normal tissues and cancer. *Intl J Biol Sci* **2012,** 8, 470-85.

144.   Kilkenny, C.; Browne, W. J.; Cuthill, I. C.; Emerson, M.; Altman, D. G. Improving Bioscience Research Reporting: The ARRIVE Guidelines for Reporting Animal Research. *Plos Biology* **2010,** 8.

145.   Robinson, D. R.; Wu, Y.-M.; Vats, P.; Su, F.; Lonigro, R. J.; Cao, X.; Kalyana-Sundaram, S.; Wang, R.; Ning, Y.; Hodges, L.; Gursky, A.; Siddiqui, J.; Tomlins, S. A.; Roychowdhury, S.; Pienta, K. J.; Kim, S. Y.; Roberts, J. S.; Rae, J. M.; Van Poznak, C. H.; Hayes, D. F.; Chugh, R.; Kunju, L. P.; Talpaz, M.; Schott, A. F.; Chinnaiyan, A. M. Activating ESR1 mutations in hormone-resistant metastatic breast cancer. *Nature Genetics* **2013,** 45, 1446-U197.

146.   Toy, W.; Shen, Y.; Won, H.; Green, B.; Sakr, R. A.; Will, M.; Li, Z.; Gala, K.; Fanning, S.; King, T. A.; Hudis, C.; Chen, D.; Taran, T.; Hortobagyi, G.; Greene, G.; Berger, M.; Baselga, J.; Chandarlapaty, S. ESR1 ligand-binding domain mutations in hormone-resistant breast cancer. *Nature Genetics* **2013,** 45, 1439-U189.

147.   Merenbakh-Lamin, K.; et al. D538G Mutation in Estrogen Receptor-alpha: A Novel Mechanism for Acquired Endocrine Resistance in Breast Cancer. *Cancer Res* **2013,** 73, 6856-64.

148.   Osborne, C.; et al. Crosstalk between estrogen receptor and growth factor receptor pathways as a cause for endocrine therapy resistance in breast cancer. *Clin Cancer Res* **2005,** 11, 865S-70S.

149.   Hao, L.; et al. Notch-1 activates estrogen receptor-alpha-dependent transcription via IKK alpha in breast cancer cells. *Oncogene* **2010,** 29, 201-13.

150.   Axerio-Cilies P; See RH; Zoraghi R; Worral L; Lian T; Stoynov N; Jiang J; et al. Cheminformatics-driven discovery of selective, nanomolar inhibitors for staphylococcal pyruvate kinase. *ACS Chem Biol* **2012,** 7, 349-58.